

การดูดซับโลหะหนักโดยใช้สาหร่ายมหภาคสีเขียวชนิดช่อพริกไทย (*Caulerpa lentillifera*) และ
ซีโอไลต์ที่ดัดแปลงจากถ้ำลอยถ่าน



นายธเนศบวรจวบ อภิตติกุล

สถาบันวิทยบริการ จุฬาลงกรณ์มหาวิทยาลัย

วิทยานิพนธ์นี้เป็นส่วนหนึ่งของการศึกษาตามหลักสูตรปริญญาวิทยาศาสตรดุษฎีบัณฑิต

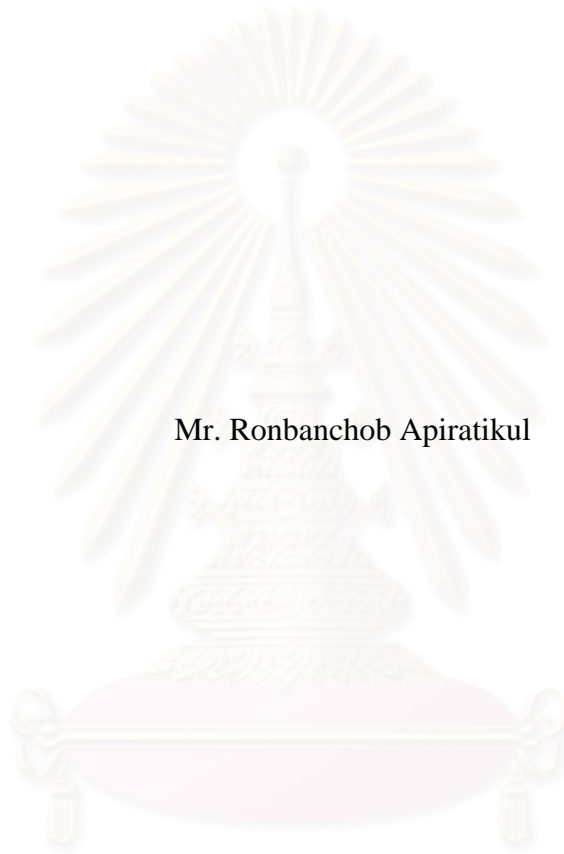
สาขาวิชาการจัดการสิ่งแวดล้อม (สหสาขาวิชา)

บัณฑิตวิทยาลัย จุฬาลงกรณ์มหาวิทยาลัย

ปีการศึกษา 2549

ลิขสิทธิ์ของจุฬาลงกรณ์มหาวิทยาลัย

SORPTION OF HEAVY METALS BY GREEN MACRO ALGA, CAULERPA
LENTILLIFERA AND MODIFIED ZEOLITE FROM COAL FLY ASH



Mr. Ronbanchob Apiratikul

สถาบันวิทยบริการ
จุฬาลงกรณ์มหาวิทยาลัย

A Dissertation Submitted in Partial Fulfillment of the Requirements
for the Degree of Doctor of Philosophy Program in Environmental Management
(Interdisciplinary Program)
Graduate School
Chulalongkorn University
Academic Year 2006
Copyright of Chulalongkorn University

รณบรรจบ อภิรติกุล : การดูดซับโลหะหนักโดยใช้สาหร่ายมหภาคสีเขียวชนิดช่อพริกไทย และซีโอไลต์ที่ดัดแปลงจากถ้ำลอยถ่าน (SORPTION OF HEAVY METALS BY GREEN MACRO ALGA, CAULERPA LENTILLIFERA AND MODIFIED ZEOLITE FROM COAL FLY ASH) อ.ที่ปรึกษา : รศ. ดร. ประเสริฐ ภูวสันต์, 171 หน้า

งานวิจัยนี้ประกอบด้วยสองส่วนหลัก ๆ คือ การศึกษาเกี่ยวกับการดูดซับโลหะหนักด้วยสาหร่ายช่อพริกไทยซึ่งเป็นวัสดุเหลือใช้ทางการเกษตร และ การศึกษาการดูดซับโลหะหนักด้วยซีโอไลต์ชนิดเอ็กซ์ที่ดัดแปลงจากถ้ำลอยถ่านซึ่งเป็นกากของเสียจากอุตสาหกรรม


สำหรับงานการดูดซับโลหะหนักด้วยกระบวนการทางชีวภาพโดยใช้สาหร่ายช่อพริกไทย ผลการศึกษาแสดงว่า จลนพลศาสตร์ของการดูดซับสามารถอธิบายได้ด้วยสมการปฏิกิริยาอันดับสอง ก่อการถ่ายเทมวลสารภายนอกและการแพร่ภายในอนุภาคเป็นกลไกที่ควบคุมการเคลื่อนที่ของโลหะหนักจากสารละลายไปสู่ตำแหน่งที่เกิดการดูดซับ ข้อมูลการดูดซับที่สภาวะสมดุล ณ อุณหภูมิคงที่สอดคล้องกับแบบจำลองของซีฟส์ที่มีค่าตัวแปรในตำแหน่งยกกำลังเข้าใกล้หนึ่งแสดงว่าการดูดซับดังกล่าวสามารถอธิบายได้ด้วยแบบจำลองของแลงเมียร์เช่นกัน สาหร่ายช่อพริกไทยสามารถดูดซับตะกั่วได้สูงที่สุด รองลงมาคือ ทองแดง และ แคดเมียม ตามลำดับ พลังงานที่ใช้ในการดูดซับโลหะหนักที่คำนวณได้จากแบบจำลองของลูบินิน-เรดิชเควิชมีค่าอยู่ในช่วง 4-6 กิโลจูลต่อโมล แสดงว่าแรงดึงดูดทางไฟฟ้าสถิตเป็นแรงที่สำคัญในกระบวนการดูดซับ ความสามารถในการดูดซับลดลงเมื่อค่าพีเอชของสารละลายลดลง การศึกษาการดูดซับสารละลายที่มีโลหะหนักทองแดง แคดเมียม และตะกั่ว ผสมกันสองโลหะ โดยสาหร่ายช่อพริกไทยพบว่าแบบจำลองการแก่งแย่งการดูดซับเพียงบางส่วนสามารถอธิบายผลการทดลองได้เป็นอย่างดี ผลการศึกษาแสดงให้เห็นว่าเมื่อมีโลหะหนักสองชนิดในสารละลายจะทำให้ความสามารถในการดูดซับโลหะหนักทั้งสองมีค่าลดลง แสดงว่ามีการใช้ตำแหน่งดูดซับร่วมกันในการดูดซับโลหะหนักทั้งสาม ตะกั่วมีอิทธิพลในการรบกวนการดูดซับมากที่สุด รองลงมาคือ ทองแดง และ แคดเมียม ตามลำดับ การที่มีตะกั่วในสารละลายโลหะหนักผสมสองชนิดจะทำให้ความสามารถในการดูดซับโลหะหนักอีกตัวลดลงอย่างมาก แบบจำลองการดูดซับโลหะสองชนิดสามารถนำมาอธิบายผลของพีเอชต่อการดูดซับโลหะหนักหนึ่งชนิด หมู่ฟังก์ชันที่ทำให้หน้าในการดูดซับโลหะหนักด้วยสาหร่ายช่อพริกไทย คือ หมู่คาร์บอกซิล หมู่ไฮดรอกซิล หมู่ซัลโฟเนต หมู่เอมีน และ หมู่ไฮโดรฟิลิก โดยแคดเมียมจะถูกดูดซับด้วยเอมีน และ หมู่ไฮโดรฟิลิก เป็นส่วนมาก แบบจำลองของโทมัสสามารถอธิบายข้อมูลการดูดซับที่ได้จากการทดลองในระบบคอลัมน์ได้ดี ระหว่างการดูดซับพบว่าแคลเซียม แมกนีเซียม และ แมงกานีสได้หลุดออกมาจากสาหร่ายช่อพริกไทยแสดงว่ากลไกการแลกเปลี่ยนไอออนเป็นกลไกที่สำคัญในการดูดซับด้วยสาหร่ายดังกล่าว

การดัดแปลงถ้ำลอยในงานวิจัยนี้ด้วยวิธีหลอมรวมกับโซเดียมไฮดรอกไซด์พบว่าได้ซีโอไลต์ชนิดเอ็กซ์ที่มีค่าความสามารถในการแลกเปลี่ยนไอออนบวกประมาณ 140 มิลลิเอควิวเลนตต่อ 100 กรัม ซีโอไลต์ที่ได้สามารถใช้เป็นตัวดูดซับที่มีประสิทธิภาพในการกำจัดทองแดง แคดเมียม และตะกั่ว จลนพลศาสตร์ของการดูดซับสามารถอธิบายได้ด้วยสมการปฏิกิริยาอันดับสอง เวลาที่การดูดซับเข้าสู่สมดุลจะนานขึ้นเมื่อเพิ่มความเข้มข้นเริ่มต้นของโลหะหนักหรือเมื่อลดอัตราส่วนซีโอไลต์ต่อปริมาตรน้ำเสีย อย่างไรก็ตามการดูดซับจะเข้าสู่สมดุลภายใน 120 นาที การถ่ายเทมวลสารภายนอกเป็นกลไกที่กำหนดการเคลื่อนที่ของตะกั่วจากสารละลายไปสู่ตำแหน่งดูดซับสำหรับกรณีความเข้มข้นเริ่มต้นของตะกั่วมีค่าต่ำและกรณีอัตราส่วนซีโอไลต์ต่อปริมาตรน้ำเสียนั้นสูงมีค่ามาก ส่วนการแพร่ภายในอนุภาคเป็นกลไกที่ควบคุมการเคลื่อนที่ของทองแดงในกระบวนการดูดซับสำหรับทุกความเข้มข้นเริ่มต้น สำหรับแคดเมียมพบว่ากลไกการถ่ายเทมวลสารภายนอกและการแพร่ภายในอนุภาคเป็นกลไกที่ควบคุมการเคลื่อนที่ทุกๆความเข้มข้นเริ่มต้น ซีโอไลต์ชนิดเอ็กซ์ในงานวิจัยนี้สามารถดูดซับตะกั่วได้สูงที่สุด รองลงมาคือ ทองแดง และแคดเมียม ตามลำดับ พลังงานที่ใช้ในการดูดซับโลหะหนักที่อยู่ในช่วงการดูดซับทางกายภาพ ความเข้มข้นเริ่มต้นของโลหะหนักและอัตราส่วนซีโอไลต์ต่อปริมาตรน้ำเสียเป็นตัวควบคุมความสามารถในการดูดซับและร้อยละการกำจัดที่สภาวะสมดุล งานวิจัยนี้ได้พัฒนาแบบจำลองขึ้นเพื่ออธิบายปรากฏการณ์ดังกล่าวโดยแบบจำลองได้ถูกพิสูจน์ด้วยผลการทดลองเพิ่มเติมว่ามีความถูกต้อง

สาขาวิชา การจัดการสิ่งแวดล้อม

ปีการศึกษา 2549

ลายมือชื่อนิสิต 

ลายมือชื่ออาจารย์ที่ปรึกษา 

4789796920: MAJOR ENVIRONMENTAL MANAGEMENT

KEY WORD: BIOSORPTION / WASTEWATER TREATMENT / FUSION / CEC
 RONBANCHOB APIRATIKUL: SORPTION OF HEAVY METALS BY
 GREEN MACRO ALGA, CAULERPA LENTILLIFERA AND MODIFIED
 ZEOLITE FROM COAL FLY ASH. THESIS ADVISOR: ASSOC. PROF.
 PRASERT PAVASANT, Ph.D. 171 PP.

This dissertation comprised two main parts which are the investigations of the biosorption of heavy metal ions by agricultural waste (green macroalga, *Caulerpa lentillifera*) and by Zeolite X modified from coal fly ash (CFA).

The biosorption of Cu^{2+} , Cd^{2+} , and Pb^{2+} by a dried green macroalga *Caulerpa lentillifera* was investigated. The sorption kinetic data could be fitted to the pseudo second order kinetic model. The governing transport mechanisms in the sorption process were both external mass transfer and intra-particle diffusion. Isotherm data followed the Sips isotherm model with the exponent of approximately unity suggesting that these biosorption could be described reasonably well with the Langmuir isotherm. The maximum sorption capacities of the various metal components on *Caulerpa lentillifera* biomass could be prioritized in order from high to low as: $\text{Pb}^{2+} > \text{Cu}^{2+} > \text{Cd}^{2+}$. The sorption energies obtained from the Dubinin-Radushkevich model for all sorption systems were in the range of 4 – 6 kJ mol^{-1} indicating that a physical electrostatic force was potentially involved in the sorption process. The sorption capacity decreased with a decrease in pH. The sorption of Cu^{2+} , Cd^{2+} , and Pb^{2+} by a dried green macroalga *Caulerpa lentillifera* in binary components systems was investigated. The partial competitive binary isotherm model was proven to be effective in describing the experimental data. The model and experimental data of each binary component system demonstrated that the presence of the secondary metal ion always reduced the total sorption capacity of the biomass. This implied that there existed the same pooled binding sites for the sorption of all of these heavy metal ions. Pb^{2+} was demonstrated to be the most uptaken species, followed by Cu^{2+} and Cd^{2+} . The presence of Pb^{2+} significantly suppressed the sorptions of Cu^{2+} and Cd^{2+} than it was by the presence of Cu^{2+} and Cd^{2+} . Similarly the sorption of Cd^{2+} was more disturbed by the presence of Cu^{2+} than that of Cu^{2+} by Cd^{2+} . The effect of pH on metal sorption could also be described using similar fundamentals with the sorption of binary metal component, and the partial competitive model could also be applied to predict the effect of pH on the sorption of these metals. It was demonstrated that a decrease in pH resulted in a reduction in the sorption capacity and sorption affinity. Carboxyl, hydroxyl, sulfonate, amine, and amide functional groups in the alga could be responsible for the sorption of all heavy metals while Cd^{2+} could mainly form bond with amine and amide groups and had difficulty in forming bonds with the other groups. Thomas model could well describe the breakthrough data from column experiments. Ca^{2+} , Mg^{2+} , and Mn^{2+} were the major ions released from the algal biomass during the sorption which revealed that ion exchange was one of the main sorption mechanisms.

The CFA was modified to zeolite X using the fusion method with cationic exchange capacity (CEC) of about 140 meq/100g. The zeolite was used as an effective sorbent for removing of Cu^{2+} , Cd^{2+} , and Pb^{2+} . The pseudo second order kinetic model was appropriate for the description of the kinetic performance of the sorption. Although it took longer to reach equilibrium for experiments at higher initial metal concentration and lower sorbent dose, all sorption reached equilibrium within 120 minutes. External mass transfer step seemed to take part as a rate limiting step for the sorption of Pb^{2+} at low initial concentration and high sorbent dose. In the contrary, the process was controlled more significantly by intraparticle diffusion step at high initial concentration and low sorbent dose. However, Cu^{2+} was found to be generally controlled by intraparticle diffusion step at all concentration range examined in this work. The sorption of Cd^{2+} , on the other hand was controlled both by external mass transfer and intraparticle diffusion steps at all range of initial concentration. Langmuir and Dubinin-Radushkevich isotherms were applied to describe equilibrium data. The order of maximum sorption capacity in a unit of mol kg^{-1} was: Pb^{2+} (2.03) > Cu^{2+} (1.43) > Cd^{2+} (0.870). The sorption energy fell in the range of physisorption. Equilibrium sorption capacity and removal percentage were governed by both initial concentration and sorbent dose. A general mathematical model was developed for describing the sorption under the variations in initial metal concentration and zeolite doses. This model was proven to be reasonably accurate with additional sets of experiments.

Field of study: Environmental Management Student's signature Ronbanchob
 Academic year 2006 Advisor's signature Prasert Pavasant

ACKNOWLEDGEMENTS

Firstly, I would like to express my deepest gratitude to my thesis advisor, Associate Professor Dr. Prasert Pavasant, for his huge encouragement, invaluable supports, and kind guidance dedicated to me during my doctoral learning. Not only did he teach me a lot of things regarding academic knowledge he has been an impressive example and role model for me which is better than wordy teaching and these made me develop my thoughts and my characters so much. He is like a craftsman who cuts and polishes a diamond until it shines splendidly. He is not just only advisor but is one of the important persons that I respect beside my parents. This dissertation would not have been accomplished without his excellent supervision.

I would like to sincerely thank the Thailand Research Fund for their financial support for this research work via Royal Golden Jubilee Ph.D. scholarship.

In addition, I desire to thank Dr. Aticha Chaisuwan for teaching me about a fundamental chemistry of zeolite. I also thank Dr. Manaskorn Rachakornkij, Asst. Dr. Pairat Kaewsarn, Dr. Chantra Tongcumpou, Dr. Punjaporn Weschayanwiwat, and Asst. Dr. Khemarath Osathaphan for participating as my dissertation committee. Moreover, I would like to thank all anonymous editors and reviewers of my publications for the criticisms, comments, and suggestions which improved the quality of this dissertation.

Special gratitude to Banchong farm owner, Mr. Banchong Nisaphawanit and his wife at Chachoengsao province for supporting algal material and National Power Supply Co. Ltd. (Thailand) for providing coal fly ash.

Special thanks should also be directed towards my friends at the Department of Chemical Engineering, Chulalongkorn University especially Dr. Porntip Wongsuchoto (P' Poo) for their warm supports and imperative helps. Moreover, I would like to express gratitude to Miss Parichat Norranattrakul for the very nice supports for every thing during my doctoral learning such as doing some laboratory work, writing the reference, helping some discussion about the work, and especially the great will that she has continuously been giving to me.

Finally, I feel proud to dedicate this thesis with all respects to my beloved parents for their love, encouragement, and inspiration throughout my entire study.

CONTENTS

	Pages
ABSTRACT IN THAI.....	iv
ABSTRACT IN ENGLISH	v
ACKNOWLEDGEMENTS	vi
CONTENTS.....	vii
LIST OF TABLES	xi
LIST OF FIGURES	xiii
ABBREVIATIONS	xv
CHAPTER I INTRODUCTION.....	1
1.1 Motivations	1
1.2 Objectives.....	2
1.3 Scopes of this work	3
1.4 Hypotheses	3
1.5 Benefits from this work.....	3
CHAPTER II BACKGROUND AND LITERATURES REVIEW	4
PART I HEAVY METALS	4
2.1 Definition of heavy metals	4
2.2 Copper, Cadmium and Lead	4
2.3 Treatment technologies for wastewater containing heavy metals.....	6
PART II BASIC SORPTION THEORY	7
2.4 Sorption kinetics.....	8
2.5 Sorption kinetic models based on reaction order	9
2.6 Sorption kinetic models based on mechanism	11
2.7 Sorption isotherm.....	13
2.8 Parameters influencing sorption.....	16
2.8.1 Effect of sorbent dosage	16
2.8.2 Effect of sorbate initial concentrations.....	16
2.8.3 Effect of pH.....	17
2.8.4 Effect of particle size.....	19

	Pages
PART III BIOSORPTION OF HEAVY METALS	39
2.9 Definition and advantage of biosorption.....	39
2.10 Biosorbent	39
2.10.1 Chitinous biosorbent.....	39
2.10.2 Microbial biosorbent	40
2.10.3 Algal biosorbent	40
2.11 <i>Caulerpa lentillifera</i> biomass.....	41
PART IV SORPTION WITH ZEOLITE FROM COAL FLY ASH.....	43
2.12 Coal fly ash	43
2.13 Zeolite	44
2.13.1 History of zeolites	44
2.13.2 Structure of zeolites.....	45
2.13.3 Applications of zeolite.....	47
2.13.4 Formation of zeolite	48
2.13.5 Heavy metal sorption using zeolite	51
CHAPTER III RESEARCH METHODOLOGY	53
3.1 Materials.....	53
3.1.1 Equipments.....	53
3.1.2 Glassware	54
3.1.3 Chemical Reagents	54
3.2 Methodology for biosorption part	55
3.2.1 Algal collection and preparation	55
3.2.2 Glassware preparation	55
3.2.3 Preparation for synthetic wastewater	55
3.2.4 Determination of effect of particle size of sorbent on biosorption kinetics.....	56
3.2.5 Determination of effect of initial concentration and sorption isotherm	56
3.2.6 Determination of effect of pH on sorption isotherm	57
3.2.7 Study of biosorption in binary component batch system	58
3.2.8 Biosorption in fixed-bed column.....	58

	Pages
3.3 Methodology for zeolite part.....	59
3.3.1 Coal fly ash (CFA) collection and preparation	59
3.3.2 Conversion of coal fly ash to zeolite	59
3.3.3 Analysis of original coal fly ash and zeolite product	60
3.3.4 Determination for effect of initial metal concentration on sorption kinetics by zeolite.....	61
3.3.5 Determination of effect of sorbent dose on sorption kinetic by zeolite	61
3.3.6 Determination of effect of sorbent dose and sorbate initial concentration on sorption equilibrium study (Sorption isotherm study)	62
3.4 Control of Experiments	62
CHAPTER IV METAL SORPTION USING <u>CAULERPA LENTILLIFERA</u>	63
4.1 Effect of particle size on characteristic of sorption capacity-contact time	63
4.2 Sorption kinetics.....	64
4.3 Sorption isotherm	66
4.4 Energy of sorption VS Biosorption mechanism.....	68
4.5 Effect of pH.....	68
4.6 Biosorption of heavy metal in binary component and modeling	71
4.6.1 Model development for binary component systems.....	72
4.6.2 Model selection and interpretation	75
4.7 Partial competitive model in describing the effect of pH on metal sorption ...	82
4.7.1 Modified partial competitive model for prediction effect of pH.....	82
4.7.2 Prediction of q_{max} and b	85
4.8 Potential sorption characteristics for metal sorption.....	89
4.9 Biosorption in fixed bed column.....	91
4.10 Metal release VS Biosorption mechanism	97
4.11 Concluding remarks	100

	Pages
CHAPTER V ZEOLITE FORMATION AND UTILIZATION FOR METAL SORPTION	101
5.1 Effect of NaOH:CFA	101
5.2 Sorbent characterization.....	102
5.3 Effect of initial concentration on sorption kinetics	105
5.4 Effect of sorbent dose on sorption kinetics	108
5.5 Mechanism in sorption kinetics	111
5.6 Sorption isotherm	115
5.7 Effect of sorbent dose and initial concentration on sorption equilibrium.....	117
5.8 Model verification.....	119
5.9 Concluding remarks	120
 CHAPTER VI COMPARISION BETWEEN <u>CAULERPA LENTILLIFERA</u> AND ZEOLITE X MODIFIED FROM COAL FLY ASH	 127
6.1 Sorption point of view.....	127
6.2 Economic point of view	128
 CHAPTER VII CONCLUSIONS AND RECOMMENDATIONS	 130
7.1 Summaries, achievements and contributions	130
7.2 Suggestions and recommendations	131
 REFERENCES	 132
APPENDICES	144
BIOGRAPHY	153

LIST OF TABLES

	Pages
Table 2.1 Basic informations for Copper, Cadmium, and Lead.....	5
Table 2.2 Effect of sorbent dose on sorption kinetics.....	20
Table 2.3 Effect of sorbent dose on sorption equilibrium	22
Table 2.4 Effect of sorbate initial concentration on sorption kinetics	25
Table 2.5 Effect of sorbate initial concentration on sorption equilibrium.....	28
Table 2.6 Effect pH on sorption kinetics	30
Table 2.7 Effect pH on sorption equilibriums	32
Table 2.8 Effect particle size on sorption kinetics	35
Table 2.9 Effect particle size on sorption equilibriums	37
Table 2.10 Conversion of ash to zeolite.....	49
Table 2.11 Metal sorption by various types of zeolite.....	52
Table 4.1 Model parameters for the sorption of various metals	65
Table 4.2 Isotherm parameters.....	67
Table 4.3 Comparison between maximum sorption capacities (q_{max}) for various sorbents.....	67
Table 4.4 Effect of pH on Langmuir isotherm parameters for metal ion sorption by dried <i>Caulerpa lentillifera</i>	69
Table 4.5 Parameters of binary sorption isotherms	76
Table 4.6 Percentage reduction in sorption capacity of primary metal ion with the presence of secondary metal ion	78
Table 4.7 Parameters of the pH prediction model*	83
Table 4.8 Details of functional groups involved with metal biosorption by <i>Caulerpa lentillifera</i>	90
Table 4.9 Fixed bed biosorption parameters.....	94
Table 4.10 Relationship between heavy metal uptake and metal release during biosorption.....	98

	Pages
Table 5.1 Elemental composition of zeolite (amount in % by weight)	102
Table 5.2 Sorption kinetic parameters (C_0 range of 0 – 5 mol m ⁻³).....	106
Table 5.3 Sorption kinetic parameters (sorbent dose range of 0.5 – 3 g L ⁻¹).....	109
Table 5.4 Sorption kinetic parameters based on reaction mechanism.....	112
Table 5.5 Sorption isotherm.....	115
Table 5.6 Parameters for model verification.....	121
Table 5.7 Maximum sorption capacities for heavy metals of various sorbents.....	122
Table 6.1 Summary of maximum sorption capacity of the two sorbents	128
Table 6.2 Estimated cost of 1 kg <i>Caulerpa lentillifera</i>	128
Table 6.3 Estimated cost of 1 kg Zeolite X modified from CFA	129



สถาบันวิทยบริการ
จุฬาลงกรณ์มหาวิทยาลัย

LIST OF FIGURES

	Pages
Figure 2.1 Overall sorption mechanism.....	8
Figure 2.2 <i>Caulerpa lentillifera</i> biomass.....	42
Figure 2.3 Primary Building Unit (Tetrahedral Unit) of Zeolite.....	45
Figure 2.4 Negative charge in PBU frame work of zeolite.....	45
Figure 2.5 Secondary Building Unit (SBU) of Zeolite.....	46
Figure 4.1 Effect of contact time on sorption capacity.....	63
Figure 4.2 Weber-Morris kinetic model for metals sorption by <i>Caulerpa lentillifera</i>	65
Figure 4.3 Sips and Langmuir isotherm plots for metal ion sorptions by <i>Caulerpa lentillifera</i>	67
Figure 4.4 Effect of pH on sorption isotherms	70
Figure 4.5 Three-dimensional sorption isotherm surface for Pb^{2+} - Cu^{2+} system.....	79
Figure 4.6 Three-dimensional sorption isotherm surface for Pb^{2+} - Cd^{2+} system.....	80
Figure 4.7 Three-dimensional sorption isotherm surface for Cu^{2+} - Cd^{2+} system	81
Figure 4.8 Effect of pH on equilibrium sorption capacity on <i>Caulerpa lentillifera</i> ..	84
Figure 4.9 Relationships between maximum sorption capacity (q_{max}) and pH	87
Figure 4.10 Relationships between sorption affinity (b) and pH.....	88
Figure 4.11 Effect of bed depth on breakthrough curve	95
Figure 4.12 Effect of flow rate on breakthrough curve	96
Figure 4.13 Amounts of metal ions released during the column sorption experiment	99

	Pages
Figure 5.1 Effect of NaOH:CFA ratio on CEC.....	101
Figure 5.2 XRD characteristic peak of original CFA and obtained zeolite.....	103
Figure 5.3 SEM micrograph of original CFA and obtained zeolite.....	103
Figure 5.4 Particle size distribution of zeolite	104
Figure 5.5 Relationship between surface charge of zeolite and pH.....	104
Figure 5.6 Relationship between contact time and sorption capacity (q) at various concentration using sorbent dose of 1 g L^{-1}	107
Figure 5.7 Relationship between contact time and sorption capacity (q) at various sorbent dose using initial concentration of 5 mol m^{-3}	110
Figure 5.8 Sorption isotherm with kinetic tracking plots	116
Figure 5.9 Relationship between sorption parameters (q_e and %Removal) of Pb^{2+} and operating parameters (C_o and X_o)	123
Figure 5.10 Relationship between sorption parameters (q_e and %Removal) of Cu^{2+} and operating parameters (C_o and X_o).....	124
Figure 5.11 Relationship between sorption parameters (q_e and %Removal) of Cd^{2+} and operating parameters (C_o and X_o).....	125
Figure 5.12 Accuracy of the models prediction.....	126

ABBREVIATIONS

A	=	cross sectional area of column
AAS	=	Atomic Absorption Spectrophotometer
A_s	=	specific surface area of biomass
b	=	affinity for the single component system
b'	=	affinity constant for the simultaneously bonding of two metals with the same binding site
B	=	free binding site
$b(\text{pH})$	=	affinity for the single component system as a function of pH
b_{HM}	=	affinity constant of the metal ion on the protonated binding site
b_{M}	=	affinity constants for metal 'M' (primary component) = $1/K_{\text{M}}$
BM	=	binding site occupied with metal 'M'
b_{MH}	=	sorption affinity of proton on the binding site already occupied by metal ion
b_{MN}	=	affinity constant for the bonding of metal 'N' with the binding site already occupied with metal 'M'
BMN	=	binding site simultaneously occupied with metals 'M' and 'N'
b_{N}	=	affinity constants for metal 'N' (secondary component) = $1/K_{\text{N}}$
BN	=	binding site occupied with metal 'N'
b_{NM}	=	affinity constant for the bonding of metal 'M' with the binding site already occupied with metal 'N'
B_t	=	total binding site
C or C_f	=	sorbate concentration after sorption (liquid phase)
C_e	=	equilibrium concentrations
C_e	=	sorbate equilibrium concentration after sorption (liquid phase)
$C_e[\text{M}]$	=	equilibrium concentration of metal 'M' (primary component)
$C_e[\text{N}]$	=	equilibrium concentration of metal 'N' (secondary component)
CEC	=	cation exchange capacity
C_{eff}	=	effluent concentration as a function of time.
CFA	=	coal fly ash
C_o	=	initial sorbate concentration (liquid phase)
C_s	=	concentration of sorbate at the surface of sorbent

C_t	=	sorbate concentration at time 't' (liquid phase)
D, D_e	=	effective diffusion coefficient
DI	=	deionized
d_p	=	mean particle diameter
E	=	mean sorption energy
\bar{E}	=	average of error from all experimental data
E_i	=	error at point i
g	=	gram
h	=	hour
h	=	initial sorption rate
HSAB	=	hard and soft acid base
I	=	intercept of sorption capacity axis (Eq. 2.15)
ICP	=	Inductively Coupled Plasma
K	=	equilibrium constant for the simultaneously bonding of two metals with the same binding site
k_1	=	the pseudo-first order rate constant
k_2	=	the pseudo-second order rate constant
K_a	=	acid dissociation equilibrium constant of binding site
k_{ads}	=	adsorption rate constant
K_{ads}	=	Langmuir sorption rate constant
k_{des}	=	desorption rate constant
K_f	=	Freundlich constant
kg	=	kilogram
kJ	=	kilojoule
K_L	=	liquid-solid external mass transfer coefficient
K_M	=	equilibrium constant of the binding site which bonding with metal 'M'
K_{MN}	=	equilibrium constant for the bonding of metal 'N' with the binding site already occupied with metal 'M'
K_N	=	equilibrium constant of the binding site which bonding with metal 'N'
K_{NM}	=	equilibrium constant for the bonding of metal 'M' with the binding site already occupied with metal 'N'
K_p	=	linear equilibrium partition coefficient

k_{TH}	=	Thomas rate constant
K_{WM}	=	Weber and Morris intraparticle diffusion rate
L	=	litre
L	=	bed height of column
L_{min}	=	depth the column required to reach the breakthrough immediately after operated
M	=	first sorbate component (metal ion) in the solution
m	=	mass of sorbent
m^3	=	cubic metre
$m_{biomass}$	=	mass of biomass (kg)
m_{eff}	=	total mass of metal released from the fixed-bed column
meq	=	milliequivalent
mg	=	milligram
min	=	minute
mL	=	millilitre
mM	=	millimolar
mmol	=	millimole
mol	=	mole
m_{pore}	=	total mass of metal left in the pore of biomass bed that was not uptaken
MTZ	=	mass transfer zone
n	=	Freundlich exponent
N	=	number of the experimental data.
N	=	second sorbate component (metal ion) in the solution
n_s	=	Sips exponent
PBU	=	primary building unit
q	=	sorption capacity
\bar{q}	=	average of actual sorption capacity from total experimental data
Q	=	volumetric flow-rate
$q[M]$	=	sorption capacity of metal 'M' (primary component)
$q[M+N]$	=	sum of sorption capacity of the two metal components
$q[N]$	=	sorption capacity of metal 'N' (secondary component)
$q_{c,i}$	=	calculated sorption capacity datum at point i
q_e	=	equilibrium sorption capacity (solid phase phase)

q_i	=	actual sorption capacity experimental datum at point i
q_m	=	maximum sorption capacity for the binary components system
q_{\max}	=	maximum sorption capacity for the single component system
$q_{\max}(\text{pH})$	=	maximum sorption capacity for the single component system as a function of pH
$q_{\max, \text{HM}}$	=	maximum sorption capacity of metal ion on protonated binding site
$q_{\max, \text{M}}$	=	maximum sorption capacity of metal ion on unprotonated binding site
q_{mc}	=	maximum metal sorption capacity calculated from Thomas model
R^2	=	determination coefficient
r_f	=	retardation factor
R_g	=	universal gas constant ($8.314 \times 10^{-3} \text{ kJ mol}^{-1} \text{ K}^{-1}$)
rpm	=	round per minute
SBU	=	secondary building unit
t	=	sorption time
T	=	temperature
$t_{50\%}$	=	time require $C_{\text{eff}}/C_o = 0.5$
t_b	=	breakthrough time
t_e	=	exhaust time
TLV	=	threshold limit value
u	=	superficial velocity
u_{pw}	=	pore water velocity
V	=	volume of solution
V_b	=	breakthrough volumn
V_v	=	void volume (m3)
X_o	=	sorbent dose
β	=	activity coefficient of Dubinin-Radushkevich isotherm model
ε	=	porosity
μm	=	micrometer
ρ_b	=	bulk density of the biomass
ρ_p	=	packing density

CHAPTER I

INTRODUCTION

1.1 Motivations

Heavy metals are among the major concerns in wastewater treatment. Heavy metals are often derived from heavy industries, such as electroplating and battery factories. The treatment of this type of wastewater involves high cost techniques. Sorption with a low cost sorbent has lately been introduced as an alternative treatment technique for this type of wastewater. Often the new development involves the transformation of unused materials into sorbents. For instance, agricultural wastes, i.e. corn cob, soybean hull, and sunflower stalks have been shown to be cheap and good sorbents in the removal of heavy metal ions (Cu^{2+} , Zn^{2+} and Ni^{2+}) (Sanguanduan, 2002) and the industrial waste such as cement kiln dust could also be used as low cost sorbents for sequestering heavy metal ions (Cu^{2+} , Ni^{2+} , Pb^{2+} , Cd^{2+} and Co^{2+}) from aqueous solutions (Pigaga et al., 2005).

Caulerpa lentillifera is a marine macro alga commonly found in culture ponds. It uptakes and keeps a balance of nitrogen compounds in the culture systems such as shrimp farms (Chokwiwattanawanit, 2000). However, its rapid growth necessitates a regular removal of the excess quantity. Previous works (Sungkum, 2002, Apiratikul, 2003 and Suthiparinyanont, 2003) illustrated the possibility of using this agricultural waste for the biosorption of positively charged contaminants such as heavy metals in an aqueous solution. Therefore, turning this unwanted agricultural waste into a viable sorbent presents a potential solution to the management of solid waste, the research area which has gained significant attention in recent years.

Coal fly ash (CFA) from industrial processes is considered waste which requires a regular management including transportation, and a disposal of such waste to landfill generally necessitates a costly investment not to mention the requirement of land for the landfill. A conversion of CFA to something useful has always obtained research interest. Zeolite is among the common product derivatives from CFA as CFA often is constituted of silica and alumina at high content and these two components are the basic foundation in the formation of zeolite.

This work intended to utilize agricultural and industrial wastes as low cost sorbent in the removal of heavy metal ions from the wastewater. For agricultural waste, this investigation extended from the previous works by Sungkum (2002), Apiratikul (2003) and Suthiparinyanont (2003) for which *Caulerpa lentillifera* was employed as a source of biosorbent. The work not only focused rigorously on the mechanism of sorption of heavy metals by such sorbent, but also it included the aspect of binary sorption in more detail where a proper isotherm model for such system was proposed. For the industrial waste, coal fly ash was employed as a model system. A preliminary work was conducted to investigate the possibility in the conversion of coal fly ash to zeolite with high cation exchange capacity, and the potential in using the zeolite product to sequester heavy metals was examined. Characteristics of sorbents and fundamentals for the sorption of heavy metals were thoroughly investigated.

1.2 Objectives

The main objective of this research was to investigate the utilization of *Caulerpa lentillifera* biomass and zeolite from CFA in the removal of Cu^{2+} , Cd^{2+} and Pb^{2+} from aqueous solution (synthetic waste) by sorption process. The sub-objectives are as follows:

For algal biosorbent part:

- to determine the mechanism of metal removal by *Caulerpa lentillifera* biomass
- to determine the efficiency of *Caulerpa lentillifera* biomass for removal of heavy metal ions from aqueous solution.

For zeolite part:

- to study the feasibility of utilizing CFA as sources of silica and alumina for zeolite synthesis using the fusion method
- to determine the mechanism of metal removal by zeolite obtained from CFA
- to determine the efficiency of the zeolite for removal of heavy metal from aqueous solution and compare with *Caulerpa lentillifera*.

1.3 Scopes of this work

For algal biosorbent part:

- *Caulerpa lentillifera* biomass from Banchong farm, Chachoengsao province, was selected as biosorbent.
- Heavy metal ions of interests were Cu^{2+} , Cd^{2+} and Pb^{2+} .
- The pH range for the dissolution of heavy metal ions was 1.5 – 5.

For zeolite part:

- CFA from National Power Supply Co. Ltd. was employed as raw material.
- Zeolites were synthesized using the fusion method according to method of Molina and Poole (2004).
- Heavy metal ions of interests were Cu^{2+} , Cd^{2+} and Pb^{2+} .
- Sorption experiments were conducted only in batch scale.

1.4 Hypotheses

- The algal biomass and the zeolite from CFA could remove heavy metal ions in aqueous solution.
- The fusion method could produce zeolite which has high cation exchange capacity.

1.5 Benefits from this work

The results from this research facilitated the understanding of the sorption behavior for the heavy metals and lead to a better design of the sorption system for the actual wastewater treatment. Furthermore, this work also provided the criteria in obtaining zeolite with high cation exchange capacity by the fusion method which can be used as effective ion exchanger for metal removal in wastewater. The outcome of this work could simultaneously solve two environmental problems. Firstly, agricultural and industrial wastes were reduced since they were utilized to the sorbent. Secondly, the heavy metal wastewater could be purified by the inexpensive sorbent obtained from unwanted raw materials.

CHAPTER II

BACKGROUND AND LITERATURES REVIEW

PART I HEAVY METALS

2.1 Definition of heavy metals

The word “heavy metal” is widely used and does not have strict definition. Many authors defined heavy metals as metals which have specific gravities greater than five (Sengupta, 2002; Tan, 2000; Wild, 1993). Some definitions stated that heavy metals included the elements in periodic table with atomic number between 21 and 84 excluding metals in Lanthanide series (Kaewsarn, 2000), and some reported that heavy metals should include those metals with atomic number higher than 26 (Kojima and Lee, 2001). In an environmental point of view, heavy metals refer to toxic elements which are harmful to creature and environment. However, it is generally known that some of these toxic elements such as copper, manganese, zinc, etc. are essential in tiny quantity for the growth of living cells, and they will only be harmful when present in great quantity.

2.2 Copper, Cadmium and Lead

Copper is a nice reddish metal which is malleable, ductile, and an extremely good conductor of both heat and electricity. It is softer than iron but harder than zinc and can be polished to a bright finish. It is used in many applications as followings: 1) Electronic apparatus such as electrical cables, electrical wires and switches, 2) Building construction such as plumbing and roofing, 3) Industrial equipments such as heavy exchanger and alloy castings, electroplated protective. Copper can dissolve in nitric acid and hot concentrated sulfuric acid, dissolve slowly in hydrochloric and dilutes sulfuric acid but only when exposed to the atmosphere. The toxicity of metallic copper is very low. However, many copper (II) salts can cause adverse health effects such as they are destructive to membranes and cause nausea vomiting, stomachaches, dizziness and diarrhea. Intentionally high uptakes of copper may cause liver and kidney damage and even death.

Cadmium is a lustrous, silver-white, ductile, very malleable metal. Its surface has a bluish tinge and the metal is soft enough to be cut with a knife, but it tarnishes in

air. It can be soluble in acids, especially nitric acid, but insoluble in alkalis. Mainly, it is used in battery industry, coatings and plating, and stabilizers for plastics. Furthermore, it can be used as a barrier in controlling nuclear fission since it can absorb proton. Cadmium can cause many adverse effects including the destruction of lung and kidney functions, diarrhea, stomach pains and severe vomiting, bone fracture, reproductive failure and possibly even infertility, damage to the central nervous system, damage to the immune system, and finally possibly DNA damage or cancer development.

Lead is a bluish-white lustrous metal. It is very soft, highly malleable, ductile, and poor electrical conductivity. It has been used widely since 5000 BC for application in metal products, battery, cables and pipelines, alloys, electroplating, and also in paints and pesticides industries. In addition, it can be used in many industries such as, dye and pigment, etc. In the past, tetraethyl lead was used in gasoline to increase octane number. Lead can cause many adverse effects such as disruption of the biosynthesis of haemoglobin and anaemia, rising in blood pressure, kidney damage, miscarriages and subtle abortions, disruption of nervous systems and brain damage, declined fertility of men through sperm damage, and diminished learning abilities of children.

Table 2.1 Basic informations for Copper, Cadmium, and Lead.

Metal symbol Data	Cu	Cd	Pb
Atomic number	29	48	82
Atomic weight	63.546	112.4	207.2
Periodic Table	group IB	group IIB	group IVA
Oxidation states	+1, +2	+2	+2, +4
Vanderwaals diameter	2.56 Å	3.08 Å	3.08 Å
Ionic diameter	1.92 Å (+1) 1.38 Å (+2)	1.94 Å (+2)	2.64 Å (+2) 1.68 Å (+4)
Specific gravity	8.96 at 20°C	8.65 at 20°C	11.35 at 20°C
Melting point	1083°C at 1 atm	320.9°C at 1 atm	327.4°C at 1 atm
Boiling point	2595°C at 1 atm	765°C at 1 atm	1755°C at 1 atm
Method of Analysis	AAS or ICP	AAS or ICP	AAS or ICP
TLV	1 mg m ⁻³	0.05 mg m ⁻³	0.05 mg m ⁻³
Standard value for industrial effluent*	< 2 mg L ⁻¹	< 0.03 mg L ⁻¹	< 0.2 mg L ⁻¹

*Notification of the Ministry of Science, Technology and Environment, No. 3 B.E. 2539 (1996) issued under the Enhancement and Conservation of the National Environmental Quality Act B.E. 2535 (1992), published in the Royal Government Gazette, Vol. 113 Part 13-D, dated February 13, B.E. 2539 (1996).

2.3 Treatment technologies for wastewater containing heavy metals

There are a lot of treatment technologies for heavy metal including precipitation, electrolytic recovery, membrane separation, ion exchange, evaporation, carbon adsorption, and biosorption (Sungkum, 2002). These techniques except biosorption have more efficiency with the wastewater containing high concentration of heavy metal. In contrast, if the concentration of heavy metals is low (e.g. less than 100 mg L⁻¹), the relatively high cost will render these techniques unattractive. Also, some of the treatment techniques were less effective for wastewater containing low level of heavy metals. Biosorption is perhaps the most economical treatment method compared with other techniques (Banerjee, 2000) and suitable with the wastewater containing heavy metal concentration lower than 100 mg L⁻¹ (Volesky, 1990).



สถาบันวิทยบริการ
จุฬาลงกรณ์มหาวิทยาลัย

PART II BASIC SORPTION THEORY

The sorption is fundamentally the attachment of one type of material onto surface of another material type. The materials that are sorbed are called sorbate whereas the sorbent is the sorbing species. Examples of sorbents include activated carbon (AC), silica gel, alumina, fly ash, zeolite, biomass etc. The sorption can be occurred by two mechanisms, adsorption and ion exchange. In this work, adsorption is a process which heavy metal ions adhere to binding site on solid surface of sorbent without releasing other positive charge ions which are already previously attached on the binding site. Ion exchange is a process that heavy metal ions located in the solution replace the cations located in the sorbent.

The binding forces associated with the sorption process can be used to categorize the type of sorption. The sorption process occurred due to physical forces is defined as physical sorption or physisorption. On the other hand, the sorption process due to chemical forces is called chemical sorption or chemisorption. Sorption can also occur due to the combination of both physical and chemical forces. Physical sorption mainly involved with two types of physical forces. One is electrostatic or Coulombic force and the other is London force. The chemical sorption generally involved with the covalent bonding such as the metal complexation and chelation by the binding site of sorbent. The sorption energy of chemical sorption is higher than that of physical sorption.

The efficiency of sorption is generally indicated by the sorption capacity (q) which can be calculated from following:

$$q = \frac{V}{m}(C_o - C_f) = \frac{C_o - C_f}{X_o} \quad (2.1)$$

where q represents the amount of metal uptaken per unit mass of the biomass (mol kg^{-1}), V the volume of the solution (m^3), m the dry mass of the algae (kg), X_o the sorbent concentration or sorbent dose (kg m^{-3}), C_o and C_f the initial and final concentrations (mol m^{-3}), respectively.

2.4 Sorption kinetics

The sorption kinetics is the study of the changes in the time course of sorption characteristics under the same operating conditions. Generally the sorption includes 4 steps as follows:

- 1) Sorbate transfers from bulk solution to boundary film (Fig. 2.1 (a)).
- 2) Sorbate transfers from the boundary film to surface of sorbent (external mass transfer step) (Fig. 2.1 (b)).
- 3) Sorbate transfers from the sorbent surface to intraparticle active site or binding site (intraparticle diffusion step) (Fig. 2.1 (c))
- 4) Sorption of the sorbate on the active site or binding site of sorbent (Fig. 2.1 (d))

However, Steps 1 and 4 generally rapidly occur and do not consider as the rate limiting steps while the slower Steps 3 and/or 4 are mainly considered as rate limiting step(s).

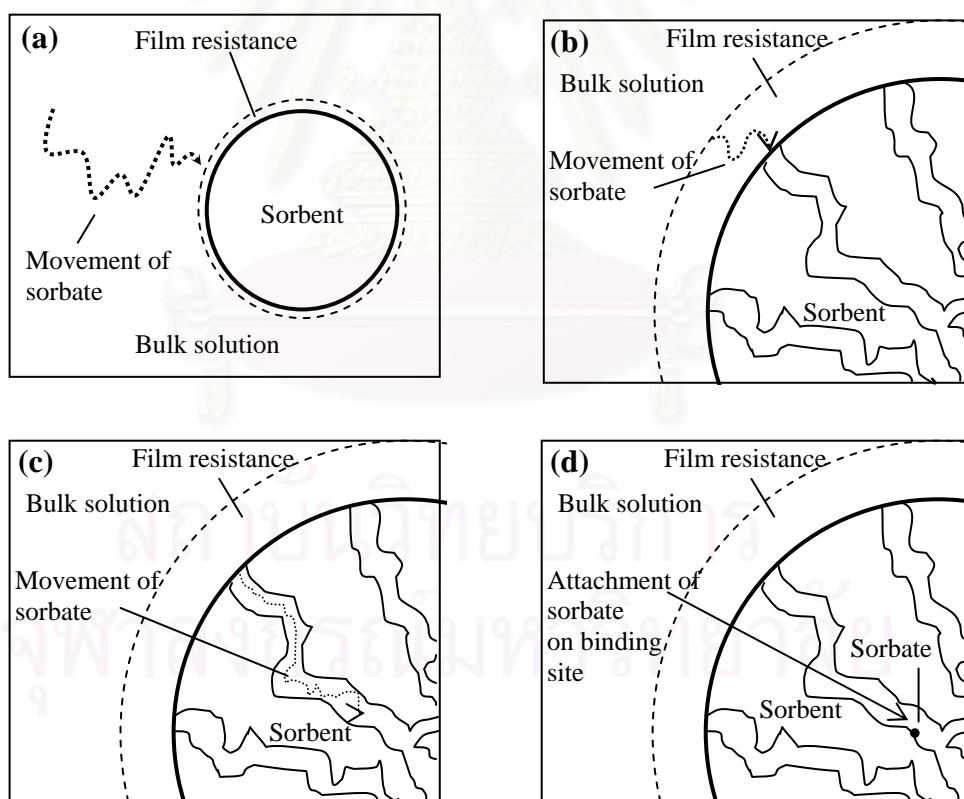


Figure 2.1 Overall sorption mechanism

The data on kinetics such as sorption rate, rate limiting step(s), and equilibrium time are important in sorption system design.

2.5 Sorption kinetic models based on reaction order

Sorption kinetic models based on reaction order are proposed which are further used to determine the time to reach equilibrium and initial sorption rate. These models can be separated into two groups, concentration based model and sorption capacity based model.

Examples of the concentration based models are the first and second order models which are following:

First order model:

$$\frac{dC}{dt} = kC \quad (2.2)$$

Integrating Eq. 2.2 from $t = 0$ to $t = t$ and $C = 0$ to $C = C$ and rearranging the equation gives:

$$\ln \frac{C}{C_o} = kt \quad (2.3)$$

Second order model:

$$\frac{dC}{dt} = k'C^2 \quad (2.4)$$

Integrating Eq. 2.4 from $t = 0$ to $t = t$ and $C = 0$ to $C = C$ and rearranging the equation gives:

$$\frac{1}{C} = \frac{1}{C_o} + k't \quad (2.5)$$

where C is the concentration at time ' t ' (mol m^{-3}), C_o the initial concentration (mol m^{-3}), t the contact time (min), k (min^{-1}) and k' ($\text{m}^3 \text{mol}^{-1} \text{min}^{-1}$) the first and second order rate constants, respectively, of the concentration based kinetic model.

However, the two models based on concentration are not as frequently used in sorption kinetic study as the sorption capacity based models.

The first sorption capacity based model was based on pseudo-first order assumption developed by Lagergren (1898) who studied liquid–solid phase sorption of oxalic acid and malonic acid onto charcoal. The model can be expressed in Eq. (2.6).

$$\frac{dq}{dt} = k_1(q_e - q) \quad (2.6)$$

Integrating Eq. 2.6 from $t = 0$ to $t = t$ and $q = 0$ to $q = q$ and rearranging the equation gives:

$$q = q_e(1 - e^{-k_1 t}) \quad (2.7)$$

Another sorption capacity based model was pseudo-second order rate equation which was firstly used for describing the sorption kinetics of divalent metal onto peat biomass by Ho (1995). In order to distinguish between the first and second order kinetic concentration based and sorption capacity based models, Ho's kinetic model was named as pseudo-second order model which can be expressed as:

$$\frac{dq}{dt} = k_2(q_e - q)^2 \quad (2.8)$$

Integrating Eq. 2.8 from $t = 0$ to $t = t$ and $q = 0$ to $q = q$ and rearranging the equation gives:

$$q = \frac{q_e^2 k_2 t}{1 + q_e k_2 t} \quad (2.9)$$

In Eqs 2.6 – 2.9, t is the contact time (min), q the sorption capacity of metal ion at time ' t ' (mol kg⁻¹), q_e the sorption capacity at equilibrium (mol kg⁻¹), k_1 the pseudo-first order rate constant (min⁻¹), k_2 the pseudo-second order rate constant (kg mol⁻¹ min⁻¹). The assumption of pseudo-second order model was that the sorption process may follow second-order and that chemisorption occurs involving valency forces through sharing or the exchange of electrons between the peat and divalent metal ions as covalent forces (Ho, 1995).

However, Azizian (2004) reported that the pseudo-first and pseudo-second order models previously derived and used by Ho and all of researchers in the literatures had, in fact, different applications. He proved that any sorption system which high initial sorbate concentration compared with the amount of sorbate sorbed on sorbent per volume of solution seemed to prefer pseudo-first order kinetic models and the pseudo-first order rate constant is the linear function of initial concentration. In case of the sorbate with moderate or low initial concentration, the sorption kinetics seemed to obey the pseudo-second order and the pseudo-second order rate constant is a complex function of initial concentration. This illustrated that fitting with first or second order kinetic did not involve with the physical or chemical sorptions as the sorption mechanism.

2.6 Sorption kinetic models based on mechanism

The kinetic models based on mechanism are useful as they allow the prediction of the performance of process system which assists in developing a better process by appropriately solving and correcting the problems.

One of important mechanistic models is the intraparticle diffusion model which is represented by the following partial differential equation:

$$\frac{\partial C}{\partial t} = D_e \left(\frac{\partial^2 C}{\partial r^2} + \frac{2}{r} \frac{\partial C}{\partial r} \right) \quad (2.10)$$

One of the closed form solutions of Eq. 2.10 was given by Boyd et al. (1947) in infinite series as shown in Eq. 2.11:

$$q = q_e \left(1 - \frac{6}{\pi^2} \sum_{n=1}^{\infty} \frac{\exp\left(-\frac{4n^2 \pi^2 D_e t}{d_p^2}\right)}{n^2} \right) \quad (2.11)$$

The approximation of the above equation for the whole range of operating time proposed by Vermeulen (1953) was:

$$q = q_e \sqrt{1 - \exp\left(-\frac{4\pi^2 D_e t}{d_p^2}\right)} \quad (2.12)$$

During the early stage (t approaches zero), the term $-\frac{4\pi^2 D_e t}{d_p^2}$ can be approximated to zero. Hence, the Vermeulen's equation can be simplified using basic knowledge of Taylor series leading to:

$$q = q_e \sqrt{\frac{4\pi^2 D_e t}{d_p^2}} = \frac{2q_e \pi \sqrt{D_e}}{d_p} \sqrt{t} \quad (2.13)$$

In Eqs. 2.10 – 2.13, t is the contact time (min), q the sorption capacity of metal ion at time ' t ' (mol kg⁻¹), q_e the sorption capacity at equilibrium (mol kg⁻¹), D_e the effective diffusion coefficient (m² min⁻¹), d_p the mean particle diameter (m).

Eq. 2.13 is consistent with Weber and Morris sorption kinetic model (Weber and Morris, 1962) as expressed in Eq. 2.14. This model was often employed to investigate the sorption kinetic mechanism:

$$q = K_{WM} \sqrt{t} \quad (2.14)$$

where q is the sorption capacity at time ' t ' (mol kg^{-1}), K_{WM} the Weber and Morris intraparticle diffusion rate ($\text{mol kg}^{-1} \text{min}^{-0.5}$), and t the contact time of biomass in the heavy metal ion solution (min). The exhibited y-axis interception (sorption capacity axis) could be interpreted that the sorption kinetic process was regulated by two main mechanisms, i.e. intraparticle diffusion and external mass transfer. The Weber and Morris intraparticle diffusion rate (K_{WM}) can be calculated from

$$q = I + K_{WM} \sqrt{t} \quad (2.15)$$

where I is the intercept of vertical axis (same unit with q), $I = 0$ can be interpreted that only intraparticle diffusion considered as rate limiting step while $I > 0$ mean both external mass transfer and intraparticle diffusion considered as rate limiting step (Acemioglu, 2004, Kalavathy, 2005, Shen and Duvnjak, 2005, Önal, 2006 and Srivastava, In Press). In addition, the slope of the plot of q vs \sqrt{t} could also be attributed to the various types of pore in sorbent, i.e. macropore, mesopore, and micropore (Allen et al., 1989).

The intraparticle diffusion coefficient can be calculated by comparing the coefficient of square root of time in Eq. 2.13 and Eq. 2.14 then rearranges the relation to obtain diffusion coefficient as shown in Eq. 2.16.

$$D = \left(\frac{d_p K_{WM}}{2q_e \pi} \right)^2 \quad (2.16)$$

However, a slightly different quantitative correlation was proposed by Crank in 1975 as in Eq. 2.17.

$$D = \pi \left(\frac{d_p K_{WM}}{12q_e} \right)^2 \quad (2.17)$$

In addition, Crank (1975) proposed the equation to determine the sorption capacity at infinite time (q approach to q_e) as Eq. 2.18.

$$q = q_e \left(1 - \frac{6}{\pi^2} e^{-\frac{4\pi^2 D_e t}{d_p^2}} \right) \quad (2.18)$$

Another important process involved with sorption mechanism is the external mass transfer process which can be calculated from:

$$\frac{dq}{dt} = K_L A_s (C - C_s) \quad (2.19)$$

where K_L is the liquid-solid external mass transfer coefficient (m s^{-1}), A_s the specific surface area of biomass ($\text{m}^2 \text{kg}^{-1}$), C the liquid phase concentration of sorbate at time ' t ' in the bulk solution (mol m^{-3}), and C_s the concentration of sorbate at the surface of sorbent (mol m^{-3}). The parameter K_L can be determined using limit theorem as:

$$\lim_{t \rightarrow 0} \frac{dq}{dt} = \lim_{t \rightarrow 0} K_L A_s (C - C_s) \quad (2.20)$$

At $t=0$, C approaches C_o and C_s approaches zero and therefore:

$$K_L = \frac{\lim_{t \rightarrow 0} \frac{dq}{dt}}{A_s C_o} = \frac{h}{A_s C_o} \quad (2.21)$$

where C_o is the initial concentration used (mol m^{-3}), and h the initial sorption rate ($\text{mol kg}^{-1} \text{min}^{-1}$) which can be determined from initial slope of the relationship between q and t using pseudo-first or pseudo-second order kinetic models (Eqs. 2.6 and 2.8). Hence, h is equal to $q_e k_1$ and $q_e^2 k_2$ for sorption that fits pseudo-first and pseudo-second kinetic model, respectively. The specific surface area (A_s , $\text{m}^2 \text{kg}^{-1}$) can be calculated using the following equation:

$$A_s = \frac{6}{\rho_b d_p} \quad (2.22)$$

where ρ_b is the bulk density of the biomass (kg m^{-3}) and d_p the average particle diameter (m).

2.7 Sorption isotherm

Sorption isotherm is the relationship between sorption capacity and sorbate concentration at equilibrium and constant temperature. The sorption isotherm is the most favorite criterion in evaluation of sorption efficiency and used as basic information in designing the sorption system. There are two methods for the determination of the sorption isotherm, (i) by varying sorbate concentration and fix sorbent concentration, and (ii) by varying sorbent concentration and fix sorbate concentration then completely mix the sorbate and sorbent together until the system approaches its equilibrium where the time to reach equilibrium is obtained from the kinetic study.

Generally the isotherms can be presented by mathematical models. The first model was linear isotherm which can be derived according to Davidson and McDougal (1973) as following:

$$\frac{dq}{dt} = k_{ads} \frac{\varepsilon}{\rho_b} C - k_{des} q \quad (2.23)$$

At equilibrium $\frac{dq}{dt} = 0$, $C = C_e$, $q = q_e$ thus

$$q_e = \frac{k_{ads}}{k_{des}} \frac{\varepsilon}{\rho_b} C_e = K_p C_e \quad (2.24)$$

However, the linear isotherm is only suitable for the case of low concentration.

The next frequently used isotherm is Freundlich isotherm proposed by Freundlich, the German chemist, in 1907 (Freundlich, 1907). The isotherm can be derived according to Davidson and McDougal (1973) as following:

$$\frac{dq}{dt} = k_{ads} \frac{\varepsilon}{\rho_b} C^n - k_{des} q \quad (2.25)$$

At equilibrium $\frac{dq}{dt} = 0$, $C = C_e$, $q = q_e$ thus

$$q_e = \frac{k_{ads}}{k_{des}} \frac{\varepsilon}{\rho_b} C_e^n = K_f C_e^n \quad (2.26)$$

In Eqs. 2.23 – 2.26, q and C are sorption capacity (mol kg^{-1}) and concentration (mol m^{-3}) at time ' t ', respectively. q_e and C_e are sorption capacity (mol kg^{-1}) and concentration (mol m^{-3}) at equilibrium, respectively. t is contact time (min), k_{ads} and k_{des} are the sorption and desorption rate constants (min^{-1}), respectively, ρ_b the bulk density (kg m^{-3}), ε the porosity (no unit), K_p the linear equilibrium partition coefficient ($\text{m}^3 \text{kg}^{-1}$), K_f the Freundlich constant ($\text{mol}^{1-n} \text{m}^3 \text{kg}^{-n}$), n the Freundlich exponent (no unit).

The Freundlich isotherm is widely used as it can explain sorption at a higher range of concentration than the linear isotherm. However, Freundlich isotherm is still only suitable for moderate concentration due to the fact that, at high concentration, the binding is limited and the sorption capacity can no longer increase with the concentration.

Langmuir isotherm (Langmuir, 1918) is the one of the most important models which is also frequently used, like Freundlich isotherm. At the beginning, the two isotherms were used with the sorption of gas on the solid phase and were subsequently applied with sorption of contaminants in liquid phase on solid phase. The isotherm can

be derived according to Selim and Iskandar (1999) based on the assumption of monolayer sorption and one binding site per one sorbate as following:

$$\frac{dq}{dt} = K_{ads} C(q_m - q) - k_{des} q \quad (2.27)$$

At equilibrium $\frac{dq}{dt} = 0$, $C = C_e$, $q = q_e$ and lets $K_{ads}/k_{des} = b$ thus

$$q_e = \frac{q_{max} b C_e}{1 + b C_e} \quad (2.28)$$

The advantage of the Langmuir isotherm is that it is more realistic than linear and Freundlich isotherms as it provides a limit of sorption site while the previous isotherms do not. This good point makes the Langmuir model suitable for predicting in wider range of concentration than linear and Freundlich models. Furthermore, the parameter q_{max} is one of major criteria in evaluation of sorption efficiency.

Sips isotherm (Sips, 1948) is another interesting isotherm as it extends the Langmuir isotherm to many sorbates per one binding site. The isotherm can be derived as follows:

$$\frac{dq}{dt} = K_{ads} C^{n_s} (q_m - q) - K_{des} q \quad (2.29)$$

At equilibrium $\frac{dq}{dt} = 0$, $C = C_e$, $q = q_e$ and lets $K_{ads}/k_{des} = b$ thus

$$q_e = \frac{q_{max} b C_e^{n_s}}{1 + b C_e^{n_s}} \quad (2.30)$$

In Eqs. 2.27 – 2.30, q , q_e , C , C_e , k_{des} , and t take the same meanings as Eqs. 2.23 – 2.26, K_{ads} the Langmuir sorption rate constant ($\text{m}^3 \text{mol}^{-1} \text{min}^{-1}$), q_{max} the maximum amount of metal ion uptaken per unit mass of the biomass (mol kg^{-1}), b the affinity constant ($\text{m}^3 \text{mol}^{-1}$), n_s the Sips exponent (no unit).

The Sips isotherm can be used in wider concentration range due to the leveling off for the binding site like the Langmuir isotherm. However, the Sips isotherm has a disadvantage that it contains three fitting parameters while the Langmuir and Freundlich isotherm contain only two fitting parameters. Thus, the parameters of Sips isotherm cannot be easily determined by linear regression analysis but must be determined by non linear regression analysis.

Dubinin-Radushkevich isotherm model (Dubinin and Radushkevich, 1947) was used to estimate the sorption energy. This isotherm expression is shown in Eq. 2.31

$$q_e = q_{max} e^{\beta(R_g T \ln(1+C_e^{-1}))^2} \quad (2.31)$$

where parameters q_e , q_{max} , C_e have same meanings as those in Sips isotherm model, β the activity coefficient ($\text{mol}^2 \text{kJ}^{-2}$), R_g the universal gas constant ($8.314 \times 10^{-3} \text{kJ mol}^{-1} \text{K}^{-1}$) T the temperature (K). The activity coefficient obtained from Dubinin-Radushkevich isotherm model (β) was suggested to be related to the mean sorption energy as expressed in Eq. 2.32 (Hobson, 1969):

$$E = \frac{1}{\sqrt{-2\beta}} \quad (2.32)$$

where E represents the mean sorption energy (kJ mol^{-1}), and β the activity coefficient ($\text{mol}^2 \text{kJ}^{-2}$).

2.8 Parameters influencing sorption

There are many parameters that have significant influence on the sorption characteristics e.g. sorbent dose, sorbate initial concentrations, pH and particle size of sorbent. These are detailed in this section.

2.8.1 Effect of sorbent dosage

Effect of sorbent dose on kinetic parameters

Increasing sorbent dosage resulted in high sorption rate since the amount of availability of sorption site is increased and the sorbate can be quicker removed. However, there are few cases that sorption rate decreased when the sorbent dosage was increased as reported by Malkoc (In press). The details are concluded in Table 2.2.

Effect of sorbent dose on equilibrium parameters

The equilibrium sorption capacity was found to decrease beside the decreasing in equilibrium concentration and increasing in removal percentage when increasing in sorbent dose at the same initial concentration of sorbate. Furthermore, the time required to reach equilibrium is increased when the sorbent dosage decreased. The details are concluded in Table 2.3.

2.8.2 Effect of sorbate initial concentrations

Effect of sorbate initial concentrations on kinetic parameters

Many researchers reported the increasing in initial concentration resulted in increasing in Weber and Morris rate constant (K_{WM}) and initial sorption rate (h). Aksu and İsoğlu (2005) explained the reason of the relationship between initial concentration and initial sorption rate that the higher initial concentration provides a more important driving force to overcome all mass transfer resistance of sorbate between the aqueous and solid phases, hence, a higher initial concentration of sorbate will increase the sorption rate. There is some exception in report of Malkoc (In press) that a decrease in initial sorption rate was caused by an increase in initial concentration.

Other parameters such as diffusion coefficient (D), external mass transfer, etc. were generally found to be unknown relation between initial concentrations. Additional informations are concluded in Table 2.4.

Effect of sorbate initial concentrations on equilibrium parameters

An increase in initial concentration was found to increase the equilibrium sorption capacity in low and medium range of concentration. However, higher initial concentration was found to only slightly increase or have no effect on equilibrium sorption capacity since the increase in concentration gradient acted as an increasing driving force and also enhanced the interaction between sorbate and sorbent, leading to an increasing equilibrium sorption until sorbent saturation is achieved (Oliveira et al., 2005 and Srivastava et al., In Press).

In addition, decreasing in removal percentage was observed with an increase in initial concentration. Shukla et al. (2005) explained the reason for this phenomenon that the higher concentrations, the availability of adsorbing sites of adsorption per mass of adsorbate became fewer and hence the percentage removal of sorbate decreased.

The time to reach equilibrium was found to be independent on initial sorption capacity. Additional informations are concluded in Table 2.5.

2.8.3 Effect of pH

The pH of the solution affects the sorption process via changing in surface charge of the sorbents through dissociation of functional groups of the binding site as well as the degree of ionization and speciation of sorbate. These subsequently lead to a shift in reaction kinetics and the equilibrium characteristics of the sorption process (Elliott and Huang (1981).

Effect of pH on kinetic parameters

When the pH was increased the Weber-morris coefficient (K_{WM}) and diffusion coefficient seemed to decrease. However, the effect of pH on other sorption parameters could not be well concluded. Additional informations are concluded in Table 2.6.



สถาบันวิทยบริการ
จุฬาลงกรณ์มหาวิทยาลัย

Effect of pH on equilibrium parameters

The equilibrium sorption capacity and removal percentage were found to increase with increasing pH. However, these parameters started decreasing when the pH reached very range. This could be due to an increasing negative charged sorption site which responded for binding positive charged contaminants such as metal ions, and at a very high pH, metals could form soluble hydroxyl complexes and resulted in a decrease in sorption capacity (Shukla, 2005). Additional informations are concluded in Table 2.7.

2.8.4 Effect of particle size

Effect of particle size on kinetic parameters

Literature showed that an increase in the particle size generally led to a decreasing Pseudo-first order rate constant but increasing in external mass transfer and intraparticle diffusion coefficients. However, Pseudo-second order rate constant was generally not found to be influenced by particle size. Additional informations are concluded in Table 2.8.

Effect of particle size on equilibrium parameters

Generally, a decrease in particle size resulted in an increase in sorption capacity and removal percentage since smaller size provides the higher sorption site. However, some reported no significant changed in sorption capacity and removal percentage when the particle size was changed such as Vijayaraghavan et al. (2006). In addition, the time to reach equilibrium is often found to take longer at the larger particle size. Additional informations are concluded in Table 2.9.

สถาบันวิทยบริการ
จุฬาลงกรณ์มหาวิทยาลัย

Table 2.2 Effect of sorbent dose on sorption kinetics

Sorption system (Sorbent/Sorbate)	Independent variable	Dependent variable						Control variable					References
	Dosage range of sorbent	Initial sorption rate (<i>h</i>)	<i>k₁</i> (Eq. 2.6)	<i>k₂</i> (Eq 2.8)	<i>K_{ym}</i> (Eq. 2.15)	<i>K_L</i> (Eq. 2.19)	<i>D</i> (Eq. 2.10)	<i>C_o</i>	Particle size	Agitation rate	pH	Temperature (°C)	
Palm kernel fiber / Pb ²⁺	Increase from 1.5 to 5 g L ⁻¹	Increase from 195 to 250.79 mg g ⁻¹ min ⁻¹	Not defined	Increase from 0.0859 to 0.44079 mg g ⁻¹ min ⁻¹	Not defined	Not defined	Not defined	120 mg L ⁻¹	50–60 μm	200 rpm	5	36 ± 4 .	Ho and Ofomaja , 2006
<i>Thuja orientalis</i> / Ni ²⁺	Increase from 1 to 5 g L ⁻¹	Decrease from 383.12 to 39.79 mg g ⁻¹ min ⁻¹	Decrease from 0.366 to 0.084 min ⁻¹	No general trend	Decrease from 1.151 to 0.149 mg g ⁻¹ min ^{-0.5}	Not defined	Not defined	100 mg L ⁻¹	250–500 μm	300 rpm	4	25	Malkoc, In press)
shale oil ash / dyes	Increase from 0.5 to 2 kg m ⁻³	Not defined	Not defined	Not defined	Not defined	Constant 0.25×10 ⁻⁵	Constant 1×10 ⁻¹⁰	200 mg L ⁻¹	150-250 μm	400 rpm	Not defined	25	Al-Qodah, 2000

Table 2.2 Effect of sorbent dose on sorption kinetics (cont.)

Sorption system (Sorbent/Sorbate)	Independent variable	Dependent variable		Control variable					References
	Dosage range of sorbent	initial sorption rates (h)	k_2 (Eq 2.8)	C_0	Particle size	Agitation rate	pH	Temperature °C	
Baker's yeast / Cd^{2+}	Increase from 0.1 to 2.0 g/100 mL	Increase from 1.8 to 2.41 $mg\ g^{-1}\ min^{-1}$ and fitted with $h=2.23m_s^{0.1003}$	Increase from 0.018 to $10.94\ g\ mg^{-1}\ min^{-1}$ and fitted with $k_2=2.46m_s^{2.142}$	$10\ mg\ L^{-1}$	Not defined	120 rpm	6.5	27	Vasudevan et al., 2003
Baker's yeast / Ni^{2+}	0.5 to 8 g/100 mL	Increase from 0.427 to 0.447 according to $h=0.431m_s^{0.0167}$	Increase from $3.88e-3$ to 0.124 according to $k_2=8.42 \times 10^{-3} m_s^{1.389}$	$100\ mg\ L^{-1}$	Not defined	120 rpm	6.75	Room temperature	Padmavathy et al., 2003

สถาบันวิทยบริการ
จุฬาลงกรณ์มหาวิทยาลัย

Table 2.3 Effect of sorbent dose on sorption equilibrium

Sorption system (Sorbent/Sorbate)	Independent variable	Dependent variable		Control variable						References
	Dosage range of sorbent	%Removal	q_e	C_o	Particle size	Agitation rate	pH	Temp. (°C)	Agitation times	
Rice husk ash. / Cd^{2+} , Ni^{2+} and Zn^{2+}	In creased from 1 to 15 g L ⁻¹	Increase from 3 to 30 % for Cd 8 to 43% for Ni 20 to 62 for Zn	Not defined	100 mg L ⁻¹	150.47 μm (average size)	150 rpm	6	30	5 h	Srivastava et al., 2006
<i>Thuja orientalis</i> / Ni^{2+}	Increase from 1 to 15 g L ⁻¹	Increase from 57.2 to 84.5%	Decrease from 57.47 to 16.92 mg g ⁻¹	100 mg L ⁻¹	250–500 μm	300 rpm	4	25	30 min	Malkoc, In press
palm kernel fiber / Pb^{2+}	Increase from 1 to 15 g L ⁻¹	Increase from 59.6 to 99.2% according to %Re = $m_s / (c + d m_s)$	Decrease from 47.6 to 23.8 mg L ⁻¹ according to $q_e = a m_s + b$	120 mg L ⁻¹	50–60 μm	200 rpm,	5	36 ± 4	20 min	Ho and Ofomaja , 2006

Table 2.3 Effect of sorbent dose on sorption equilibrium (cont.)

Sorption system (Sorbent/Sorbate)	Independent variable	Dependent variable		Control variable						References
	Dosage range of sorbent	%Removal	q_e	C_o	Particle size	Agitation rate	pH	Temp. (°C)	Agitation times	
mango seed kernel powder / methylene blue	Increase from 0.01 to 0.06 g / 100 mL	Increase from 61.33 to 96.17%	Decrease from 184 to 48.085 mg g ⁻¹ $m_s = 0.0003q_e / (0.0242q_e - 1)$ for solution 100 mL	100 mg L ⁻¹	60-85 mesh (BSS)	95 rpm	8	30	48 h	Kumar and Kumaran, 2005
Baker's yeast / Cd ²⁺	increase from 0.1 to 2 g / 100 mL	Not defined	decrease from 9.95 to 0.47 mg g ⁻¹ according to $q_e = 0.951m_s^{-1.0193}$ for 100 mL solution	100 mg L ⁻¹	Not defined	120 rpm	6.5	27	1500 min	Vasudevan et al., 2003

Table 2.3 Effect of sorbent dose on sorption equilibrium (cont.)

Sorption system (Sorbent/Sorbate)	Independent variable	Dependent variable		Control variable						References
	Dosage range of sorbent	Time to reach equilibrium	q_e	C_o	Particle size	Agitation rate	pH	Temp. (°C)	Agitation times	
Sorbent: Baker's yeast Sorbate: Ni ²⁺	0.5 to 8 g L ⁻¹	60 min for 0.5 – 1 g L ⁻¹ and 20-30 min for 4 – 8 g L ⁻¹	decrease from 10.48 – 1.90 mg g ⁻¹ according to $q_e = 7.15m_s^{-0.686}$	100 mg L ⁻¹	Not defined	120 rpm	6.75	Room temperature	90 min	Padmavathy et al., 2003

สถาบันวิทยบริการ
จุฬาลงกรณ์มหาวิทยาลัย

Table 2.4 Effect of sorbate initial concentration on sorption kinetics

Sorption system (Sorbent/Sorbate)	Independent variable	Dependent variable				Control variable					References
	Range of initial concentration	initial sorption rates (h)	k_1 (Eq. 2.6)	k_2 (Eq 2.8)	K_{wm} (Eq. 2.15)	Dosage of sorbent	Particle size	Agitation rate	pH	Temp. (°C)	
<i>Thuja orientalis</i> / Ni ²⁺	Increase from 50 to 400 mg L ⁻¹	Decrease from 66.22 to 58.9 mg g ⁻¹ min ⁻¹	Increase from 0.132 to 0.445 min ⁻¹	Increase from 0.194 to 0.312 g mg ⁻¹ min ⁻¹	No general trend	5 g L ⁻¹	250–500 μm	300 rpm	4	25	Malkoc, In press
Synthetic Na-rich buserite / uranyl ions	Increase from 0.28 to 11.86 μmol L ⁻¹	Increase from 0.014 to 0.606 μmol g ⁻¹ min ⁻¹	Not defined	No general trend	Not defined	Not defined	Not defined	200 rpm	4	room temperature	Montes-Hernandez and Rih, In press
H ₃ PO ₄ ⁻ activated rubber wood sawdust / Cu ²⁺	Increase from 10 to 40 ppm	No general trend	No general trend	Decrease from 0.7324 to 0.0846 g mg ⁻¹ min ⁻¹	Increase from 0.432 to 2.813 mg g ⁻¹ min ^{-0.5}	5 g L ⁻¹	74 μm	180 rpm	6	30	Kalavathy et al., 2005

Table 2.4 Effect of sorbate initial concentration on sorption kinetics (cont.)

Sorption system (Sorbent/Sorbate)	Independent variable	Dependent variable						Control variable					References
	Range of initial concentration	Initial sorption rate (h)	k_1 (Eq. 2.6)	k_2 (Eq. 2.8)	K_{vm} (Eq. 2.15)	K_L (Eq. 2.19)	D (Eq. 2.17)	Dosage of sorbent	Particle size	Agitation rate	pH	Temp. ($^{\circ}\text{C}$)	
agricultural waste sugar beet pulp / Cu^{2+}	Increase from 25 to 260 ppm	Increase from 0.8 to 1.3 $\text{mg g}^{-1} \text{min}^{-1}$	Decrease from 7.09×10^{-2} to $3.96 \times 10^{-2} \text{min}^{-1}$	Decrease from 66.61×10^{-3} to 15.12 $\times 10^{-3} \text{g mg}^{-1} \text{min}^{-1}$	Increase from 1.99 to 4.38 $\text{mg g}^{-1} \text{min}^{-0.5}$	Decrease from 17.7×10^{-2} to $4.1 \times 10^{-2} \text{cm min}^{-1}$	Not defined	1 g L^{-1}	250 μm	150 rpm	4	25	Aksu and İsoğlu, 2005
polymerized banana stem / Pb^{2+}	Increase from 10 to 100 mg L^{-1}	Not defined	Not defined	Not defined	Not defined	Not defined	increases from 1.42 $\times 10^{-8}$ to $2.12 \times 10^{-8} \text{cm}^2 \text{s}^{-1}$	2 g L^{-1}	96 μm	200 rpm	6	30	Noeline et al., 2005

Table 2.4 Effect of sorbate initial concentration on sorption kinetics (cont.)

Sorption system (Sorbent/Sorbate)	Independent variable	Dependent variable					Control variable					References
	Range of initial concentration	Initial sorption rate (h) ($\text{mg g}^{-1} \text{min}^{-1}$)	k_1 (Eq. 2.6)	k_2 (Eq. 2.8) ($\text{g mg}^{-1} \text{min}^{-1}$)	K_{wm} (Eq. 2.15) ($\text{mg g}^{-1} \text{min}^{-0.5}$)	D (Eq. 2.12) ($\text{m}^2 \text{s}^{-1}$)	Dosage of sorbent	Particle size	Agitation rate	pH	Temp. ($^{\circ}\text{C}$)	
Rice husk ash. / Cd^{2+} , Ni^{2+} and Zn^{2+}	Increase from 50 to 500 ppm	Increase Cd 0.4288 – 3.1789 Ni 1.1309 – 3.0213 Zn 1.6503 – 3.6616	No general trend	Decrease Cd 0.1511- 0.0228 Ni 0.1913- 0.0156 Zn 0.1630- 0.0115	Increase Cd 0.0501- 0.3598 Ni 0.0550- 0.4518 Zn 0.0713- 0.5585	No general trend Average for Cd 6.842×10^{-13} Average for Ni 5.780×10^{-13} Average for Zn 6.848×10^{-13}	10 g L ⁻¹	150.47 μm (average size)	150	6	30	Srivastava et al., In press

จุฬาลงกรณ์มหาวิทยาลัย

Table 2.5 Effect of sorbate initial concentration on sorption equilibrium

Sorption system (Sorbent/Sorbate)	Independent variable	Dependent variable			Control variable						References
	Range of initial concentration	Time to reach equilibrium	q_e	%Removal	Sorbent dose	Particle size	Agitation rate	pH	Temp. (°C)	Agitation times	
H ₃ PO ₄ ⁻ activated rubber wood sawdust / Cu ²⁺	Increase from 10 to 40 mg L ⁻¹	240 min for all concentration	Increase from 1.997 to 5.764 mg g ⁻¹	Not defined	5 g L ⁻¹	74 μm	180 rpm	6	30	240 min	Kalavathy et al., 2005
<i>Thuja orientalis</i> / Ni ²⁺	Increase from 50 to 400 mg L ⁻¹	7 min for all concentrations	Increase from 10 to 55 mg g ⁻¹	Decrease from 93.25 to 68%	5 g L ⁻¹	250–500 μm	300 rpm	4	25	30 min	Malkoc, In press
Agricultural waste sugar beet pulp / Cu ²⁺	Increase from 25.6 to 258.8 mg L ⁻¹	1 h for 200 ppm 3 h for 100 ppm	Increase from 11.8 to 28.5 mg g ⁻¹	Decrease from 45.9 to 11.0%	1 g L ⁻¹	250 μm	150 rpm	4	25	24 h	Aksu and Işoğlu, 2005
polymerized banana stem / Pb ²⁺	Increase from 10 to 100 mg L ⁻¹	60 min for all concentration	Increase from 11.8 to 28.5 mg g ⁻¹	Not defined	2 g L ⁻¹	96 μm	200 rpm	6	30	240 min	Noeline et al., 2005

Table 2.5 Effect of sorbate initial concentration on sorption equilibrium (cont.)

Sorption system (Sorbent/Sorbate)	Independent variable	Dependent variable			Control variable					References
	Range of initial concentration	Time to reach equilibrium	q_e	Sorbent dose	Particle size	Agitation rate	pH	Temp. (°C)	Agitation times	
Bacterial dead <i>Streptomyces rimosus</i> / Pb ²⁺	Increase from 10 to 800 mg L ⁻¹	180 h	Increase from about 7 to 135 mg g ⁻¹	3 g L ⁻¹	50–160 µm.	250 rpm	unadjusted pH	Not defined	240 h	Selatnia et al., 2004
Rice husk ash. / Cd ²⁺ , Ni ²⁺ and Zn ²⁺	Increase from 50 – 500 ppm	120 min	Increase from 1.6844 to 11.7862 mg-Cd g ⁻¹ Increase from 2.4311 to 13.8947 mg-Ni g ⁻¹ Increase from 3.1819 to 17.844 mg-Zn g ⁻¹	10 g L ⁻¹	150.47 µm (average size)	150	6	30	300 min	Srivastava et al., In Press

Table 2.6 Effect pH on sorption kinetics

Sorption system (Sorbent/Sorbate)	Independent variable	Dependent variable						Control variable					References
	Range of pH	Initial sorption rate (<i>h</i>)	k_1 (Eq. 2.6)	k_2 (Eq. 2.8)	K_{wm} (Eq. 2.15)	K_L (Eq. 2.19)	D (Eq. 2.12)	Dosage of sorbent	C_0	Particle size	Agitation rate	Temp. (°C)	
Palm kernel fiber / Pb ²⁺	Increase from 3 to 5	Increase from 55.6 to 170 mg g ⁻¹ min ⁻¹	Not defined	K_2 increase from 0.0376 to 0.106 g mg ⁻¹ min ⁻¹	Not defined	Not defined	Not defined	1.5 g L ⁻¹	120 mg L ⁻¹	50–60 μm	200 rpm	36 ± 4	Ho and Ofomaja, 2006
Chitin / Cr ⁶⁺	Increase from 2 to 4	Not defined	Not defined	Not defined	Decrease from 3.29, 2.25, 1.73 mmol g ⁻¹ s ^{-0.5}	Decrease from 1.9×10 ⁻³ , 1.11×10 ⁻³ , 0.62×10 ⁻³ cm s ⁻¹	No general trend 9.05×10 ⁻¹⁰ , 10.7×10 ⁻¹⁰ , 5.78×10 ⁻¹⁰ cm ² s ⁻¹	1 g L ⁻¹	1.923 mM	250–420 μm	Not define	25	Sag&Aktay, 2000
Eggshells / Cr ³⁺	3 to 5	Not defined	Not defined	0.00281, 0.001988, 0.0073 g mg ⁻¹ min ⁻¹	Not defined	Not defined	Not defined	5 g L ⁻¹	200 mg L ⁻¹	100 μm	150 rpm	20 ± 1	Chojnacka, 2005

Table 2.6 Effect pH on sorption kinetics (cont.)

Sorption system (Sorbent/Sorbate)	Independent variable	Dependent variable			Control variable				References	
	Range of pH	K_{wm} (Eq. 2.15)	K_L (Eq. 2.19)	D (Eq. 2.12)	Dosage of sorbent	C_o	Particle size	Agitation rate		Temp. (°C)
Chitosan / V^{4+}	Increase	No general trend	Increase	No general trend	0.1 g L ⁻¹	50 mg L ⁻¹	< 125 μm	400 rpm	20 ± 1	Jansson-Charrier et al., 1996
	3	7.26	1.2×10 ⁻⁴	1.02×10 ⁻¹⁴						
	4	2.61	2.1×10 ⁻⁴	0.43×10 ⁻¹⁴						
	5	3.95 mg g ⁻¹ min ^{-0.5}	2.5×10 ⁻⁴ m s ⁻¹	1.6×10 ⁻¹⁴ m ² s ⁻¹						

Table 2.7 Effect pH on sorption equilibriums

Sorption system (Sorbent/Sorbate)	Independent variable	Dependent variable		Control variable						References
	Range of pH	Time to reach equilibrium	q_e	Sorbent dose	C_o	Particle size	Agitation rate	Temp. (°C)	Agitation times	
H ₃ PO ₄ ⁻ activated rubber wood sawdust / Cu ²⁺	2 - 8	Not define	increase from 0.46 to 3.825 mg g ⁻¹ for pH 2 – 6 and decrease for 6-8	5 g L ⁻¹	20 mg L ⁻¹	74 μm	180 rpm	30	240 min	Kalavathy et al., 2005
Palm kernel fiber / Pb ²⁺	3 - 6	About 10 min for all pH	Increase 38.5 to 47.6 mg g ⁻¹ For 3-5 and decrease from 47.6 - 40 mg g ⁻¹ for 5-6	1.5 g L ⁻¹	120 mg L ⁻¹	50–60 μm	200 rpm	36 ± 4.	20 min	Ho and Ofomaja, 2006

Table 2.7 Effect pH on sorption equilibriums (cont.)

Sorption system (Sorbent/Sorbate)	Independent variable	Dependent variable			Control variable						References
	Range of pH	Time to reach equilibrium	q_e	%Removal	Sorbent dose	C_o	Particle size	Agitation rate	Temp. (°C)	Agitation times	
Saw dust / Ni^{2+}	1-10	Not define	Not define	No Ni removal at pH 1 – 2 But sharply increase 0 – 69 % for pH 2 -4 then slightly increase from 69 – 78% for pH 4-9 and drop from 78 – 62 % for pH 9 -10	Not define but range from 10 – 50 $g L^{-1}$	3 $mg L^{-1}$.	Not define	80 rpm	23	24 hr	Shukla (2005)
Wheat bran / Cd^{2+}	4-10	120 min for all pH	Increase from 0.19 to 0.5 $mg g^{-1}$ with increase of pH from 4.0 to 8.6 and thereafter removal decrease from 0.5 to 0.08 $mg g^{-1}$ with an increase of pH from 8.6 to 10.0	Increase from 30.85% to 80.16% with increase of pH from 4.0 to 8.6 and thereafter removal decrease from 80.16% to 12.62% with an increase of pH from 8.6 to 10.0	1 g / 50 mL	12.5 $mg L^{-1}$	<178 μm	125	30	200 min	Singh et al., 2006

Table 2.7 Effect pH on sorption equilibriums (cont.)

Sorption system (Sorbent/Sorbate)	Independent variable	Dependent variable	Control variable						References
	Range of pH	q_e	Sorbent dose	C_o	Particle size	Agitation rate	Temp. (°C)	Agitation times	
Rice husk ash. / Cd ²⁺ , Ni ²⁺ and Zn ²⁺	2-10	<p>Cd Increase from 0.2 – 0.4 mg g⁻¹ for pH 2-4 Increase from 0.4 – 2.9 mg g⁻¹ for pH 4 – 7 and constant until pH 10</p> <p>Ni Increase from 0.5– 1.3 mg g⁻¹ for pH 2-4 Increase from 1.3 – 4.4 mg g⁻¹ for pH 4 - 8 and constant until pH 10</p> <p>Zn Increase from 0.7– 1.2 mg g⁻¹ for pH 2-3 Increase from 1.2 – 6.3 mg g⁻¹ for pH 4 - 7 and constant until pH 10</p>	10 g L ⁻¹	100 mg L ⁻¹	150.47 μm (average size)	150	30	5 h	Srivastava et al, 2006

Table 2.8 Effect particle size on sorption kinetics

Sorption system (Sorbent/Sorbate)	Independent variable	Dependent variable		Control variable					References
	Size range	k_1 (Eq. 2.6)	k_2 (Eq 2.8)	Sorbent dose	C_o	Agitation rate	pH	Temp. (°C)	
Scoria (a vesicular pyroclastic rock with basaltic composition) / Zn^{2+}	Decrease from 0.5 – 2 mm 0.2 – 0.5 mm 0.1 – 0.2 mm and <0.1 mm	Increase from 1.51×10^{-3} to $7.92 \times 10^{-3} \text{ min}^{-1}$ when decrease size from 0.5 – 2 mm to <0.1 mm	Not defined	3g / 30 mL	20 mM	150 rpm	3.0 ± 0.1	25	Kwon, 2005
Chitin / Cd^{2+}	<0.20; 0.20–0.63; 0.63–1.25; 1.25–2.50; 2.50–4.10; 4.10–6.30 mm	Not defined	No general trend $2.91 \times 10^{-3} \text{ g mg}^{-1} \text{ min}^{-1}$ $0.69 \times 10^{-3} \text{ g mg}^{-1} \text{ min}^{-1}$ $1.41 \times 10^{-3} \text{ g mg}^{-1} \text{ min}^{-1}$ $3.65 \times 10^{-3} \text{ g mg}^{-1} \text{ min}^{-1}$ $2.12 \times 10^{-3} \text{ g mg}^{-1} \text{ min}^{-1}$ $0.61 \times 10^{-3} \text{ g mg}^{-1} \text{ min}^{-1}$	0.6 g /300 mL	100 mg L^{-1}	Not defined	Not controlled	25	Benguella and Benaissa, 2002

Table 2.8 Effect particle size on sorption kinetics (cont.)

Sorption system (Sorbent/Sorbate)	Independent variable	Dependent variable			Control variable					References
	Size range	K_{wm} (Eq. 2.15)	K_L (Eq. 2.19)	D (Eq. 2.12)	Sorbent dose	C_0	Agitation rate	pH	Temp. (°C)	
Chitin prepared from crab shells / Cr^{6+}	Increase from 250 – 420 μm to 595 – 841 μm	Decreased from 433×10^{-3} to 2.74×10^{-3} $mmol\ g^{-1}\ s^{-0.5}$	increasing 1.67×10^{-3} to 2.27×10^{-3} $cm\ s^{-1}$	Increase from 7.53×10^{-10} to 31.1×10^{-10} $cm^2\ s^{-1}$	1 $g\ L^{-1}$	of 2.885 mM	Not defined	2	25	Sag and Aktay, 2000
Chitosan / V^{4+}	Increase from <125 to 125 – 250 to 250 - 500 to 500 - 1000 μm	No general trend 0.91 3.2 1.52 2.19 $mg.\ g^{-1}\ s^{-0.5}$	Increase from 2.1×10^{-4} to 6.5×10^{-4} to 20.6×10^{-4} to 34.9×10^{-4} $m\ s^{-1}$	Increase from 0.43×10^{-14} to 2.85×10^{-14} to 2.97×10^{-14} to 16.5×10^{-14}	0.1 $g\ L^{-1}$	50 $mg\ L^{-1}$	400 rpm	4	20 ± 1	Jansson-Charrier et al., 1996

สถาบันวิทยบริการ
จุฬาลงกรณ์มหาวิทยาลัย

Table 2.9 Effect particle size on sorption equilibriums

Sorption system (Sorbent/Sorbate)	Independent variable	Dependent variable		Control variable						References
	Size range	q_e	%Removal	Sorbent dose	C_o	Agitation rate	pH	Temp. (°C)	Agitation time	
crab shell particles / Co^{2+} and Cu^{2+}	Decrease from 1.117, 0.767, 0.597, 0.456 mm	Co Highly Increase from 235 $mg\ g^{-1}$ to 260 $mg\ g^{-1}$ for decreasing size 1.117 to 0.767 and slightly increase from 260 to about 262 $mg\ g^{-1}$ for decreasing size 0.767 to 0.456 mm Cu Highly Increase from 181 $mg\ g^{-1}$ to 193.5 $mg\ g^{-1}$ for decreasing size 1.117 to 0.767 and unchanged for decreasing size from 0.767 to 0.456 mm	Co Highly Increase from 59 % to 65% decreasing size 1.117 to 0.767 and slightly increase from 65% to about 66% for decreasing size 0.767 to 0.456 mm Cu Highly Increase from 46% to 49% decreasing size 1.117 to 0.767 and unchanged for decreasing size from 0.767 to 0.456 mm	5 $g\ L^{-1}$	2000 $mg\ L^{-1}$ for 2 metals	150 rpm	6	Not defined	6 h	Vijayaraghavan et al., 2006
<i>Tectona grandis</i> L.f. leaves / Cu^{2+}	Increase from 75 to 212 μm	Not defined	Decrease from 85.67% to 64.18%	0.1g / 30 mL	20 $mg\ L^{-1}$	180 rpm	5	Room temp.	3 h	Kumar et al 2006

Table 2.9 Effect particle size on sorption equilibriums (cont.)

Sorption system (Sorbent/Sorbate)	Independent variable	Dependent variable			Control variable						References
	Size range	Time to reach equilibrium	q_e	%Removal	Sorbent dose	C_o	Agitation rate	pH	Temp. (°C)	Agitation time	
Scoria (a vesicular pyroclastic rock with basaltic composition) / Zn^{2+}	Increase from < 0.1 mm 0.1 – 0.2 0.2 – 0.5 0.5 – 2 mm	12 h for all size the smallest size and 24 h for the others	Increase from 0.77, 5.71, 10 and 11 mg g^{-1} when increase size from the largest size to smallest size	In crease from 5% to 44% , 77%, and 86 % when increase from the largest size to smallest size	3g / 30 mL	20 mM	150 rpm	3.0 ± 0.1	25	36 h	Kwon et al., 2005
Chitin prepared from crab shells / Cr^{6+}	Increase from 250 – 420 μm to 595 to 841 μm	Increasing the particle size resulted in a greater time to reach equilibrium.	Not defined	Not defined	1 g L^{-1}	of 2.885 mM	Not defined	2	25	3000 min	Sag and Aktay, 2000
Manganese nodule residue / Cd^{2+}	Decrease from >0.152, 0.104–0.152, 0.076–0.104 0.053–0.076 mm	1 h for the small lest size 4 h for the largest size	Not defined	99% for the small lest size 98.1% for the largest size	1 g / 100 mL	200 mg L^{-1}	120 rpm	5.5	30	8 h	Agrawal and Sahu, 2006

PART III BIOSORPTION OF HEAVY METALS

2.9 Definition and advantage of biosorption

Biosorption can be defined as the passive sequestering of contaminant such as heavy metal ions by metabolically inactive biomass which is different from bioaccumulation as the later involved with the metabolism activities (Volesky, 2004). Like the sorption process, the biosorption occurred by same mechanisms (adsorption and/or ion exchange) and same binding forces (physical and chemical forces). The two mechanisms can simultaneously or individually occur, however, ion exchange was proved to be a principal mechanism in metal biosorption by algal biomass (Davis et al. 2003a, Davis et al. 2003b and Volesky, 2004)

The advantage of biosorption is low operating cost since the raw materials are easily available (Banerjee, 2002). In addition, the biosorption is easily controllable since the process is independent of metabolism activities and does not generate chemical sludge like precipitation. Furthermore, the spent biomass after heavy metal biosorption process can be reused by recovering the metal attached on the biosorbent which, in some cases, is easy and more economic than recovering the metal from chemical sludge (Volesky, 2004).

2.10 Biosorbent

The biomass used in biosorption called as biosorbent can be any biological materials. Mainly, the biosorbent can be divided into three groups as follows:

- Chitinous biosorbent e.g. Shrimp, krill, squid, crab shell etc.
- Microbial biosorbent e.g. bacteria, fungi, and yeast
- Algal biosorbent

2.10.1 Chitinous biosorbent

The chitinous biosorbent can be used in heavy metal biosorption process since chitin consisting of (1,4) 2-acetamide-2-deoxy-D-glucose units which have ability to form the complex with the metal. The source chitinous material can be obtained from waste of seafood industrial process.

2.10.2 Microbial biosorbent

The bacteria sorbent can be obtained from waste products from fermentation industries. Metal removal using bacteria sorbent can occur by micro-precipitation process (McLean and Beveridge, 1990), complexation and electrostatic attraction (Brierley and Vance, 1988). Gram positive bacteria can bind the positive charged contaminants, e.g. metal ions, better than gram negative bacteria since the gram positive bacteria have teichoic and teichuronic acids at the outer surface while the gram negative do not. In addition, the gram positive bacteria contain higher layer of peptidoglycan polymer than the gram negative bacteria. These three biomolecular compounds (teichoic, teichuronic acids and peptidoglycan) contain negative charged function groups, for example, carboxyl group which facilitates biosorption process such as adsorption or ion exchange. Overall, the gram positive bacteria have more negative charged from these substances than the gram negative bacteria resulting in higher binding site for biosorption of positive charged contaminants (Brierley and Vance, 1988; McLean and Beveridge, 1990; Volesky, 2004).

The fungi is one of the generally used as biosorbents due to its low cost and comfortably acquired as the waste from some industries involved with microorganism such as food or beer industry. The types of fungi mainly used as biosorbent such as *Rhizopus* sp., *Absidia* sp., *Penicillia* sp., and *Aspergillus* sp. Among these, *Rhizopus* sp. and *Absidia* sp. are found to have high sorption capacity for metals while *Aspergillus* sp. do not. However, *Aspergillus* sp., the filamentous fungi, such as *Aspergillus niger* have an advantage in biosorptions process since they can grow in pellet which makes it easy for the subsequent separation from wastewater. The problems in using fungi as biosorbent are that the fungi are not easy to filter from the wastewater (excluded for *Aspergillus* sp.) and the impurities from fermentation broth residues could affect metal uptake (Volesky, 2004). The main binding site in metal biosorption by fungi is cell wall which largely consists of about 90% of polysaccharides (Remacle, 1990) such as glucan or mannan and some of protein and chitin/chitosan fiber.

2.10.3 Algal biosorbent

Another biomaterial frequently used as biosorbent is alga. The algae can easily grow in the nature and commonly found in seawater or freshwater depending on types of algal biomass. There are many advantages in using algae as biosorbent, for example, 1) they are readily available, 2) they spend low operating cost, 3) they provide

generally high metal sorption capacity, 4) they provide more regular quality than microbial biosorbent, 5) They are comfortable in operation since they require a little pretreatment such as drying for transportation and storage while microbial sorbents are often too small in particle size for direct column application and therefore requires granulation before used and this increases the costs and difficulties in operation (Kratochvil et al., 1995).

The biosorption by algal biomass occurs at the cell wall where ion exchange plays a major role and complexation can also occur (Davis et al. 2003). However, some type of algae such as *Cryptophyta* sp. and *Pyrrhophyta* sp. (Lee, 1989) do not have cell wall, which results in the lower potential in metal sorption than the algae with cell wall. The algal cell wall mostly comprises amorphous matrix of biomolecular compounds depending on type of algal biomass such as alginic acid, Fucoidan, etc. The minor constituents of algal cell are fibrillar skeletons such as cellulose, mannan, xylan, etc. In addition, the top of alga is mucilage which consists of complex hetero-polysaccharides such as involving galactose, arabinose, xylose, rhamnose, glucuronic acid, etc. (Lee, 1989). These biomolecular compounds provide many functional groups involved with metal biosorption mechanism. The principal functional groups responds for metal biosorption by algal biomass, especially marine algae, are carboxyl group (COOH) and sulfonate group (SO₃H) while the subordinate one is hydroxyl group (OH) (Volesky, 2004). This is because the carboxyl and sulfonate groups have the lower dissociation constant (pK_a) than hydroxyl group resulted in the wider range of pH which the groups have negative charge and can act as the effective binding site in metal biosorption.

2.11 *Caulerpa lentillifera* biomass

Caulerpa lentillifera is a green macroalga classified in

Kingdom: *Plantae*

Division : *Chlorophyta* (Green algae)

Class : *Chlorophyceae*

Order : *Caulerpales*

Family : *Caulerpaceae*

Genus : *Caulerpa*

Specie : *Caulerpa lentillifera*

The characteristics of this algal specie are siphonous form with septum cover cell to produce gametangium in reproducing. Generally *Caulerpa lentillifera* is found on the rock or sand in shallow water near coral reef. The branch's height are 1-6 cm. and consist of small green bulb with sphere shape with diameter around 1.5 – 2 mm arranged look like a bunch of pepper (See the detail in Fig. 2.2).

This alga is commonly found on the coral rubble, among the sponges, in the lagoon, and on ashore. The best condition for the growth of this algal biomass is sand or mud at bottom of shallow lagoons with calm saline water at salinity in range of 30 – 35 ppt. It does not tolerate for wide fluctuations in salinity or very low levels of salinity.

Caulerpa lentillifera is the most popular edible species of genus *Caulerpa*. In Philippines, Malaysia and Indonesia, this alga is freshly eaten as salad and it is also fed to livestock and fish. In Thailand, it often used to treat wastewater containing nitrogen compounds in shrimp ponds (Chokwiwattanawanit, 2000). Its rapid growth makes it common for the farmers to discard the excess biomass. Previous works (Sungkum, 2002, Apiratikul, 2003 and Suthiparinyanont, 2003) has shown that this alga is an unwanted agricultural material but could well be employed as an effective biosorbent for positively charged contaminants such as heavy metal ions.



Figure 2.2 *Caulerpa lentillifera* biomass

PART IV SORPTION WITH ZEOLITE FROM COAL FLY ASH

2.12 Coal fly ash

The coal fly ash (CFA) is a by product from combustion process using coal as fuel. CFA is carried out from the combustion chamber by the hot exhausted gas along the stack and generally is separated from the gas by some kinds of separator e.g. electrostatic precipitator, baghouse, cyclone collector, etc.

The characteristics of coal fly ash (as reported in Tongkam, 2000) are a fine particle with a round and sphere shape, light brown to gray in coloring depend on the amount of carbon in the coal. It has low specific gravity about 1.9 – 2.69 and low plasticity. The chemical compositions of coal fly ash depend on the type of coal used and combustion condition. However, silica, alumina, ferrous, and calcium constitute main compositions (95 – 99 % by weight).

The coal fly ash can be harmful on respiratory system, e.g. it can be the cause of pneumonia since CFA is a fine particle and can irritate the respiratory system. Furthermore, it can raise the pH of soil because CFA mainly contains alkaline property induced from CaO and MgO in its composition. These problems tend to increase in the future since a higher amount of CFA has been shown to be each year.

Due to its high silica and alumina contents, CFA is considered a potential precursor for zeolite. Converting coal fly ash to zeolite is a one of alternatives since the the coal fly ash has silica and alumina rich in chemical composition which can used as raw material in the zeolite making process.

สถาบันวิทยบริการ
จุฬาลงกรณ์มหาวิทยาลัย

2.13 Zeolite

2.13.1 History of zeolites

The word zeolite come from two Greek words “zein (ζειν)” which means “to boil” and “lithos (λιθος)” which means “stone”. This word was named by Cronstedt, a Swedish mineralogist, when he discovered new mineral in 1756. The mineral easily swells and loses water when heated, the characteristics that gives it’s the name zeolite. However, the mineral was later named as “stilbite” (Turatum, 2002 and Tongkam, 2000). Damour found the capability in sorption of alcohol, benzene, chloroform, carbonsulfide and mercury by dehydrated zeolite in 1840 (Tongkam, 2000). Weigel and Steinhoff reported in 1925 that chabazite can adsorb water, methyl and ethyl alcohols, and formic acid but excluded acetone, ether, and benzene. McBain (1926) explained this phenomena that zeolite could act itself as molecular sieve.

In 1945, Barrer used natural zeolite (chabasite) for separating gas molecules by the principle of molecular sieve and sorption phenomena. He proposed that the pore of zeolite could be divided into three groups based on the size of adsorbed molecules, i.e . micropore, mesopore, and macropore. After that, zeolites were used as a catalyst in applied for catalysis processes (Breck, 1974).

The first discoverer of the synthetic zeolites was Robert M. Milton from Union Carbide Corporation who successfully synthesized Zeolite A and Zeolite B(P) at the end of 1949. Later, in 1950, Zeolite X was synthesized at high purity. The two new zeolites, A and X, form the basis of a worldwide industry in gas and liquid separation and purification in the coming decades (Rabo and Schoonover, 2001).

There are more than 7,000 report papers and 2,000 US-Patent about zeolite published during 1948 to 1972 (Breck, 1974) and the zeolite literatures (papers and patent) of the world continually grow at rate about 100 publications per week (Turatum, 2002). These emphasize the significance of zeolite technology in a current technological era.

2.13.2 Structure of zeolites

Zeolites are crystalline aluminum-silicates, with structure made up of three dimensional framework of $[\text{SiO}_4]^{4-}$ and $[\text{AlO}_4]^{5-}$ tetrahedral units where Si or Al is central atom. The tetrahedral unit or generally called as primary building unit (PBU) linked to each other at corners by sharing their oxygens as shown in Fig 2.2 (Querol et al., 2002 and Breck, 1974). The length of covalent bonding from central to oxygen atom is 1.61 aungstrom and the distance between oxygen atoms (length of line and dash line in Fig. 2.3) is 2.62 aungstrom (Breck, 1974). A negative charge in the PBU framework of zeolite is caused by Al atom (Fig. 2.4). This negative charge can be balanced naturally by cations (e.g. Na^+ , K^+) in the zeolite structure, and the existence of cations could interchange with other cations e.g. heavy metals in the solutions, allowing effective cation exchange process.

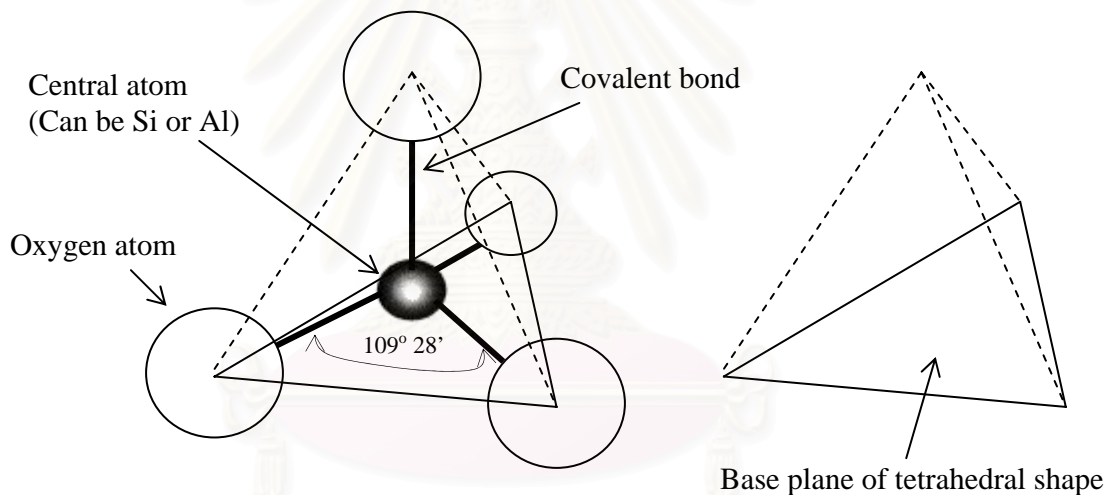


Figure 2.3 Primary Building Unit (Tetrahedral Unit) of Zeolite

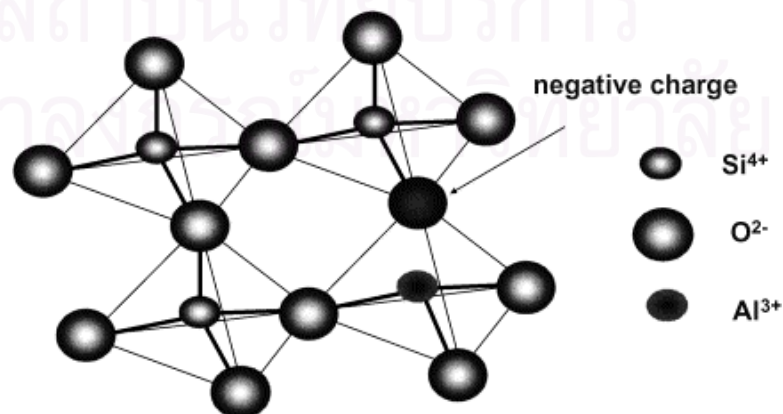
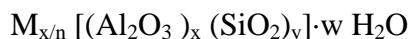


Figure 2.4 Negative charge in PBU frame work of zeolite (Picture from Querol et al., 2002)

From above concept the unit cell formula of zeolite can be represented as follows:



where M represents the cation with has valency n, x and y are a number of PBU with aluminium and silicon as a central atom, respectively, w is a number of water molecule in the unit cell.

The bigger structure of zeolite can be considered as secondary building unit (SBU) which consists of several PBUs lined up in geometric shapes. The example of SBU is the ring of four tetrahedral units denoted as S4R (Single 4 Rings), as shown in Fig. 2.4. However, the square shape is easily used to represent S4R as each angel represents the PBU. This square structure is denoted as “4” in Fig. 2.5. Szoztak (1989) categorized such SBUs into sixteen types as shown in Fig. 2.5 and all of zeolites contain some of these SBUs. These SBUs are currently used as the basis in the classification of zeolites.

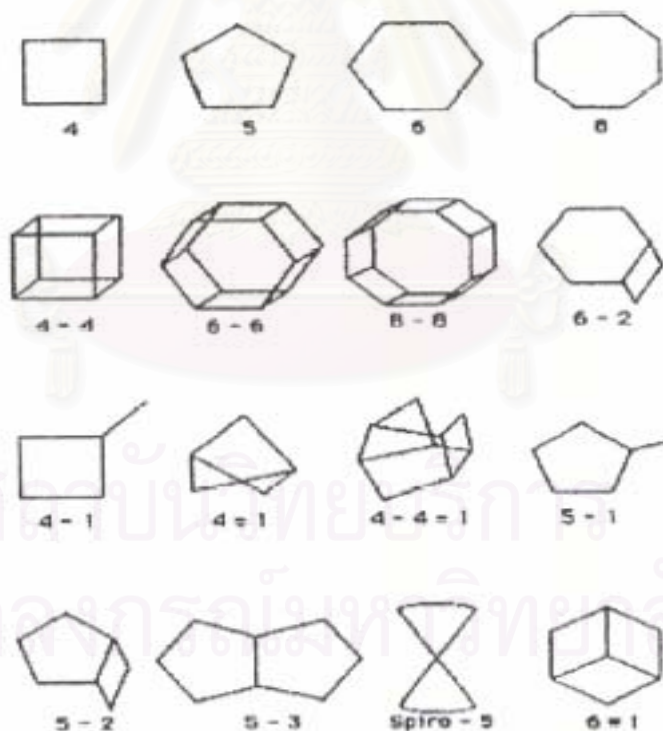


Figure 2.5 Secondary Building Unit (SBU) of Zeolite
(Picture from Szoztak, 1989)

2.13.3 Applications of zeolite

With their unique properties, zeolites have a major impact on the field of science and industry. The industrial interest in zeolites continues unabated at the dawn of the 21st century. International technical conferences devoted to zeolite science are numerous and growing (Rabo and Schoonover, 2001).

Nowadays, zeolites are widely used in many fields such as

1. Used as catalyst in many reaction process e.g. Hydrogenation, Alkylation, and Isomerization
2. Used as sorbent for removing contaminants e.g. heavy metals, toxic gas, dyes, organic pollutants such as benzene, alcohol etc.
3. Used as cation exchanger for many applications such as
 - a. Water softener: since Ca^{2+} and Mg^{2+} cause the hardness in water, hence these cations can be exchange with cation in zeolite e.g. Na^+ or K^+ . For this properties, zeolite can be used as detergent binder instead of phosphate, leading to less adverse effects on water environment as the phosphate cause the algae bloom.
 - b. Other sorption processes: Remove another cation pollutants such as heavy metals, ammonium ion etc.
4. Used in metal recovery processes: heavy metals can be recovered after zeolite removed the heavy metals from liquid phase

In the field of environmental engineering, zeolite mainly involves with air pollution control and the adsorption of contaminant in the wastewater as a new alternative adsorbent since they have low cost but high ion selectivity compared with ion exchange resin (Alvarez-Ayuso et al., 2003) and their ability for easily successive regeneration (Gupta et al., 2004 and Steenbruggen and Hollman, 1998). Furthermore, the spent zeolites after used as adsorbent in absorbing heavy metal can be used as the catalyst for lean- NO_x reduction technology at higher temperature application such as municipal solid waste incinerator. Subbiah et al. (2003) proved that the copper ion exchanged synthetic zeolite (Cu/SUZ-4) was the best metal cation for lean- NO_x removal catalysis over a wide range of temperature 350 to 600°C compared with Ag, Fe and Co.

2.13.4 Formation of zeolite

Zeolite occurred by two ways: 1) by natural way called as natural zeolite, and 2) by human called as synthetic zeolite. The natural zeolites may be found in natural deposits. They can be naturally formed by the alkaline activation and/or percolating with hot ground water of glassy volcanic rocks (Querol et al., 2002 and Barrer, 1982). After these processes the glass fraction in volcanic rock is converted into zeolites and subsequently be converted in to analcime and feldspar, respectively. The processes may take tens to thousands of years in natural conditions (Steenbruggen and Hollman, 1998). So the synthesis of zeolites in the laboratory conditions is necessary for the commercial zeolites developing industry to produce high quality of zeolites, to develop the desired properties of them for specific utilization, and to accelerate the time of forming them from many years to a few hours. In addition, some researchers (Pitcher et al., 2004 and Alvarez-Ayuso et al. 2003) reported the higher ability in removal efficiency, sorption capacity, adsorption affinity, and stability of synthetic zeolites than those of natural zeolites.

The synthesis of zeolites (zeolization) can be done using the starting materials containing high amount of silica and alumina (SiO_2 and Al_2O_3) like the glassy volcanic rock such as coal fly ashes (CFAs). The processes of zeolization are analogous to the formation of natural zeolites. There are three major methods in synthesis of zeolite; using organic template such as tetraethylammonium (TEAOH) couple with hydrothermal method, unusing template couple with hydrothermal method and unusing template couple with fusion method. There are some research papers reported the using unwanted material such as fly ash as raw material(s) in zeolite making process which concluded in Table 2.10.

The fusion method was found to provide higher cation exchange capacity than the hydrothermal method at the same conditions (Molina and Poole, 2004).

Table 2.10 Conversion of ash to zeolite

Type of Synthesis	Type of Zeolite synthesized	CEC* (meq/100g)	Operating condition							Reference
			NaOH:Ash ratio	Fusion temp /time	Solution Volume	Aging temp/time	Crystalization temp /time	pH of washed soluion	Drying temp /time	
Fusion	X (high peak)	210 (NH ₄ Ac)	1.2 g/g (12 g NaOH : 10 g CFA)	550°C / 1 h	85 mL of DI water	Shaking at Room Temp./12 h	90°C / 6 h	10	105°C / overnight	Molina and Poole, 2004
Hydrothermal	X,A, together with quartz and mullite (low intensity)	115 (NH ₄ Ac)	3.52 M : 10 g CFA	-	85 mL of DI water	Shaking at Room Temp./12 h	90°C / 6 h	10	105°C overnight	Molina and Poole, 2004
Hydrothermal	Faujasite (low intensity at 3 days, high intensity at 5 days)	107 (NH ₄ Ac)	2.5 parts of 2.8 M : 1 part of CFA	-	-	Stirred 30 min before static aged at Room Temp/48 h	38°C / 3 – 5 d	-	80°C / 1 d	Shih and Chang , 1996
Hydrothermal	zeolite P	-	2.5 parts of 2.8 M : 1part of CFA	-	-	Stirred 30 min before static aged at Room Temp/48 h	80°C / 0 - 3d	-	80°C / 1 d	Shih and Chang , 1996

Table 2.10 Conversion of fly ash to zeolite (cont.)

Type of Synthesis	Type of Zeolite synthesized	CEC* (meq/100g)	Operating condition							Reference
			NaOH:Ash ratio	Fusion temp /time	Solution Volume	Aging temp/time	Crystalization temp /time	pH of washed solution	Drying temp /time	
Hydrothermal	Not defined in literature	166 (NH ₄ Ac)	8 M : 50g oil shale ash	-	100 mL of base solution	-	160°C / 24 h	-	105°C / not stated in literature	Shawabkeh et al. (2004)
Hydrothermal	NaPl	186 (NaAc)	3.5 N of 8 mL : 1 mg lagoon ash	-	160 mL of base solution	-	100°C / 24 h	-	-	Kolay et al (2001)
Fusion	Faujasite	72 (NaAc)	1.2 g/g (12 g NaOH : 10 g CFA)	600°C/ 1-2 h	60 mL of DI water	Not defined / 8 h	100°C / 24 h	10-11	70°C / not defined	Somerset et al. 2005
Fusion	X	400 (NaAc)	1.2 g/g (12 g NaOH : 10 g CFA)	550°C / 2 h	50 mL of DI water	statically aged at Room Temp/12 h	100°C / 6 h	-	-	Berggaut and Singer 1996
Fusion	P	420 (NaAc)	1.2 g/g (12 g NaOH : 10 g CFA)	550°C / 2 h	50 mL of DI water	Stirred aged at Room Temp/12 h	100°C / 6 h	-	-	Berggaut and Singer 1996

* NaAc = Sodium Acetate method

NH₄Ac = Ammonium Acetate method

2.13.5 Heavy metal sorption using zeolite

In the field of sorption application, many researchers used zeolites as sorbent and found that they have high sorption capacity, sorption affinity, and cation exchange capacity for divalent sorbate. For example, Lee et al. (2000) reported the synthesized zeolites had greater adsorption capabilities for heavy metals than the original fly ash and natural zeolites. Alvarez-Ayuso et al. (2003) studied the application of zeolites in purification of metal electroplating and found that they have high adsorption capacity. Pitcher et al. (2004) used zeolites to remove dissolved heavy metals from the simulated and spiked motorway stormwater and reported that zeolites are very good for removing the studied heavy metals (Zn^{2+} , Cu^{2+} , Pb^{2+} and Cd^{2+}). Erdem et al. (2004) studied adsorption behavior of heavy metal cations (Co^{2+} , Cu^{2+} , Zn^{2+} and Mn^{2+}) by zeolites and reported that they hold great high potential to effectively remove these metal cations from industrial wastewater and could be used as a substitute for activated carbon. Additional details on the sorption capacity for some of the heavy metals on zeolite are concluded in Table 2.11. This illustrates that zeolites generally have the maximum sorption capacities for Cu^{2+} , Cd^{2+} , Pb^{2+} , and Zn^{2+} in the range of 0.7 to 2.5 mmol g^{-1} which is in a much higher level than the activated carbons where the maximum sorption capacities for these metals are in the range of 0.02 to 1.35 mmol g^{-1} .

Table 2.11 Metal sorption by various types of zeolite (At Temperature = 25°C)

Sorbent / Sorbate	Studied parameters		Operating conditions				Reference
	Maximum sorption capacity (q_{max}) mol kg ⁻¹	Sorption affinity (b) L mmol ⁻¹	Particle size	Agitation rate (rpm)	Shaking time	pH	
Zeolite A/ Cd ²⁺	2.53	0.991	-	-	3 h	-	El-Kamash et al., 2005
Zeolite A/ Zn ²⁺	1.65	0.455	-	-	3 h	-	El-Kamash et al., 2005
Clinoptilolite/ Cu ²⁺	1.4112	1.16	63–106 μm	-	5.5 h	6 – 7	Erdem et al. ,2004
Clinoptilolite / Co ²⁺	2.4413	1.75	63–106 μm	-	5.5 h	6 – 7	Erdem et al. ,2004
Clinoptilolite / Zn ²⁺	1.3385	0.85	63–106 μm	-	5.5 h	6 – 7	Erdem et al. ,2004
Clinoptilolite / Mn ²⁺	0.7678	0.33	63–106 μm	-	5.5 h	6 – 7	Erdem et al. ,2004
Na-PI / Pb ²⁺	1.286	457.29	-	300 rpm	-	-	Lee et al. ,2000
Na-PI / Cu ²⁺	1.046	103.92	-	300 rpm	-	-	Lee et al. ,2000
Na-PI / Cd ²⁺	1.156	21.91	-	300 rpm	-	-	Lee et al. ,2000
Na-PI / Zn ²⁺	1.007	8.29	-	300 rpm	-	-	Lee et al. ,2000
Faujasite / Pb ²⁺	1.229	211.34	-	300 rpm	-	-	Lee et al. ,2000
Sodalite / Pb ²⁺	0.798	214.32	-	300 rpm	-	-	Lee et al. ,2000
Analcime / Pb ²⁺	0.745	214.74	-	300 rpm	-	-	Lee et al. ,2000
Cancrinite / Pb ²⁺	0.537	205.66	-	300 rpm	-	-	Lee et al. ,2000
Na-PI / Zn ²⁺	1.007	8.29	-	300 rpm	-	-	Lee et al. ,2000
Faujasite / Pb ²⁺	1.229	211.34	-	300 rpm	-	-	Lee et al. ,2000
Sodalite / Pb ²⁺	0.798	214.32	-	300 rpm	-	-	Lee et al. ,2000
Analcime / Pb ²⁺	0.745	214.74	-	300 rpm	-	-	Lee et al. ,2000
Cancrinite / Pb ²⁺	0.537	205.66	-	300 rpm	-	-	Lee et al. ,2000

CHAPTER III

RESEARCH METHODOLOGY

3.1 Materials

3.1.1 Equipments

- Rotary Shaker, GFL, 3017
- Magnetic stirrer, Clifton UK, MSU-3
- Magnetic Bar
- pH-meter, HACH, SensIon 1 and SensIon 3
- Oven, WTB binder, FD115 (E2)
- Digital Balance (4 digits), Sartorius, BP2215
- Dessicator
- Water Purification System (For making DI water), ELGA, Ultraanalytic
- Filter paper No. 93, Whatman
- Filter paper GF/C, Toyo
- Vacuum Pump, KNF Neuberger, NO35AN. 18-IP20
- Peristaltic Pump, Watson-Marlow Sci-Q323
- Sieve Shaker and Sieve Mesh No. 10 and 20, Orto alresa, TA 002
- Refrigerator
- Inductively Couple Plasma (ICP), Vista
- Atomic Absorption Spectrophotometer, Analytik Jena
- Centrifuge, Kendro and Centrifuge Tube
- X-Ray Diffractometer, SIEMENS, D5000
- X-Ray Fluorescence spectrophotometer, ARL, 9400
- Scanning Electron Microscopy (SEM), Wealtec
- Surface area analyzer (Thermo Finnigan, Sorptomatic 1990)
- Laser Particle Size Analyzer, Malvern, Mastersizer-S long bed Ver 2.19
- Zeta Meter electrophoresis, Zeiss/3.0⁺

3.1.2 Glassware

- Erlenmeyer flasks
- Volumetric flasks
- Filtering Flasks
- Bushner Flasks
- Three ways junction
- Glass watches
- Beakers
- Pipettes
- Cylinders
- Dropper
- Funnels

3.1.3 Chemical Reagents

- Analytical grade $\text{Cu}(\text{NO}_3)_2 \cdot 2.5 \text{H}_2\text{O}$
- Analytical grade $\text{Cd}(\text{NO}_3)_2 \cdot 4 \text{H}_2\text{O}$
- Analytical grade $\text{Pb}(\text{NO}_3)_2$
- HNO_3 Conc., 69%
- NaOH anhydrous
- Deionized water (DI water)
- Ammonium Acetate
- Sodium Acetate
- Isopropyl alcohol, 99%
- pH buffer solution 4.00 ± 0.02 , Scharlau chemie
- pH buffer solution 7.00 ± 0.02 , HACH
- pH buffer solution 10.00 ± 0.02 , HACH
- Mix metal standard solution for ICP, MERCK

3.2 Methodology for biosorption part

3.2.1 Algal collection and preparation

- (1) Collect the *Caulerpa lentillifera* from Banchong Farm, Chachoengsao province
- (2) Wash the alga with deionized water
- (3) Dry the alga at 80°C for 12 hours
- (4) Store the alga in dessicator and used as whole thallus dried alga.

In most experiments, the dried alga (whole thallus) was employed directly. The ground algal biomass was used in the kinetic experiments and in the experiments where the effect of particle size was examined. In this work, the ground particles were defined as those which could pass through standard sieve number 10 but not with the standard sieve number 20. The particle size of the ground biomass was determined by Laser Particle Size Analyzer, Malvern, Mastersizer-S long bed Ver 2.19. In this work, the mean particle diameter of the ground biomass was 9×10^{-4} m

3.2.2 Glassware preparation

- (1) Wash the glassware with water
- (2) Immerse glassware in 20% HNO₃ overnight.
- (3) Wash the glassware with water to make sure there is no acid deposited inside the glassware.
- (4) Rinse the glassware with deionized water.
- (5) Dry the glassware on the shelf

3.2.3 Preparation for synthetic wastewater

- (1) Prepare stocks of heavy metal solution at 10 mol m^{-3} at a volume of 2 L from analytical grade of each heavy metal species in nitrate form i.e. Cu(NO₃)₂, Cd(NO₃)₂, and Pb(NO₃)₂
- (2) Keep stock solution in refrigerator at 4°C
- (3) Prepare synthetic wastewater with desire concentration by diluting the stock solution in (1) to the required concentration. The calculation is done by using a balance equation

$$N_1 V_1 = N_2 V_2 \quad (3.1)$$

N_1 = heavy metal's concentration of stock solution

V_1 = the required volume of stock solution

N_2 = the required heavy metal's concentration

V_2 = the required volume of solution.

3.2.4 Determination of effect of particle size of sorbent on biosorption kinetics

- (1) Prepare Cu^{2+} solution 30 mL with initial concentration of 10 mg L^{-1} at $\text{pH} = 5 \pm 0.2$
- (2) Add 0.5 g of whole thallus or ground algal biomass obtained from Section 3.2.1
- (3) Mix the solution with a rotary shaker at a rate of 150 rpm for 60 minutes at $21 \pm 1^\circ\text{C}$. The controlling of pH was done by using 0.1N nitric acid and 0.1N sodium hydroxide solutions
- (4) Separate solid phase with filter paper (Whatman No.93 and GF/C)
- (5) Triplicate the experiment by repeating Steps (1) to (4)
- (6) Measure heavy metal concentrations in the filtrate at 0 – 60 minutes by Atomic Absorption Spectrophotometer (AAS) or Inductively Coupled Plasma (ICP)
- (7) Determine the sorption capacity using Eq. 3.2 at each contact time.

$$q_t = \frac{V}{m} (C_o - C_t) \quad (3.2)$$

where q_t represents the amount of metal uptaken per unit mass of the biomass at time ' t ' (mol kg^{-1}), V the volume of the solution (m^3), m the dry mass of the algae (kg), C_o and C_t the initial concentration and the concentrations at time ' t ' (mol m^{-3}), respectively

- (8) Repeat Steps (1) to (7) with Cd^{2+} and Pb^{2+} solution.

3.2.5 Determination of effect of initial concentration and sorption isotherm

- (1) Prepare 30 mL of Cu^{2+} solution with initial concentrations in range of 0 – 3 mol m^{-3} at $\text{pH} = 5 \pm 0.2$
- (2) Add 0.5 g of whole thallus algal biomass obtained from Section 3.2.1

- (3) Mix the solution with a rotary shaker at a rate of 150 rpm for 30 minutes at $21 \pm 1^\circ\text{C}$. The controlling of pH was done by using 0.1N nitric acid and 0.1N sodium hydroxide solutions
- (4) Separate solid phase with filter paper (Whatman No.93 and GF/C)
- (5) Triplicate the experiment by repeating Steps (1) to (4)
- (6) Measure heavy metal concentrations in the filtrate at each concentration by Atomic Absorption Spectrophotometer (AAS) or Inductively Coupled Plasma (ICP)
- (7) Determine the equilibrium sorption capacity using Eq. 2.1 at each concentration
- (8) Determine the removal percentage (%Removal) from following equation.

$$\% \text{Removal} = 100 \frac{(C_o - C_f)}{C_o} \quad (3.3)$$

where C_o and C_f are the initial and final heavy metal concentrations (mol m^{-3}), respectively

- (9) Repeat Steps (1) to (8) with Cd^{2+} and Pb^{2+} solution.

3.2.6 Determination of effect of pH on sorption isotherm

- (1) Prepare 30 mL of Cu^{2+} solution with initial concentrations in range of 0 – 3 mol m^{-3} at $\text{pH} = 4 \pm 0.2$
- (2) Add 0.5 g of whole thallus algal biomass obtained from Section 3.2.1
- (3) Mix the solution with a rotary shaker at a rate of 150 rpm for 30 minutes at $21 \pm 1^\circ\text{C}$. The controlling of pH was done by using 0.1N nitric acid and 0.1N sodium hydroxide solutions
- (4) Separate solid phase with filter paper (Whatman No.93 and GF/C)
- (5) Triplicate the experiment by repeating Steps (1) to (4)
- (6) Measure heavy metal concentrations in the filtrate at each concentration by Atomic Absorption Spectrophotometer (AAS) or Inductively Coupled Plasma (ICP)
- (7) Determine the equilibrium sorption capacity using Eq. 2.1 at each concentration
- (8) Repeat Steps (1) to (7) with $\text{pH} 3 \pm 0.2$ and 1.5 ± 0.2
- (9) Repeat Steps (1) to (8) with Cd^{2+} and Pb^{2+} solution.

3.2.7 Study of biosorption in binary component batch system

- (1) Prepare 30 mL of mixture Pb^{2+} - Cu^{2+} solution with initial concentrations of each component in range of 0 – 3 mol m^{-3} at $pH = 5 \pm 0.2$
- (2) Add 0.5 g of whole thallus algal biomass obtained from Section 3.2.1
- (3) Mix the solution with a rotary shaker at a rate of 150 rpm for 30 minutes at $21 \pm 1^{\circ}C$. The controlling of pH was done by using 0.1N nitric acid and 0.1N sodium hydroxide solutions
- (4) Separate solid phase with filter paper (Whatman No.93 and GF/C)
- (5) Triplicate the experiment by repeating Steps (1) to (4)
- (6) Measure heavy metal concentrations in the filtrate at each concentration by Atomic Absorption Spectrophotometer (AAS) or Inductively Coupled Plasma (ICP)
- (7) Determine the equilibrium sorption capacity for each metal using Eq. 2.1 at each concentration
- (8) Repeat Steps (1) to (7) with mixture Pb^{2+} - Cd^{2+} and Cu^{2+} - Cd^{2+} solution.

3.2.8 Biosorption in fixed-bed column

- (1) Prepare 2000 mL of Cu^{2+} solution with initial concentrations of 0.1 mol m^{-3} at $pH = 5 \pm 0.2$ and control this pH during the sorption
- (2) Pack the ground algal biomass obtained from Section 3.2.1 in a fixed-bed column, 1.5 cm internal diameter, 4 cm in height with 1.0 g algal mass to obtain bed volume = 7.07 cm^3 and bulk density = 0.14 $g\ cm^{-3}$
- (3) Fed the synthetic wastewater into column by a peristaltic pump (Watson Marlow: Sci Q 323) at a flow rate of 6 $mL\ min^{-1}$ ($3.42\ mL\ min^{-1}\ cm^{-2}$) at $21 \pm 1^{\circ}C$
- (4) Measure metal concentrations in the effluent by Inductively Coupled Plasma (ICP)
- (5) Calculate the amount of heavy metal uptaken into the alga by the mass conservation principle where:

$$q = \frac{m_{inf} - m_{eff} - m_{pore}}{m_{biomass}} = \frac{C_o V - Q \int_0^t C_{eff}(t) dt - C_o V_v}{m_{biomass}} \quad (3.4)$$

In this equation, q represents the mass of metal uptaken onto the biomass ($mol\ kg^{-1}$), m_{inf} the total mass of metal fed into the fixed-bed column (mol),

m_{eff} the total mass of metal released from the fixed-bed column (mol), m_{pore} the total mass of metal left in the pore of biomass bed that was not uptaken (mol), $m_{biomass}$ the mass of biomass (kg), C_o the initial concentration of metal (mol m^{-3}), V the total volume of wastewater fed into column (m^3), V_v void volume (m^3), Q the volumetric flow-rate ($\text{m}^3 \text{ min}^{-1}$), t the total time that column was operated (min), and $C_{eff}(t)$ the effluent concentration as a function of time (mol m^{-3}).

- (6) Repeat Steps (1) to (5) with Cd^{2+} and Pb^{2+} solution.

3.3 Methodology for zeolite part

3.3.1 Coal fly ash (CFA) collection and preparation

- (1) Collect CFA from National Power Supply Co. Ltd., Prachin buri province
- (2) Dry the CFA at 120°C for 3 hours to get rid of humidity.
- (3) Store the CFA in dessicator.

3.3.2 Conversion of coal fly ash to zeolite

This process follows the method proposed by Molina and Poole (2004):

- (1) Weigh 10 g of dry coal fly ash in the evaporating dishes
- (2) Ground the NaOH anhydrous in pellet form to powder form using mortar and pestle
- (3) Weigh 12 g of powdered NaOH in the evaporating dishes to obtain NaOH:FA ratio = 1.2:1
- (4) Mix the powder NaOH and CFA together until the mixture is homogeneous
- (5) Fuse the mixture in furnace at 550°C for 1 hour
- (6) Homogenize the fusion products using mortar and pestle and transfer in Erlenmeyers flask with screw caps
- (7) Pour 85 mL of deionized water in each Erlenmeyer flask and close the screw cap
- (8) Shake the Erlenmeyer flasks at 150 rpm by shaker water bath at room temperature ($33 \pm 2^\circ\text{C}$) for 24 hours
- (9) Place the Erlenmeyer flasks in the oven preset the temperature at 90°C for crystallizing the product and leave the product in the oven for 2 hours

- (10) Wash the product 4 – 5 times by deionized water and separate the product by centrifugation
- (11) Dry the product in the oven at 105°C overnight
- (12) Fill the product in the zip bag and store in dessicator.

3.3.3 Analysis of original coal fly ash and zeolite product

The coal fly ash and zeolite products were analyzed using following techniques.

1). *Cation Exchange Capacity (CEC)*

Cation exchange capacity (CEC) of the products was determined using sodium acetate method according to US-EPA method 9081. This method uses 1N sodium acetate to saturate the sample. The samples were washed with 99% isopropyl alcohol and ammonium acetate was added to samples to exchange with sodium ion in the samples. The amount of sodium ions in the exchange solution were determined by AAS or ICP. The CEC values are calculated by mass balance concept.

2). *X-Ray Diffraction (XRD)*

The X-Ray Diffractometer, SIEMENS, D5000 was used to examine the crystalline phase(s) of the product using Cu K α radiation ($\lambda=0.154056$ nm), with Ni filter.

3). *X-Ray Fluorescence (XRF)*

The X-Ray Fluorescence spectrophotometer was used to determine the overall mineral composition of the product. The samples are analyzed by Test Tech Co. Ltd.

4). *Scanning Electron Microscope*

The dry solid samples were glued onto 10 mm diameter of aluminum stub by carbon tape and placed into Scanning Electron Microscope, Wealtec to study the morphology.

5). *Specific Surface Area (SAA) and Total Pore Volume (TPV)*

The Surface area analyzer, Thermo Finnigan, Sorptomatic 1990 was used for determining the specific surface area (SAA) and total pore volume (TPV) of the product using BET technique based on adsorption characteristic of N₂ gas on the sample at 77 K.

6). *Point of Zero Charge (PZC)*

The point of zero charge (PZC) was the pH that surface charge of the sample equal to zero which was determined by measuring the surface charge of product in the

deionized water solution at various pH using Zeta Meter electrophoresis, Zeiss/3.0⁺. The pH of deionized water was adjusted by nitric acid and sodium hydroxide to desired pH.

7). *Particle Size Distribution (PSD)*

The particle size distribution of product was determined by Laser Particle Size Analyze, Malvern, Mastersizer-S long bed Ver 2.19 using water as a medium.

3.3.4 Determination for effect of initial metal concentration on sorption kinetics by zeolite

- (1) Prepare 30 mL of Cu²⁺ solution with initial concentrations in range of 0 – 10 mol m⁻³ at pH = 5 ± 0.2
- (2) Add 0.03 g of zeolite product obtained from Sections 3.3.2
- (3) Mix the solution with a rotary shaker at a rate of 150 rpm for 60 minutes at 21 ± 1°C. The controlling of pH is achieved by using ammonium acetate buffer with the ratio of acetate : acetic = 15 mM : 8.24 mM
- (4) Separate solid phase with filter paper (Whatman No.93 and GF/C)
- (5) Triplicate the experiment by repeating Steps (1) to (4)
- (6) Measure heavy metal concentrations in the filtrate at 0 – 60 minutes for each initial concentration by Atomic Absorption Spectrophotometer (AAS) or Inductively Coupled Plasma (ICP)
- (7) Determine the sorption capacity using Eq. 3.2 for each concentration at each contact time
- (8) Repeat Steps (1) to (7) with Cd²⁺ and Pb²⁺ solution.

3.3.5 Determination of effect of sorbent dose on sorption kinetic by zeolite

- (1) Prepare Cu²⁺ solution 30 mL with initial concentration of 5 mol m⁻³ at pH = 5 ± 0.2
- (2) Add 0.015, 0.03, 0.06 and 0.09 g of zeolite product obtained from Sections 3.3.2
- (3) Mix the solution with a rotary shaker at a rate of 150 rpm for 60 minutes at 21 ± 1 °C. The controlling of pH is achieved by using ammonium acetate buffer with the ratio of acetate : acetic = 15 mM : 8.24 mM
- (4) Separate solid phase with filter paper (Whatman No.93 and GF/C)
- (5) Triplicate the experiment by repeating Steps (1) to (4)

- (6) Measure heavy metal concentrations in the filtrate at 0 – 60 minutes for each sorbent concentration by Atomic Absorption Spectrophotometer (AAS) or Inductively Coupled Plasma (ICP)
- (7) Determine the sorption capacity using Eq. 3.2 for each sorbent dose at each contact time
- (8) Repeat Steps (1) to (7) with Cd^{2+} and Pb^{2+} solution.

3.3.6 Determination of effect of sorbent dose and sorbate initial concentration on sorption equilibrium study (Sorption isotherm study)

- (1) Prepare 30 mL of Cu^{2+} solution with initial concentrations in range of 0 – 10 mol m^{-3} at $\text{pH} = 5 \pm 0.2$
- (2) Add 0.015, 0.03, 0.06 and 0.09 g of optimal zeolite product obtained from Sections 3.3.2. and 3.3.3
- (3) Mix the solution with a rotary shaker at a rate of 150 rpm for 60 minutes at 21 ± 1 °C. The controlling of pH is achieved by using ammonium acetate buffer with the ratio of acetate : acetic = 15 mM : 8.24 mM
- (4) Separate solid phase with filter paper (Whatman No.93 and GF/C)
- (5) Triplicate the experiment by repeating Steps (1) to (4)
- (6) Measure heavy metal concentrations in the filtrate at 60 minutes for each sorbent dose and sorbate concentration by Atomic Absorption Spectrophotometer (AAS) or Inductively Coupled Plasma (ICP)
- (7) Determine the equilibrium sorption capacity using Eq. 2.1 for each concentration and each sorbent dose
- (8) Determine the removal percentage (%Removal) from Eq. 3.3
- (9) Repeat Steps (1) to (8) with Cd^{2+} and Pb^{2+} solution.

3.4 Control of Experiments

In this research, each experiment was triplicated to ensure that obtained results were genuine. The results were reported as average values. Temperature was controlled by air condition to 20°C with error is no more than 2°C. The glasswares were exclusively used for this research to ensure that they had no contamination. No sorption of heavy metals by filter paper, glasswares, and plastic reactor tubes was observed in this work.

CHAPTER IV

METAL SORPTION USING CAULERPA LENTILLIFERA

4.1 Effect of particle size on characteristic of sorption capacity-contact time

The time-profiles of the sorption of Cu^{2+} , Cd^{2+} , and Pb^{2+} ions by whole thallus and ground biomass are given in Fig. 4.1. In all cases, the metal ion uptake was rapid with the system reaching equilibrium within 10-20 minutes and no further sorption was observed thereafter. The figure also illustrates that the ground biomass could more rapidly uptake each metal ion, and the equilibrium was reached faster than those achieved with the whole thallus. This was because particles with smaller particle size allowed a faster contact between the metal ion and the binding sites. On the other hand, the particle size did not have significant effects on the equilibrium sorption capacity indicating that the grinding did not deteriorate the integrity of the alga and all the active sites for the sorption remained mostly intact.

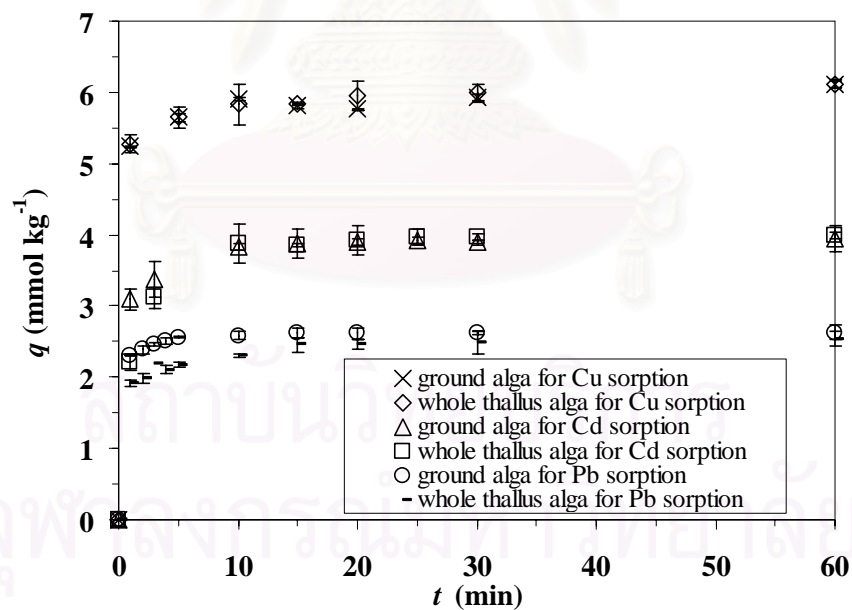


Figure 4.1 Effect of contact time on sorption capacity

4.2 Sorption kinetics

The ground biomass was selected to study for sorption kinetics. Experimental data were analyzed with the sorption kinetic models *i.e.* pseudo first order (Eq. 2.7), pseudo second order (Eq. 2.9), Vermeulen model (Eq. 2.12), Weber-Morris model (Eq. 2.15), Crank's diffusion coefficient (Eq. 2.17), and External mass transfer model (Eqs. 2.21 and 2.22). Model parameters in Eqs. 2.7, 2.9, and 2.12 were determined by a nonlinear regression analysis to avoid statistical bias. STATISTICA version 6.0 was employed for these nonlinear fittings of the experimental data and the resulting parameters of each kinetic model are summarized in Table 4.1. The experimental data were found to best follow the second order kinetic model (higher values of correlation coefficient or R^2). Hence, the model was thereafter used for calculating the initial slope (h) to determine the external mass transfer coefficient from Eq. 2.21. Table 4.1 shows that Pb^{2+} had the highest value of pseudo second order kinetic rate constant (k_2) and external mass transfer coefficient (K_L) indicating that *Caulerpa lentillifera* could uptake Pb^{2+} faster than the other metal ions

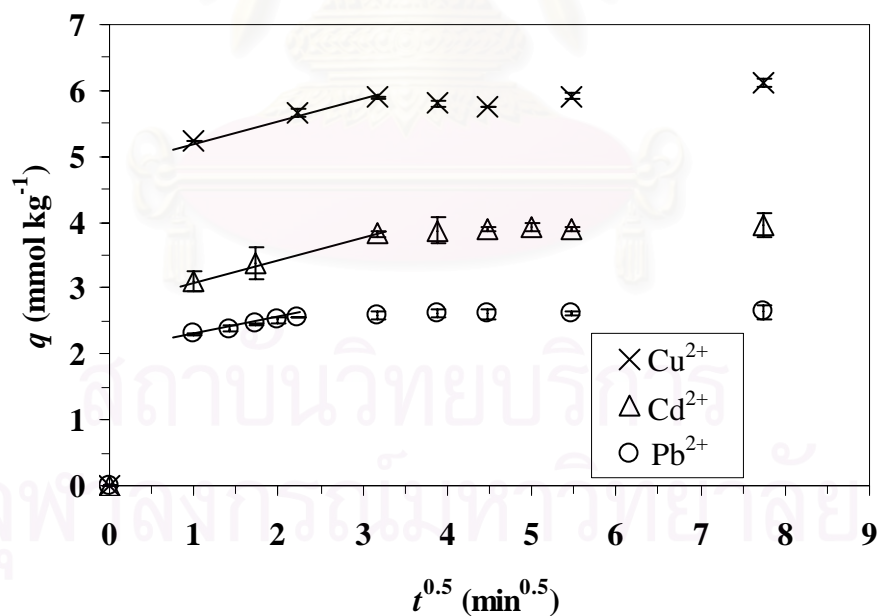
The intraparticle diffusion coefficient from the Vermeulen model was found to be in the same order magnitude for all three metal ions (about $5 \times 10^{-10} \text{ m}^2 \text{ s}^{-1}$) while the value obtained from the Weber-Morris model was significantly lower (100 times) than that from the Vermeulen model. This difference might be due to the different calculation methods of the two models. While the calculation of the Vermeulen model was based on the whole range of data, the Weber-Morris model only employed data within the linear region between the plot of q and $t^{0.5}$ (as shown by solid line in Fig. 4.2) which depended on the judgement of the "linear region", and this might induce statistical bias. In addition, the values from Vermeulen model was closed to the molecular diffusivity obtained from literature and D_o of Cu^{2+} , Cd^{2+} , and Pb^{2+} were 7.33×10^{-10} , 7.17×10^{-10} , and $9.45 \times 10^{-10} \text{ m}^2 \text{ s}^{-1}$, respectively (Dortch et al., 2005). This indicated that inner structure of the algal biomass was not complex.

Table 4.1 also illustrates that the intercept (I) of the Weber-Morris intraparticle diffusion existed for all metals indicating that there were both external mass transfer and intraparticle diffusion presented as rate limiting steps for biosorption systems. The rate of sorption might be possible with a better control of external mass transfer and intraparticle diffusion parameters such as shaking rate and temperature.

Table 4.1 Model parameters for the sorption of various metals

($d_p = 9.0 \times 10^{-4}$ m, $\rho_b = 150$ kg m⁻³, $A_s = 44.44$ m² kg⁻¹)

Model	parameters	Cu ²⁺	Cd ²⁺	Pb ²⁺
Pseudo 1 st order	$q_{e,1}$ (mmol kg ⁻¹)	5.86	3.85	2.56
	k_1 (min ⁻¹)	2.248	1.395	2.153
	R^2	0.996	0.982	0.992
Pseudo 2 nd order	$q_{e,2}$ (mmol kg ⁻¹)	6.14	3.97	2.64
	k_2 (kg mol ⁻¹ min ⁻¹)	254	621	2036
	R^2	0.999	1.000	1.000
External Mass Transfer	$h_2 = q_e^2 k_2$ (mmol kg ⁻¹ min ⁻¹)	9.57	9.80	14.19
	K_L (m s ⁻¹)	3.14×10^{-5}	5.29×10^{-5}	10.5×10^{-5}
Vermeulen Model	$q_{e,v}$ (mmol kg ⁻¹)	5.86	3.80	2.57
	D_e (m ² s ⁻¹)	5.49×10^{-10}	4.66×10^{-10}	4.82×10^{-10}
	R^2	0.996	0.981	0.993
Weber Morris Model	K_{WM} (mmol kg ⁻¹ min ^{-0.5})	0.306	0.335	0.210
	I (mmol kg ⁻¹)	4.94	2.78	2.09
	D_e (m ² s ⁻¹)	0.733×10^{-12}	2.10×10^{-12}	1.87×10^{-12}
	R^2	0.996	0.997	1.000

Figure 4.2 Weber-Morris kinetic model for metals sorption by *Caulerpa lentillifera*

4.3 Sorption isotherm

The data of sorption equilibrium was tested with Sips isotherm as expressed in Eq. 2.30. The isotherm was found to provide a reasonably accurate prediction of experimental results with the determination coefficient (R^2) of at least 0.95. Table 4.2 summarizes the parameters of Sips model where Sips exponent (n_s) for the sorption of each metal was demonstrated to be quite close to unity. This implied monolayer coverage of the heavy metal ions on the surface of the algal biomass. In other words, the biosorption of heavy metal ions on *Caulerpa lentillifera* should have taken place at the functional groups/binding sites on the surface of the alga, *i.e.* one mole of metal ion per one mole of binding site. In this case, hence, the use of Langmuir isotherm model (Eq. 2.28) for this sorption system could be regarded as appropriate. In addition, Langmuir isotherm model is more convenient to use as it can be analyzed by a simple linear regression analysis. Furthermore, Langmuir isotherm model has been more universally applied which allowed the comparison between the results with literature. Fig. 4.3 shows the predictive performance of Sips model compared with Langmuir isotherm model for the three heavy metal ions. It can be seen that a deviation of Langmuir isotherm from Sips isotherm model was only apparent at high equilibrium concentration, and within the concentration investigated in this work, the two models provided similar characteristics particularly for the sorption of Cd^{2+} . The coefficient of determination (R^2) for the fitting between experimental and predicted data using Langmuir isotherm model were equal to 0.996, 0.980, and 0.998 for Cu^{2+} , Cd^{2+} , and Pb^{2+} , respectively. The results from the Langmuir isotherm model suggested that the order of maximum sorption capacity (q_{max}) could be prioritized from high to low as: Pb^{2+} ($0.136 \text{ mol kg}^{-1}$) > Cu^{2+} ($0.125 \text{ mol kg}^{-1}$) > Cd^{2+} ($0.042 \text{ mol kg}^{-1}$), indicating that this algal biomass had more binding sites for Pb^{2+} than Cu^{2+} and Cd^{2+} , respectively. On the other hand, the Langmuir affinity constant (b) could be prioritized from high to low as: Pb^{2+} ($14.3 \text{ m}^3 \text{ mol}^{-1}$) > Cd^{2+} ($8.06 \text{ m}^3 \text{ mol}^{-1}$) > Cu^{2+} ($2.89 \text{ m}^3 \text{ mol}^{-1}$) which suggested that Pb^{2+} was the most easily bonded component to the binding sites of this alga, followed by Cd^{2+} and Cu^{2+} , respectively. The value of q_{max} in this work was compared with various reported data from literature as illustrated in Table 4.3. The removal efficiency for Cu^{2+} , Cd^{2+} , and Pb^{2+} fall in the range of 87% – 76%, 80% – 53%, and 97% – 93% for the initial concentration between 0 – 1 mol m^{-3} (See the details in Appendix C).

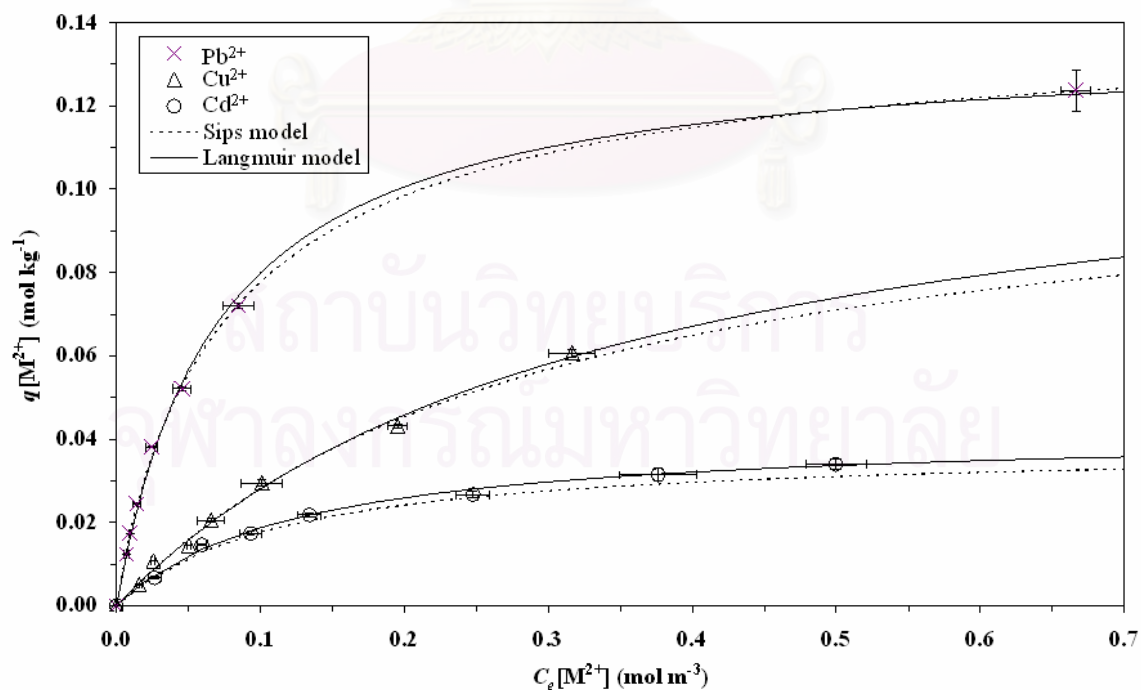
Table 4.2 Isotherm parameters (results at T = 294 K, pH = 5, X₀=0.5 g in 30 mL)

Heavy Metal Ion	Sips isotherm				Dubinin-Radushkevich isotherm			
	q_{\max} (mol kg ⁻¹)	b (m ³ mol ⁻¹)	n_s (-)	R^2	q_{\max} (mol kg ⁻¹)	β (mol ² kJ ⁻²)	E (kJ mol ⁻¹)	R^2
Cu ²⁺	0.112	3.51	1.02	0.971	0.0765	-0.0291	4.15	0.968
Cd ²⁺	0.0381	8.79	1.01	0.984	0.0354	-0.0204	4.95	0.974
Pb ²⁺	0.142	9.71	0.905	0.999	0.12	-0.0151	5.75	0.979

Table 4.3 Comparison between maximum sorption capacities (q_{\max}) for various sorbents

Sorbent	q_{\max} (mol kg ⁻¹)	pH	Reference
<i>Caulerpa lentillifera</i>	Pb(0.14) > Cu(0.13) > Cd(0.042)	5.0	This work
Juniper wood	Cd(0.0283)	4.8-5.6	Shin et al., 2007
Granular Activated Carbon	Cu(0.043) > Cd(0.0219)	5.4-5.7	Üçer et al., 2006
<i>Oryza sativa</i> L. husk	Pb(0.0415)	5	Zulkali et al., 2006
Coir	Pb(0.0912)	5.5	Conrad and Hansen, 2006
Zeolite clinoptilolite	Cu(0.405) > Pb(0.13) > Cd(0.043)	6.2	Sprynskyy et al., 2006
Pine bark	Cu(0.149) > Cd(0.126)	n.d.	Ko et al., 2004
Rice husk ash	Pb(0.061)	5.6-5.8	Feng et al., 2004
Na-Montmorillonite	Pb(0.0462)	5	Abollino et al., 2003
Turkish Beypazari low rank coal	Pb(0.0655)	5	Arpa et al., 2000
<i>Aspergillus niger</i>	Cu(0.073) > Pb(0.049) > Cd(0.035)	5.0	Kapoor and Viraragharan, 1999

n.d. = not defined

Figure 4.3 Sips and Langmuir isotherm plots for metal ion sorptions by *Caulerpa lentillifera* (same conditions as in Table 4.2)

4.4 Energy of sorption vs Biosorption mechanism

Dubinin-Radushkevich isotherm model (Eqs 2.3.1 and 2.3.2) was used to estimate the sorption energy. Again, STATISTICA was employed for nonlinear parameter fitting and the model parameters are shown in Table 4.2. The analysis from the Dubinin-Radushkevich isotherm showed that the mean sorption energies were 4.15, 4.95, and 5.75 kJ mol⁻¹ for Cu²⁺, Cd²⁺, and, Pb²⁺, respectively. Smith (1981) illustrated that the range of energy of sorption at 2 – 20 kJ mol⁻¹ could be considered physiosorption in nature. Therefore it was possible that physical means such as electrostatic force played a significant role as a sorption mechanism for the sorption of heavy metal ions in this work.

4.5 Effect of pH

The resulting sorption isotherm curves are illustrated in Fig. 4.4 which shows that sorption capacities decreased with decreasing pH. This was because of a higher concentration of positive charged hydrogen ion at lower pH which could compete with the heavy metal ion for the sorption on the binding site, and hence, resulted in a decrease in sorption capacity. On the other hand, an increase in pH meant a lower quantity of protons, which caused a decrease in the competition between proton and heavy metal ion. Hence, an increase in the sorption capacity (or removal efficiency) could be observed. In addition, the negative surface charge of the biomass also decreased when the pH was decreased (see Appendix A). This might be due to the sorption of proton on the functional groups of algal biomass resulting in a higher proportion of protonated site. This led to a lower ability in sequestering positively charged contaminants such as heavy metal ions at low pH. To ensure no interference from metal precipitation, subsequent experiments were carried out at pH less than or equal to 5. The modeling for such phenomenon is discussed in Section 4.7.2.

According to Table 4.4, the maximum sorption capacity (q_{\max}) was highest for the sorption of Pb²⁺ followed by Cu²⁺ whereas sorptions of Cd²⁺ were rather low. Cd²⁺ was the lowest uptaken metal among the three as its associated q_{\max} was the lowest for all pH levels examined in this work. The b value had different order for each pH, however, Pb²⁺ was always found to have the highest b value indicating the highest affinity to the binding site of this biomass.

Table 4.4 Effect of pH on Langmuir isotherm parameters for metal ion sorption by dried *Caulerpa lentillifera*

Metal ion	pH	Langmuir parameters	Accuracy (R^2)
Pb^{2+}	5	$q_{max} = 0.14 \text{ mol kg}^{-1}$ $b = 14.3 \text{ m}^3 \text{ mol}^{-1}$	0.99
	4	$q_{max} = 0.12 \text{ mol kg}^{-1}$ $b = 5.8 \text{ m}^3 \text{ mol}^{-1}$	0.97
	3	$q_{max} = 0.08 \text{ mol kg}^{-1}$ $b = 2.6 \text{ m}^3 \text{ mol}^{-1}$	0.97
	1.5	$q_{max} = 0.07 \text{ mol kg}^{-1}$ $b = 0.8 \text{ m}^3 \text{ mol}^{-1}$	0.91
Cu^{2+}	5	$q_{max} = 0.13 \text{ mol kg}^{-1}$ $b = 2.9 \text{ m}^3 \text{ mol}^{-1}$	0.99
	4	$q_{max} = 0.1 \text{ mol kg}^{-1}$ $b = 1.9 \text{ m}^3 \text{ mol}^{-1}$	0.96
	3	$q_{max} = 0.07 \text{ mol kg}^{-1}$ $b = 1.1 \text{ m}^3 \text{ mol}^{-1}$	0.97
	1.5	$q_{max} = 0.05 \text{ mol kg}^{-1}$ $b = 0.5 \text{ m}^3 \text{ mol}^{-1}$	0.90
Cd^{2+}	5	$q_{max} = 0.042 \text{ mol kg}^{-1}$ $b = 8.1 \text{ m}^3 \text{ mol}^{-1}$	0.98
	4	$q_{max} = 0.035 \text{ mol kg}^{-1}$ $b = 2.6 \text{ m}^3 \text{ mol}^{-1}$	0.95
	3	$q_{max} = 0.022 \text{ mol kg}^{-1}$ $b = 1.7 \text{ m}^3 \text{ mol}^{-1}$	0.99
	1.5	$q_{max} = 0.016 \text{ mol kg}^{-1}$ $b = 1.6 \text{ m}^3 \text{ mol}^{-1}$	0.96

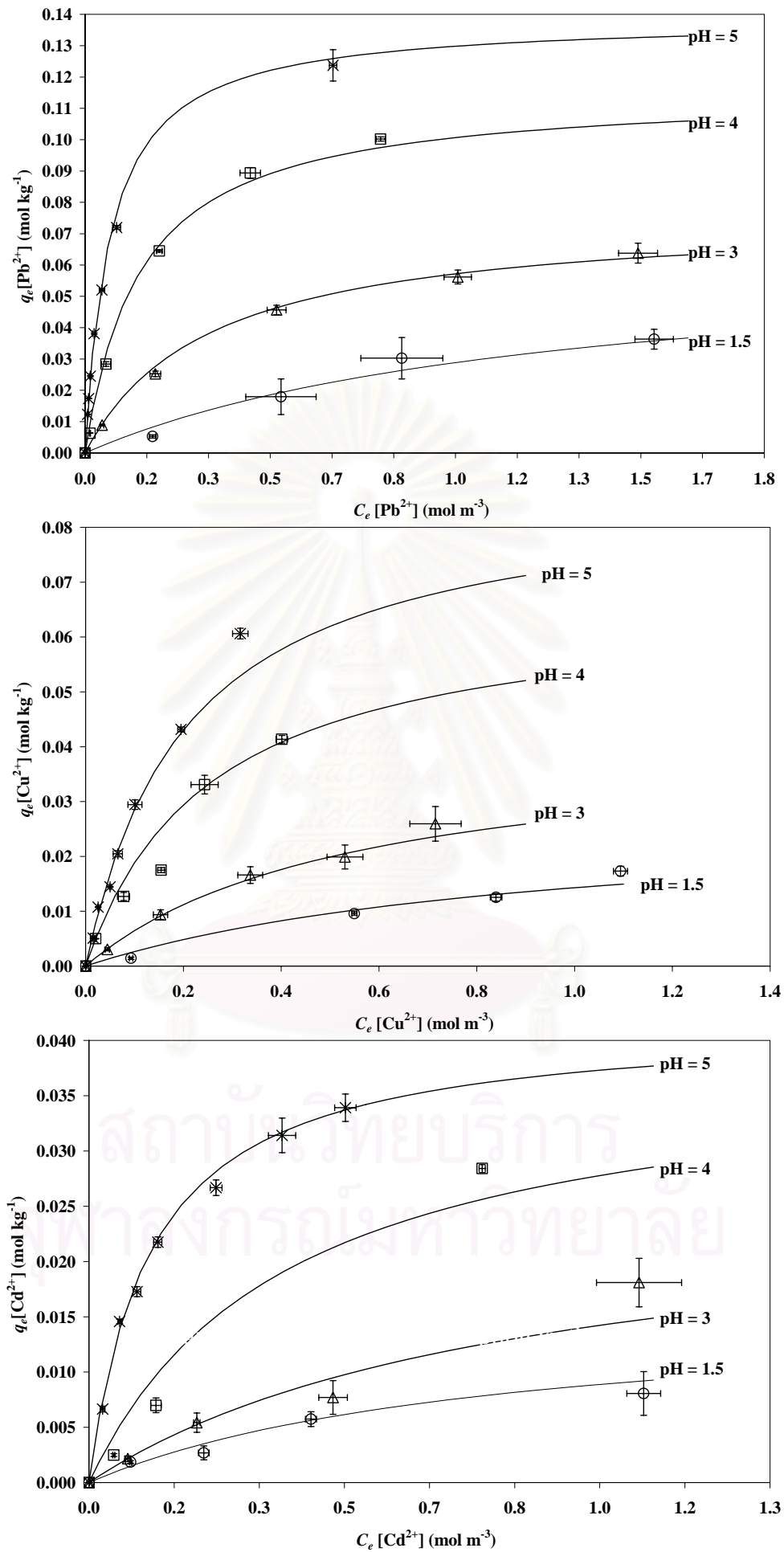


Figure 4.4 Effect of pH on sorption isotherms

4.6 Biosorption of heavy metal in binary component and modeling

To ensure the applicability of biosorption technology, more works are still needed for the sorption of a mixture of heavy metals at various operating conditions. Recent reports on the sorption of multi-component systems include that of Al-Asheh *et al.* (2000) who studied the binary sorption of Cu^{2+} , Cd^{2+} , and Ni^{2+} by pine bark using the extended Langmuir (based on competitive sorption), extended Freundlich, extended Sips, and IAST models. They found that these models could be used to describe the sorption of some binary metal systems including Cu^{2+} - Cd^{2+} , Cu^{2+} - Ni^{2+} , and Cd^{2+} - Ni^{2+} . Hammami *et al.* (2002) employed three Langmuir type models, based on competitive, uncompetitive, and multi-component sorptions, to explain the effect of Pb^{2+} on the sorption of other metals, *i.e.* Cu^{2+} , Cd^{2+} , and Zn^{2+} , by activated sludge. The results indicated that a competitive uptake was the most appropriate model, and Pb^{2+} was the most preferentially uptaken species. Ma and Tobin (2003) reported the applicability of the extended Langmuir models based on competitive sorption for the binary sorptions of Cr^{3+} - Cu^{2+} , Cr^{3+} - Cd^{2+} , and Cu^{2+} - Cd^{2+} on peat biomass. Lee and Suh (2001) examined the effect of Al^{3+} on the sorptions of Cr^{3+} , Pb^{2+} , Cu^{2+} , Cd^{2+} , and Zn^{2+} by Ca-loaded *Sargassum fluitans* biomass using a modified multi-component Langmuir isotherm (based on competitive concept). They reported that the presence of Al ion greatly diminished the uptakes of other heavy metals except that of Cr^{3+} . Alimohamadi *et al.* (2005) found that the modified Freundlich model was a better model than the modified Langmuir model in predicting the binary sorption of Pb^{2+} and Cu^{2+} by *Rhizopus arrhizus*. All the above findings suggested that, although the binary sorption could be well described using various types of models, the extended Langmuir using the competitive sorption concept was generally more commonly employed than others.

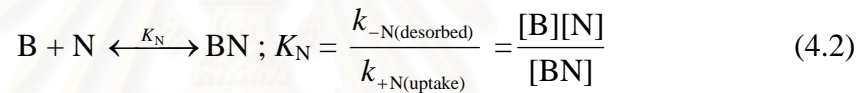
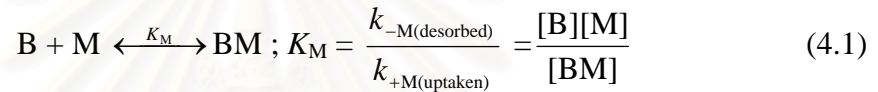
This section was intended to investigate the suitability of various types of multi-component sorption isotherm models in predicting the binary sorption of Cu^{2+} , Cd^{2+} , and Pb^{2+} . Three dimensional sorption isotherm surfaces of each binary component system were generated where the sorption behavior could be clearly illustrated.

4.6.1 Model development for binary component systems

Three different Langmuirian isotherm models with distinctive assumptions were selected for the investigation of the sorption of each pair of heavy metal species. The three assumptions were: (i) the sorption was competitive, (ii) the sorption was uncompetitive, and (iii) the sorption was partially competitive. This was to be able to identify the type of sorption taken place in each binary system.

(i) Competitive model (Model A)

The competitive model was developed under the concept of the original Langmuir model for single component systems where one binding site was only available for one sorbate. This can be written in a mathematical form as follows (Hammami *et al.*, 2002 and Ma and Tobin, 2003):



where M represents the first sorbate (metal) in the solution, N the second sorbate (metal) in the solution, B the free binding site, K_M and K_N the equilibrium constants of the binding site for metals 'M' and 'N', respectively. BM and BN were the binding sites occupied with metals 'M' and 'N', respectively. The mass balance equation for this case could be written as:

$$[B_t] = [B] + [BM] + [BN] \quad (4.3)$$

Assuming that the sorption system rapidly reached the equilibrium resulting in no changes of [BM] and [BN] with respect to time:

$$\frac{d[BM]}{dt} = 0 \text{ and } \frac{d[BN]}{dt} = 0 \quad (4.4)$$

Combining Eqs. 4.1 to 4.4 leads to:

$$[BM] = \frac{([B_t]/K_M)[M]}{1 + (1/K_M)[M] + (1/K_N)[N]} \quad (4.5)$$

Eq. 4.5 is well known as an extended Langmuir model for binary-component competitive sorption which can be written into Langmuirian type equation as expressed in Eq. 4.6:

$$q[M] = \frac{q_m b_M C_e [M]}{1 + b_M C_e [M] + b_N C_e [N]} ; b_M = 1/K_M \text{ and } b_N = 1/K_N \quad (4.6)$$

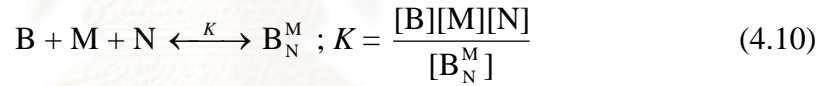
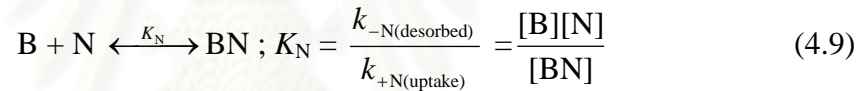
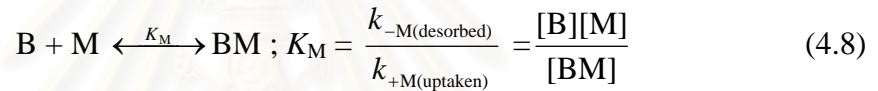
where the total metal uptake (for the two metals) can be expressed as Eq. 4.7:

$$q[M+N] = q[M] + q[N] = q_m \frac{b_M C_e[M] + b_N C_e[N]}{1 + b_M C_e[M] + b_N C_e[N]} \quad (4.7)$$

where $q[M]$ and $q[N]$ are the sorption capacities of metals 'M' (primary component) and 'N' (secondary component), respectively, $q[M+N]$ the sum of uptakes of the two metal components, $C_e[M]$ and $C_e[N]$ the equilibrium concentrations of metals 'M' and 'N', respectively, q_m the maximum sorption capacity for the binary components system, b_M and b_N the affinity constants of Langmuir model for the primary and secondary metal components, or 'M' and 'N', respectively.

(ii) *Uncompetitive model (Model B)*

This model was developed based on the assumption that the two sorbates could be simultaneously uptaken on the same binding site. The equilibrium reaction equations and the mass balance equation based on this assumption can be expressed as:



$$[B_t] = [B] + [BM] + [BN] + [B_N^M] \quad (4.11)$$

$$\frac{d[BM]}{dt} = \frac{d[BN]}{dt} = \frac{d[B_N^M]}{dt} = 0 \quad (4.12)$$

Combining these equations results in

$$[BM] + [B_N^M] = \frac{[M]\{[B_t] + [B_t](K_M / K)[N]\}}{K_M + [M] + (K_M / K_N)[N] + 2(K_M / K)[M][N]} \quad (4.13)$$

Eq. 4.13 can be rearranged in Langmuirian form as:

$$q[M] = \frac{q_{\max} (b_M C_e[M] + b' C_e[M] C_e[N])}{1 + b_M C_e[M] + b_N C_e[N] + b'(C_e[M])(C_e[N])} \quad (4.14)$$

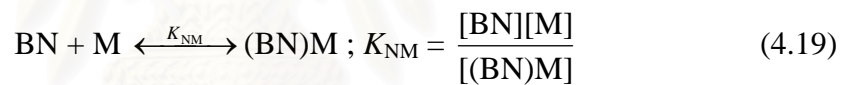
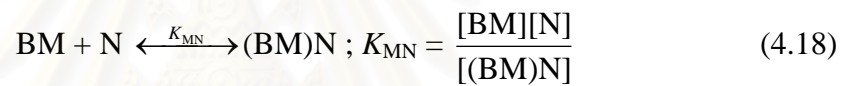
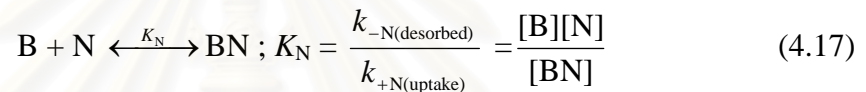
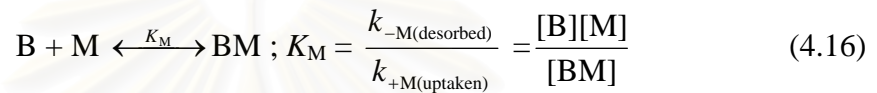
and the total uptake for the two metals as:

$$q[M+N] = q[M] + q[N] = \frac{q_{\max} (b_M C_e[M] + C_e[N] + 2b'(C_e[M])(C_e[N]))}{1 + b_M C_e[M] + b_N C_e[N] + b'(C_e[M])(C_e[N])} \quad (4.15)$$

where $q[M]$, $q[N]$, $q[M+N]$, $C_e[M]$, $C_e[N]$, q_m , b_M , and b_N take the same meanings with the Model A, K and b' are the equilibrium constant and the affinity constant for the simultaneous bonding of two metals with the same binding site, respectively.

(iii) *Partial competitive model (Model C)*

The partial competitive isotherm model was developed based on the assumption that one sorbate could attach onto only one binding site, and that the sorbate could also attach to the occupied binding sites. This meant that the occupied binding sites (with one metal) could form another linkage with other sorbates. The chemical equilibrium reaction equations and the mass balance equation based on this assumption can be expressed as:



$$[B_t] = [B] + [BM] + [BN] + [(BM)N] + [(BN)M] \quad (4.20)$$

$$\frac{d[BM]}{dt} = \frac{d[BN]}{dt} = \frac{d[(BM)N]}{dt} = \frac{d[(BN)M]}{dt} = 0 \quad (4.21)$$

Combining these equations results in

$$[BM] + [BNM] = \frac{([B_t] / K_M)[M] + ([B_t] / K_N)(1 / K_{NM})[M][N]}{1 + (1 / K_M)[M] + (1 / K_N)[N] + ((1 / K_M)(1 / K_{MN}) + (1 / K_N)(1 / K_{NM}))[M][N]} \quad (4.22)$$

Eq. 4.22 can be rearranged in Langmuirian form as:

$$q[M] = \frac{q_{\max}(b_M + b_N b_{NM} C_e[N])(C_e[M])}{1 + b_M C_e[M] + b_N C_e[N] + (b_M b_{MN} + b_N b_{NM})(C_e[M])(C_e[N])} \quad (4.23)$$

and the total uptake for the two metals as:

$$q[M+N] = q[M] + q[N] = \frac{q_{\max}(b_M C_e[M] + b_N C_e[N] + (b_M b_{MN} + b_N b_{NM})(C_e[M])(C_e[N]))}{1 + b_M C_e[M] + b_N C_e[N] + (b_M b_{MN} + b_N b_{NM})(C_e[M])(C_e[N])} \quad (4.24)$$

where K_{MN} is the equilibrium constant for metal 'N' with the binding site that is already occupied with metal 'M', K_{NM} the equilibrium constant for the bonding of metal 'M' with the binding site already occupied with metal 'N', b_{MN} and b_{NM} the affinity constants for metal 'N' with the binding site already occupied with metal 'M', and for metal 'M' with the binding site already occupied with metal 'N', respectively. Other parameters have the same meanings as those mentioned in Model B.

4.6.2 Model selection and interpretation

Parameters employed to verify the model prediction were: (i) the coefficient of determination (R^2), (ii) average of %Error, and (iii) relative standard distribution (RSD) of %Error. These are calculated from:

$$R^2 = 1 - \frac{\sum_{i=1}^N (q_i - q_{c,i})^2}{\sum_{i=1}^N (q_i - \bar{q})^2} \quad (4.25a)$$

$$E_i = \left| \frac{q_i - q_{c,i}}{q_i} \right| \quad (4.25b)$$

$$\text{Average of \%Error (\%)} = \frac{100 \times \sum_{i=1}^N E_i}{N} \quad (4.25c)$$

$$\text{RSD of \%Error (\%)} = 100 \times \sqrt{\frac{\sum_{i=1}^N (E_i - \bar{E})^2}{N \bar{E}^2}} \quad (4.25d)$$

where q_i is the actual sorption capacity at point i , $q_{c,i}$ the predicted sorption capacity at the same point as q_i , \bar{q} the average of actual sorption capacity from all experimental data, E_i the error at point i , \bar{E} the average of error from all experimental data, and N the number of experimental data.

The parameter assessment for each binary system was obtained from the non-linear estimation using STATISTICA version 6 and the results are summarized in Table 4.5. One obvious finding from this parameter estimation was that the parameter b' of Model B always had negative value which potentially indicated that the two heavy metal ions could not simultaneously bonded on the same binding site. Hence, the assumption of uncompetitive sorption became insignificant and was thereafter discarded from further consideration.

Table 4.5 Parameters of binary sorption isotherms

Metal system*	Model	$q_m \pm \sigma_{q_m}$ (mol kg ⁻¹)	$b_M \pm \sigma_{b_M}$ (m ³ mol ⁻¹)	$b_N \pm \sigma_{b_N}$ (m ³ mol ⁻¹)	$b' \pm \sigma_{b'}$ (m ³ mol ⁻¹)	$b_{MN} \pm \sigma_{b_{MN}}$ (m ³ mol ⁻¹)	$b_{NM} \pm \sigma_{b_{NM}}$ (m ³ mol ⁻¹)	Average %Error (%)	RSD of %Error (%)	R ²
Pb ²⁺ -Cu ²⁺	A	0.07 ± 0.004	44 ± 8.6	8 ± 1.3	-	-	-	22.8	21.7	0.80
	B	0.09 ± 0.01	25 ± 4	4.8 ± 0.7	-54 ± 6	-	-	-	-	-
	C	0.09 ± 0.01	25 ± 4	4.7 ± 0.5	-	1.3 ± 0.2	5.3 ± 1.3	16.5	21	0.89
Pb ²⁺ - Cd ²⁺	A	0.09 ± 0.01	21 ± 6.2	1 ± 0.2	-	-	-	30.9	37.2	0.74
	B	0.10 ± 0.01	24 ± 4.9	1.2 ± 0.1	-51 ± 8	-	-	-	-	-
	C	0.11 ± 0.01	20 ± 4.5	0.9 ± 0.17	-	0.6 ± 0.25	11 ± 1.2	25.1	23.6	0.87
Cu ²⁺ - Cd ²⁺	A	0.06 ± 0.01	10 ± 2.4	2.1 ± 0.4	-	-	-	37.4	57.5	0.68
	B	0.09 ± 0.01	5 ± 1.4	1.2 ± 0.3	-7.8 ± 1.4	-	-	-	-	-
	C	0.10 ± 0.01	4 ± 1.5	1 ± 0.3	-	1.4 ± 0.51	5.5 ± 0.49	31.7	46.6	0.78

* Primary metal (M) – Secondary metal (N)

A high R^2 , low average of percentage error (Average of %Error), and low relative standard deviation of percentage error (RSD of %Error) as shown in Table 4.5 for Model C suggested that the predictions from this model conformed well to experimental data. Model A also performed well in this regards but a lower R^2 than that of Model C meant that the accuracy of the predictions of Model C was superior. Hence, in the subsequent analysis of the three dimensional sorption isotherm surfaces, only Model C was employed.

Figs. 4.5 to 4.7 illustrate the three dimensional sorption isotherm surfaces of the binary mixture. It was noticed that the presence of secondary metal ion in the system, most of the time, resulted in a decrease in the sorption capacity of the primary metal. This antagonistic competitive effect was both observed for the sorption capacity of each single metal ion and for the total sorption capacity, particularly at high concentration range. This indicated that there was a competitive sorption between the two metals on the surface of this algal biomass. For example, the sorption capacity of Pb^{2+} was about $0.081 \text{ mol kg}^{-1}$ in a single component system (at the equilibrium concentration of $0.35 \text{ mol-Pb}^{2+} \text{ m}^{-3}$), but this was reduced to approx. $0.071 \text{ mol-Pb}^{2+} \text{ kg}^{-1}$ (12% decrease) with the presence of Cu^{2+} (at $0.1 \text{ mol-Cu}^{2+} \text{ m}^{-3}$ equilibrium concentration) and vice versa, the sorption capacity of Cu^{2+} was about $0.056 \text{ mol-Cu}^{2+} \text{ kg}^{-1}$ (at $0.35 \text{ mol-Cu}^{2+} \text{ m}^{-3}$ equilibrium concentration), and this was reduced to $0.028 \text{ mol-Cu}^{2+} \text{ kg}^{-1}$ (49% decrease) with the presence of Pb^{2+} at 0.1 mol m^{-3} equilibrium concentration.

Table 4.6 summarizes the percentage reduction in the sorption capacities of the primary metal ion when there was a secondary metal ion presented in the system. It was interesting to note that Pb^{2+} as secondary ions more effectively decreased the sorption capacity of Cu^{2+} than the effect of Cu^{2+} to Pb^{2+} . Similar effect was also observed for the mixture between Pb^{2+} and Cd^{2+} . This potentially implied that the sorption of Pb^{2+} by *Caulerpa lentillifera* biomass was more favorable than the sorptions of the other two metal ions. For the pair of Cu^{2+} and Cd^{2+} , Table 4.6 illustrates that the uptake of Cd^{2+} decreased more significantly with the presence of Cu^{2+} than the uptake of Cu^{2+} with the presence of Cd^{2+} . This indicated that Cu^{2+} was more preferable to be uptaken than Cd^{2+} .

Table 4.6 Percentage reduction in sorption capacity of primary metal ion (at $C_e = 0.35 \text{ mol m}^{-3}$) with the presence of secondary metal ion (at $C_e = 0.1 \text{ mol m}^{-3}$)*

2 nd ion \ 1 st ion	Cu ²⁺	Cd ²⁺	Pb ²⁺
Cu ²⁺	-	1.3 ± 1.2	12 ± 1.9
Cd ²⁺	6 ± 5.7	-	5.2 ± 2.3
Pb ²⁺	49 ± 7.6	26 ± 20	-

* Equilibrium concentrations (C_e) of primary and secondary metal ions were arbitrarily selected to illustrate the antagonistic effect.

Figs. 4.5(c), 4.6(c), and 4.7(c) reveal that, at a low range of equilibrium concentration for all mixtures, the total sorption increased with the presence of the secondary metal ion. This was due to the large availability of binding sites and therefore the competitive effect appeared to be insignificant. As more metals were presented in the system, the availability of binding sites when compared with the metal became limited, and hence, the competition among the metal ions was more obvious.

Table 4.5 illustrates that the total sorption capacities, q_m , were approx. 0.09, 0.11, 0.10 mol kg⁻¹ for Pb²⁺-Cu²⁺, Pb²⁺-Cd²⁺, and Cu²⁺-Cd²⁺ binary mixtures, respectively. This indicated that there was a limitation in the maximum sorption capacities at about 0.1 mol kg⁻¹. In addition, it was observed that b_M and b_N were always higher than b_{NM} and b_{MN} . For instance, $b_{Pb^{2+}}$ (24.56 m³ mol⁻¹) in the Pb²⁺-Cu²⁺ system was higher than $b_{Cu^{2+} - Pb^{2+}}$ (5.30 m³ mol⁻¹) and $b_{Cu^{2+}}$ (4.70 m³ mol⁻¹) higher than $b_{Pb^{2+} - Cu^{2+}}$ (1.30 m³ mol⁻¹). Based on the model assumptions, this finding could lead to a potential supposition that metal ions showed higher sorption affinity in bonding with the free binding site than with the binding sites occupied with another metal ion. In other words, the metal may not be easily bonded with the occupied binding sites.

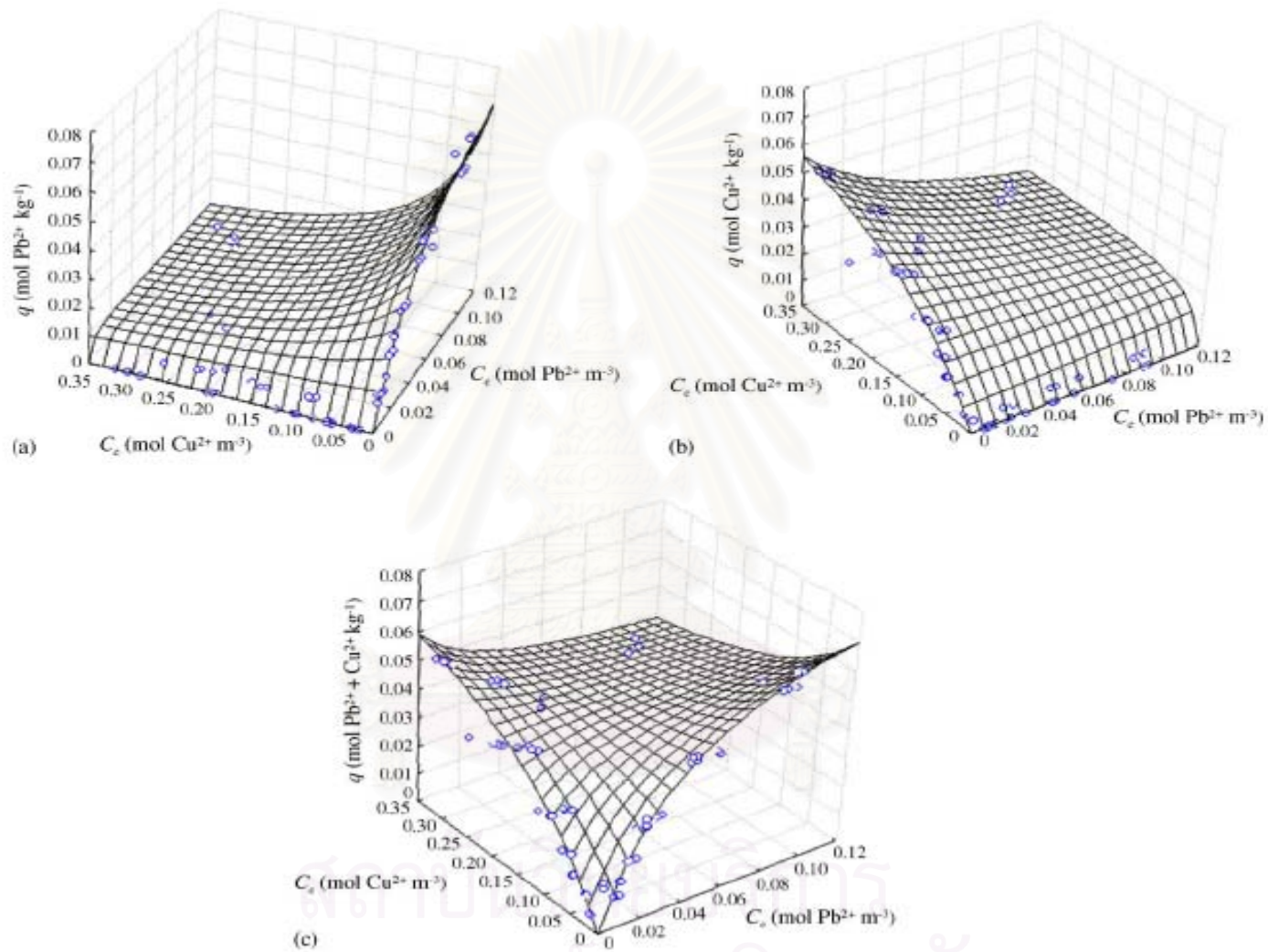


Figure 4.5 Three-dimensional sorption isotherm surface for Pb^{2+} - Cu^{2+} system. (a) Sorption capacity of Pb^{2+} ; (b) sorption capacity of Cu^{2+} ; (c) total sorption capacities ($\text{Pb}^{2+} + \text{Cu}^{2+}$).

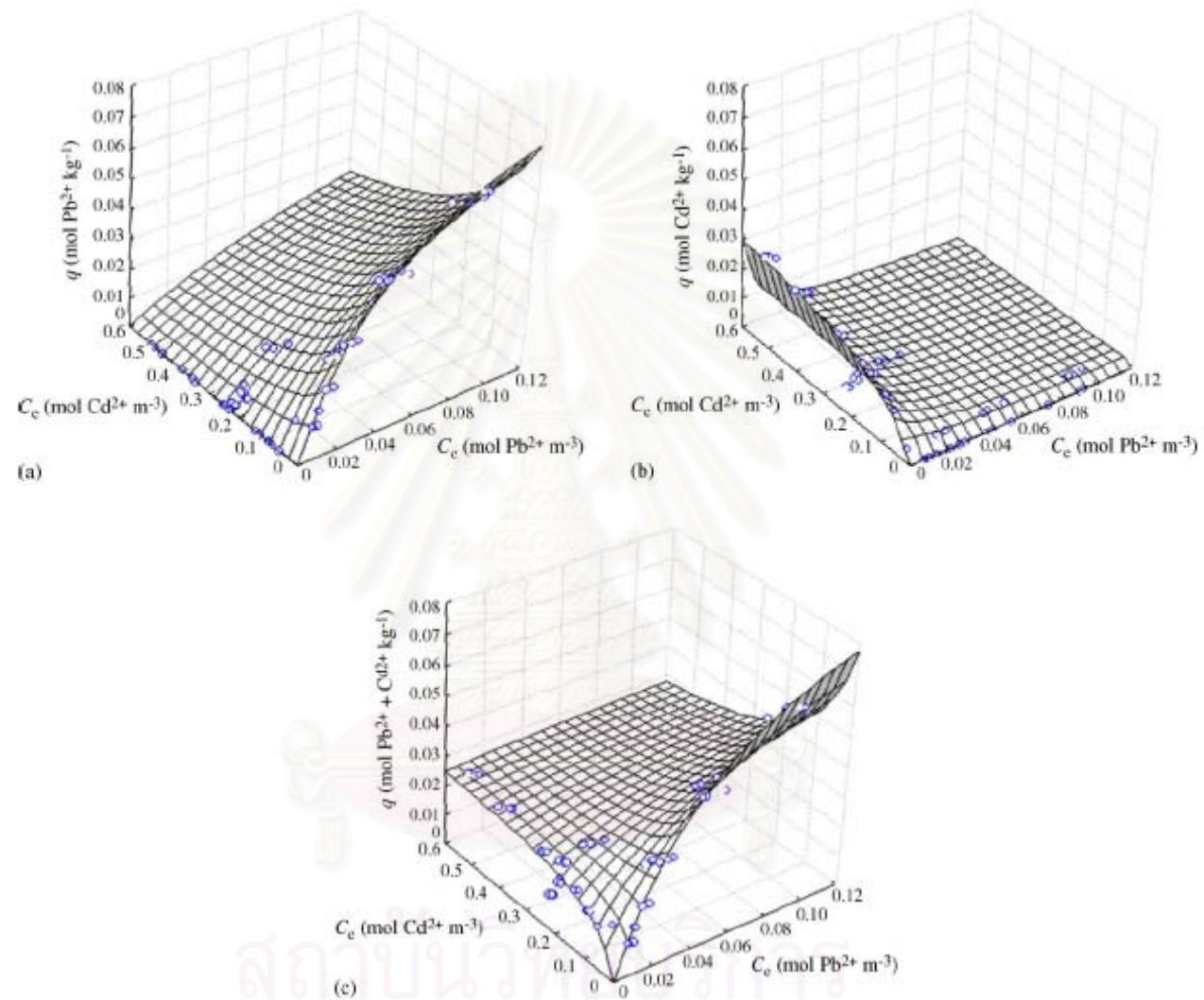


Figure 4.6 Three-dimensional sorption isotherm surface for Pb^{2+} – Cd^{2+} system. (a) Sorption capacity of Pb^{2+} ; (b) sorption capacity of Cd^{2+} ; (c) total sorption capacity ($\text{Pb}^{2+} + \text{Cd}^{2+}$).

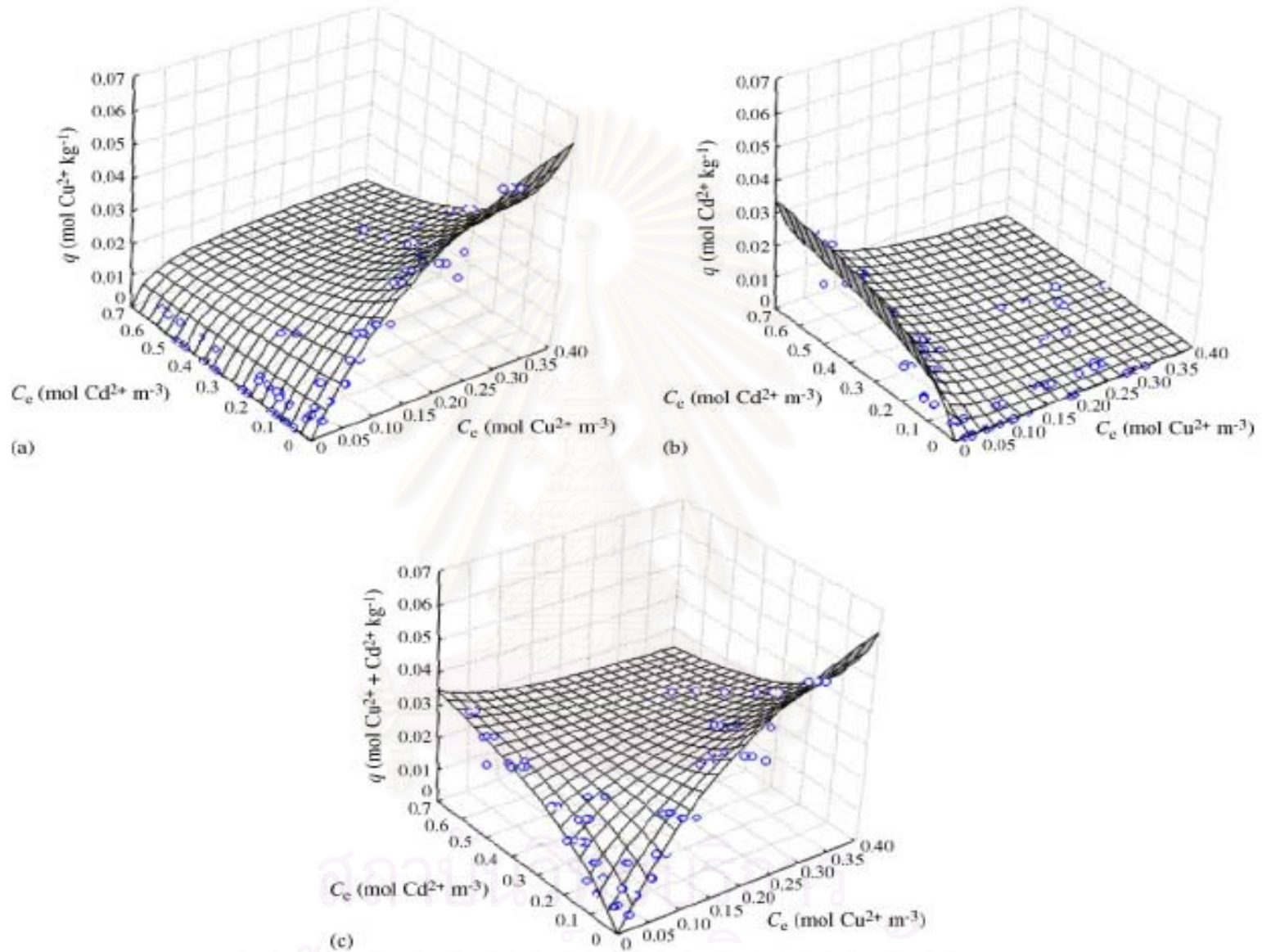


Figure 4.7 Three-dimensional sorption isotherm surface for Cu^{2+} - Cd^{2+} system. (a) Sorption capacity of Cu^{2+} ; (b) sorption capacity of Cd^{2+} ; (c) total sorption capacity ($\text{Cu}^{2+} + \text{Cd}^{2+}$).

4.7 Partial competitive model in describing the effect of pH on metal sorption

It could be seen from Table 4.4 that pH played an important role in the sorption of heavy metal ions. The fundamental explanation was that pH was inversely related to the quantity of positive charged hydrogen ion (proton). Therefore a solution with lower pH would accommodate a higher concentration of hydrogen ion than that with higher pH. This proton could compete with the heavy metal ion for the sorption on the available binding sites on the surface of the alga, and hence, resulted in a decrease in sorption capacity. This phenomenon could potentially be considered as a partial competitive effect between the metal ion and the proton. It could be that the metal ion could be attached on the free binding more easily than proton, and that the metal ion could be attached on the binding site pre-occupied by proton at a rate higher than proton being attached on the binding site pre-occupied by metal ion, and vice versa.

4.7.1 Modified partial competitive model for prediction effect of pH

Proton could be considered as another cation which interfered the sorption. The reaction of proton on the binding site could be demonstrated in a mathematical form as expressed in Eqs. 4.16 – 4.21 where N was replaced with H^+ (proton) and K_N was replaced with K_a (the acid dissociation equilibrium constant of binding site). Thus, Eq. 4.23 can be rearranged to:

$$q_e = \frac{(q_{\max,M} b_M 10^{\text{pH}} + q_{\max,HM} b_{HM} 10^{\text{p}K_a}) C_e}{(1 + b_M C_e) 10^{\text{pH}} + (1 + b_{HM} C_e) 10^{\text{p}K_a} + b_M b_{MH} C_e} \quad (4.26)$$

where $\text{p}K_a = -\log K_a$ and $\text{pH} = -\log [H^+]$, b_M takes the same meaning as that in Model C, $q_{\max,M}$ represents the maximum sorption capacity of metal ion on the free binding site, $q_{\max,HM}$ and b_{HM} the maximum sorption capacity and affinity constant of the metal ion on the binding site occupied by proton, respectively, b_{MH} the sorption affinity of proton on the binding site already occupied by metal ion.

Eq. 4.26 demonstrates that the equilibrium sorption capacity was a function of equilibrium concentration and equilibrium pH. This model was used to fit experimental data using the non-linear analysis where the model parameters are displayed in Table 4.7, and the results are shown in Fig 4.8.



Table 4.7 Parameters of the pH prediction model*

Metal	$q_{max,M} \pm \sigma_{q_{max,M}}$ (mol kg ⁻¹)	$q_{max,HM} \pm \sigma_{q_{max,HM}}$ (mol kg ⁻¹)	$b_M \pm \sigma_{b_M}$ (m ³ mol ⁻¹)	$b_{HM} \pm \sigma_{b_{HM}}$ (m ³ mol ⁻¹)	$b_{MH} \pm \sigma_{b_{MH}}$ (m ³ mol ⁻¹)	$pK_a \pm \sigma_{pK_a}$ (-)	Average %Error (%)	RSD of %Error (%)	R^2
Pb ²⁺	0.13 ± 0.01	0.05 ± 0.00	19 ± 1.2	1.2 ± 0.20	0.09 ± 0.00	4.4 ± 0.5	15.5	22.5	0.98
Cu ²⁺	0.13 ± 0.02	0.04 ± 0.00	2.9 ± 0.5	0.7 ± 0.3	0.10 ± 0.01	4.1 ± 0.7	18.0	18.1	0.96
Cd ²⁺	0.044 ± 0.004	0.016 ± 0.003	80 ± 9.7	1.3 ± 0.4	0.10 ± 0.02	6 ± 0.8	17.7	15.5	0.96

* M = Metal ion, H = Hydrogen ion

สถาบันวิทยบริการ
จุฬาลงกรณ์มหาวิทยาลัย

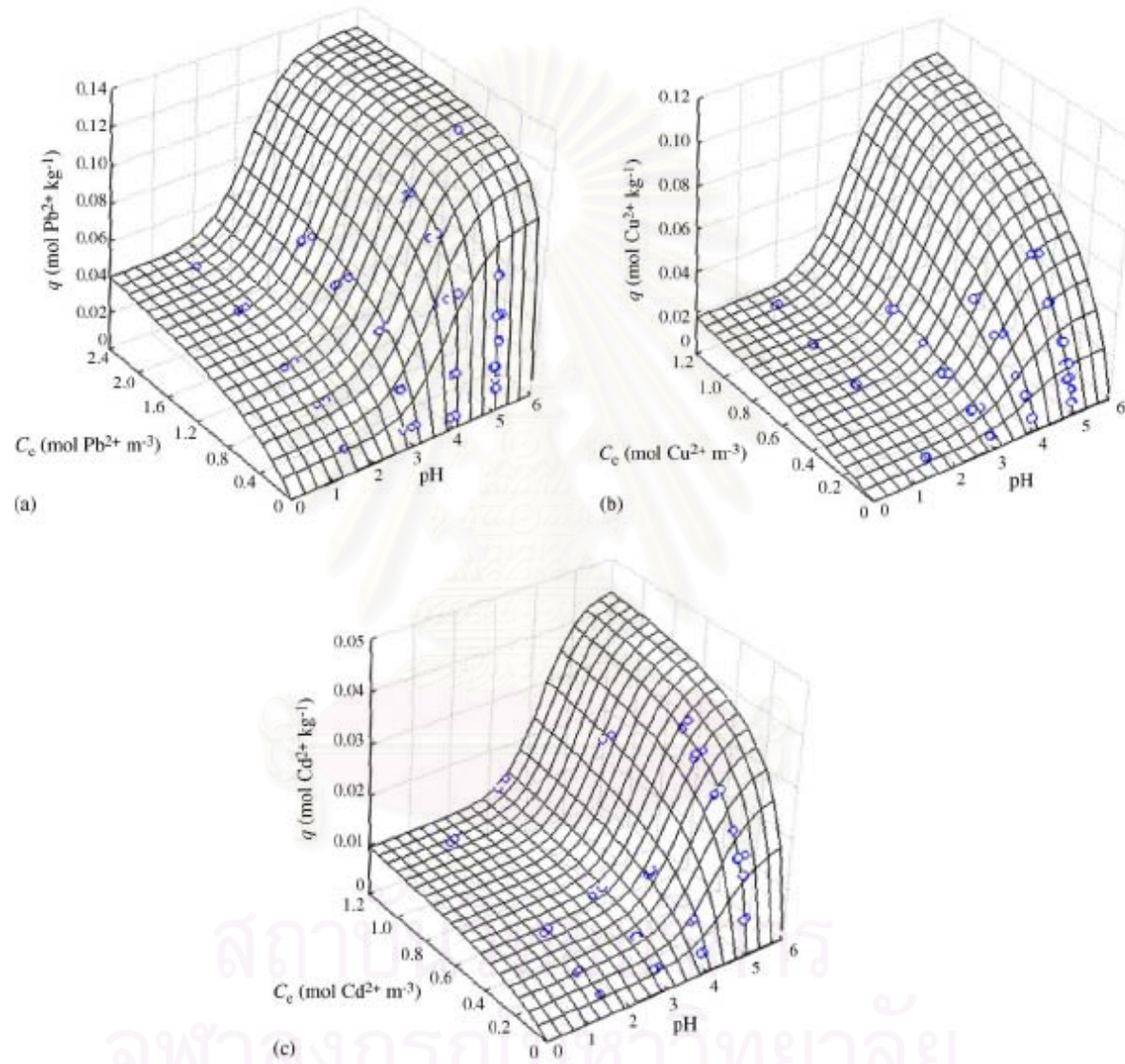


Figure 4.8 Effect of pH on equilibrium sorption capacity on *Caulerpa lentillifera*. (a) Pb^{2+} ; (b) Cu^{2+} ; (c) Cd^{2+} .

The high R^2 of more than 0.95 illustrated that the model prediction agreed reasonably well with experimental data. This indicated that the partial competitive model could be applied for the prediction of pH effect on the sorption using *Caulerpa lentillifera*. The results from Table 4.7 indicated that pK_a of Cd^{2+} was about 6 while those of Cu^{2+} and Pb^{2+} were about 4. This could imply a different main sorption site for Cd^{2+} from those for Cu^{2+} and Pb^{2+} . In addition, the maximum sorption capacity and sorption affinity of each metal on the free binding site ($q_{max,M}$, b_M) were always higher than those of metal on the same binding site pre-occupied by proton ($q_{max,HM}$, b_{HM}). This suggested that the sorption of metal mainly occurred on the free binding site rather than on the binding site already occupied by proton. However, the later binding site could also be responsible for the sorption of these metals but at different capacity and affinity. It could be that the sorption of metal to this biomass was by physical means such as electrostatic and van der waals force, and therefore the sorption could occur on both free and proton occupied binding sites. In the same way, the sorption affinity of proton attached on the binding site pre-occupied by metal ion (b_{MH}) was always lower than that of metal on both free and proton occupied binding sites (b_M , b_{HM}). This suggested that proton might not be a favorably positive charged species for the binding site in the alga when compared with the metal ion species.

4.7.2 Prediction of q_{max} and b

It can be observed from Table 4.4 that the maximum sorption capacity (q_{max}) and sorption affinity (b) changed with pH. Hence, the relationship between q_{max} and b , and pH must be determined. This could be achieved using the following technique. For single metal systems, Langmuir equation can be expressed as in Eq. 2.28 where the maximum sorption capacity q_{max} could be estimated from the limit theorem:

$$q_{max} = \lim_{C_e \rightarrow \infty} q_e \quad (4.27)$$

Similarly, the sorption affinity (b) could be determined by

$$\lim_{C_e \rightarrow 0} (q_e/C_e) = b q_{max} \quad (4.28)$$

Thus;

$$b = \frac{\lim_{C_e \rightarrow 0} (q_e / C_e)}{q_{\max}} = \frac{\lim_{C_e \rightarrow 0} (q_e / C_e)}{\lim_{C_e \rightarrow \infty} q_e} \quad (4.29)$$

This concept could be applied to the partial competitive model to predict the effect of pH on the sorption (Eq. 4.26) and the resulting expressions were obtained.

$$q_{\max}(\text{pH}) = \lim_{C_e \rightarrow \infty} q = \frac{(q_{\max, M} b_M 10^{\text{pH}} + q_{\max, \text{HM}} b_{\text{HM}} 10^{\text{pKa}})}{b_M 10^{\text{pH}} + b_{\text{HM}} 10^{\text{pKa}} + b_M b_{\text{MH}}} \quad (4.30)$$

$$b(\text{pH}) = \frac{\lim_{C_e \rightarrow 0} [q/C_e]}{q_{\max}(\text{pH})} = \frac{b_M 10^{\text{pH}} + b_{\text{HM}} 10^{\text{pKa}} + b_M b_{\text{MH}}}{10^{\text{pH}} + 10^{\text{pKa}}} \quad (4.31)$$

The results from applying Eqs. 4.30 and 4.31 in estimating the effect of pH are demonstrated in Figs. 4.9 and 4.10 where agreement between experimental data and model prediction was clearly observed. The maximum sorption capacity and sorption affinity increased with increasing pH following the S-shape curve. This meant that, at low pH, the amount of protonated binding site was higher than the unprotonated, and therefore resulting in low metal sorption character. Increasing pH resulted in an increase in the quantity of unprotonated binding sites, and hence, a higher metal metal sorption was observed. As the sorption reached its equilibrium, a further increase in pH no longer influenced the sorption characteristics and the sorption capacity was leveled off.

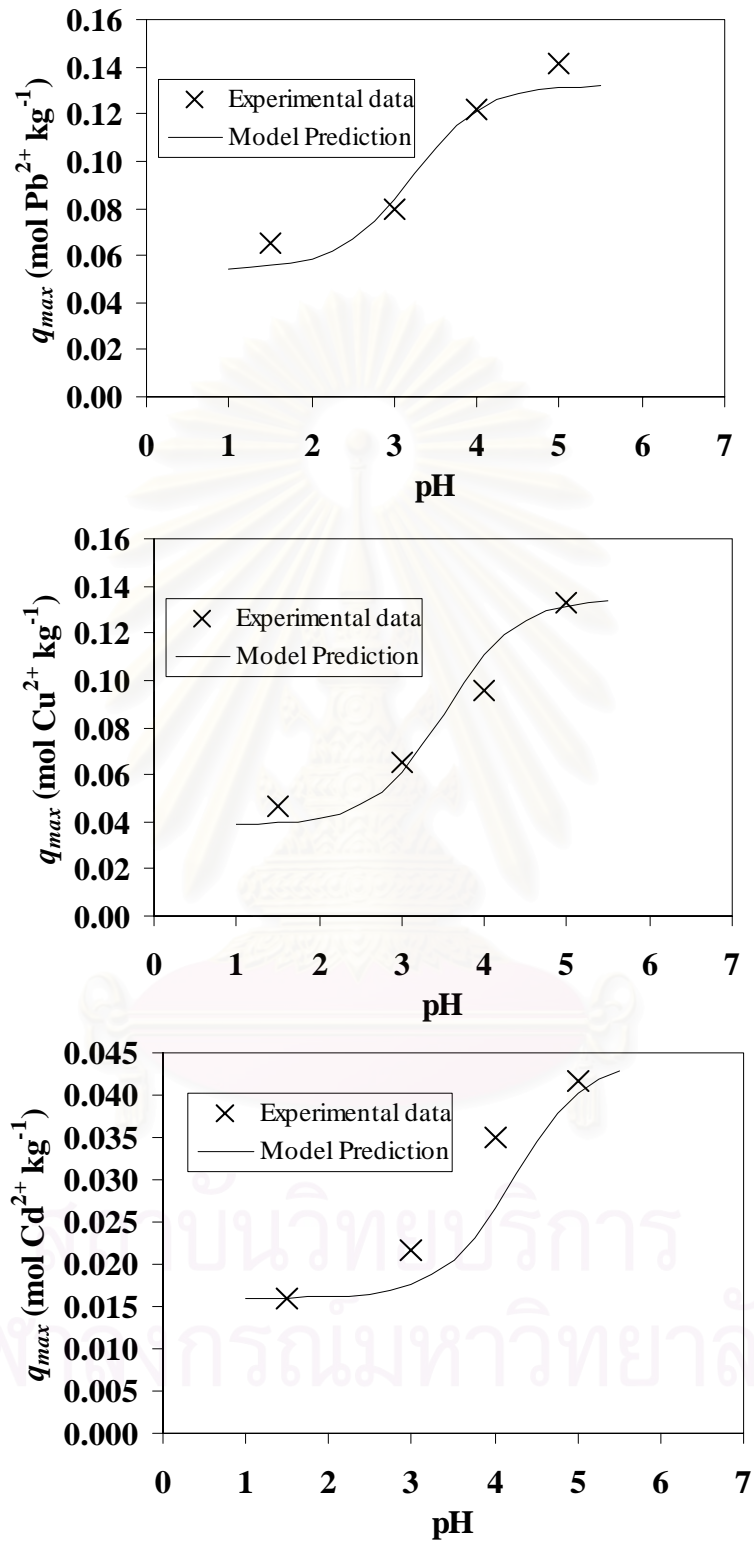


Figure 4.9 Relationships between maximum sorption capacity (q_{max}) and pH

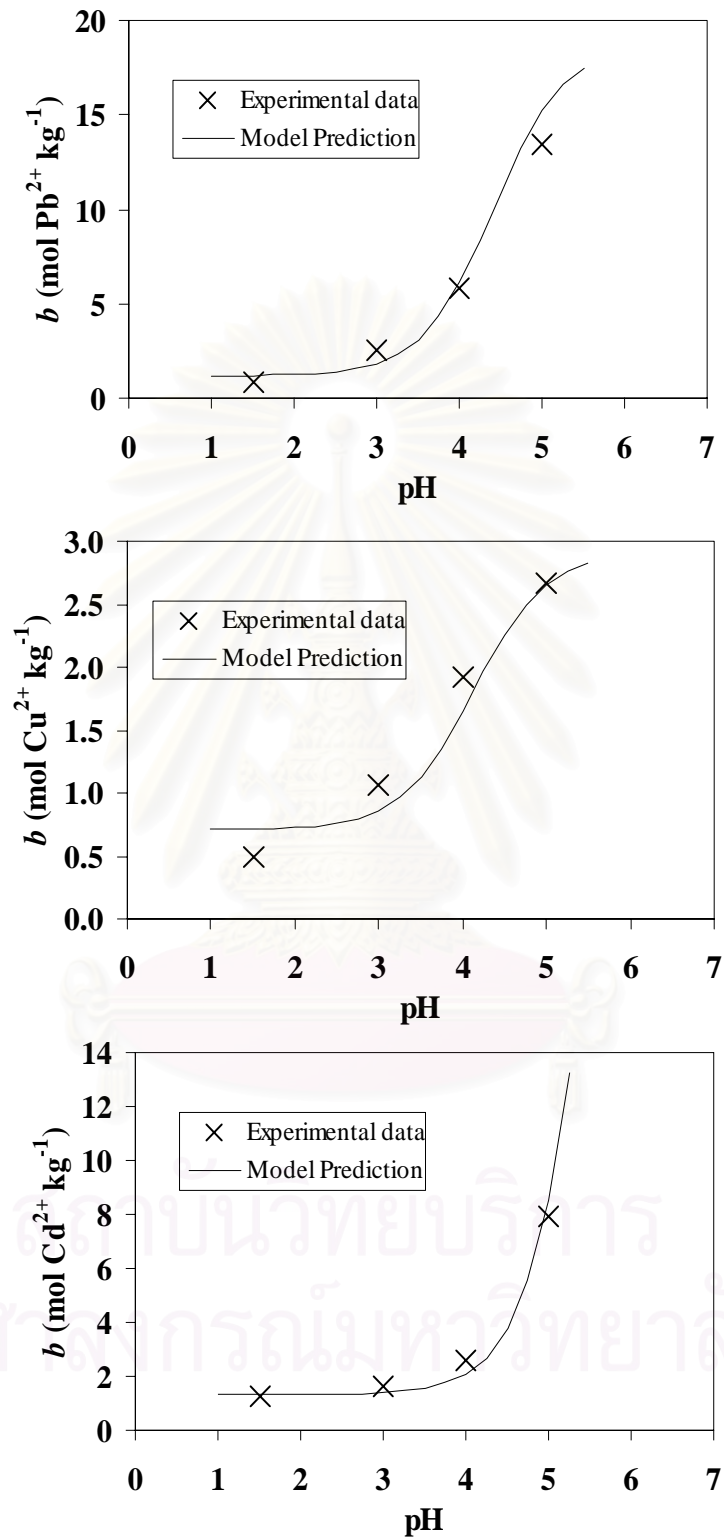


Figure 4.10 Relationships between sorption affinity (b) and pH

4.8 Potential sorption characteristics for metal sorption

Our previous work on the examination of the alga with FTIR revealed that possible functional groups involved in metal biosorption using *Caulerpa lentillifera* biomass were carboxyl, hydroxyl, sulfonate, amine, and amide (Apiratikul, 2003). Details of these functional groups are displayed in Table 4.8. This finding suggested that the sulfonate group in the algal biomass with pK_a of about 1.3 could be responsible for the sorption of Cu^{2+} , Cd^{2+} , and Pb^{2+} (as some experiments were carried out at pH as low as 1.5). In addition, the Hard and Soft Acid Base (HSAB) theory of Pearson stated that hard functional groups formed strong bonds with hard cations, soft functional groups formed strong bond with soft cations, whereas intermediate types could form bonds with any type of metals. As Cu^{2+} and Pb^{2+} were classified as intermediate type, whilst Cd^{2+} was soft (Pearson, 1963), Table 4.8 suggests that Cu^{2+} and Pb^{2+} could form bonds with all functional groups listed in this table while Cd^{2+} could mainly form bond with amine and amide groups and had difficulty in forming bonds with carboxyl, hydroxyl, and sulfonate groups. Due to the limitation on the availability of binding sites for Cd^{2+} , this theoretical interpretation might explain the finding that the sorption capacity of Cd^{2+} was always lower than those of Cu^{2+} and Pb^{2+} under the same operating conditions. This agrees with the results in Table 4.4. In fact, Table 4.7 suggests that the actual binding site for Cd^{2+} might be amine as, among all the functional groups presented in the alga, pK_a of amine ($pK_a = 8-11$) was nearest to the pK_a of the functional group of Cd^{2+} ($pK_a = 6$). However, data in Table 4.4 show that the maximum sorption capacity of Pb^{2+} was slightly higher than that of Cu^{2+} . This was due to the preferential sorption of Pb^{2+} to the binding site than Cu^{2+} . Pagnanelli et al. (2001) reported that the first hydrolysis equilibrium constant (no unit) of Pb^{2+} ($10^{-7.71}$) was higher than that of Cu^{2+} ($10^{-8.00}$) which indicated that Pb^{2+} had the higher attaching ability on the binding site than Cu^{2+} . This could also be the case for this biosorbent.

Table 4.8 Details of functional groups* involved with metal biosorption by *Caulerpa lentillifera*.

Functional group	Structural formula	pK_a	HSAB** classification
Carboxyl	$\begin{array}{c} \text{O} \\ \\ -\text{C} - \text{OH} \end{array}$	1.7 – 4.7	Hard
Hydroxyl	-OH	9.5 – 13	Hard
Sulfonate	$\begin{array}{c} \text{O} \\ \\ -\text{S} = \text{OH} \\ \\ \text{O} \end{array}$	1.3	Hard
Amine	-NH ₂	8 – 11	Intermediate
Amide	$\begin{array}{c} \text{O} \\ \\ -\text{C} - \text{NH}_2 \end{array}$	-	Intermediate

* Volesky, 2004

** Hard and Soft Acid Base theory of Pearson

สถาบันวิทยบริการ
จุฬาลงกรณ์มหาวิทยาลัย

4.9 Biosorption in fixed bed column

One of the main tools used in the investigation of the efficiency in adsorption columns is the breakthrough analysis. The breakthrough time (t_b) was defined as the time when the effluent concentration reached approx. 5% of the influent concentration ($C_{eff}/C_o = 0.05$) which represented the time that column was still active. The volume of the treated wastewater was determined by multiplying the breakthrough time with the volumetric flow rate (Q). In addition, sorbent usage dose can be determined at this point by dividing the sorbent mass in the column with the treated wastewater volume. The amount of heavy metal uptaken into the alga was determined by the mass conservation principle shown in Eq. 3.4.

The mass transfer zone (MTZ) is one of the parameters frequently employed to examine the effective height of the sorption column. MTZ is defined as the length of sorbing zone in the column which can be calculated from:

$$MTZ \text{ (cm)} = L \frac{t_e - t_b}{t_e} \quad (4.32)$$

where L refers to the bed height (cm), t_b time (min) to reach the breakthrough point or $C_{eff}/C_o = 0.05$, and t_e time (min) required to reach the exhaust point $C_{eff}/C_o = 0.95$. Several mathematical models had been proposed to describe the column performance. Thomas model (Thomas, 1948) was selected for describing the breakthrough for the fixed bed biosorption column in this study since it could be written in a simple form allowing a quick and easy interpretation of the results. Thomas model can be expressed as:

$$\frac{C_{eff}}{C_o} = \frac{1}{1 + e^{\frac{k_{TH} q_{mc} \rho_p A L}{Q} - k_{TH} C_o t}} \quad (4.33)$$

where C_{eff} represents the effluent heavy metal ion concentration (mol m^{-3}), C_o the initial heavy metal ion concentration (mol m^{-3}), k_{TH} Thomas rate constant ($\text{m}^3 \text{mol}^{-1} \text{min}^{-1}$), q_{mc} the maximum metal sorption capacity of the algal biomass (mol kg^{-1}), ρ_p the packing density (kg m^{-3}), A the cross sectional area of column (m^2), L the bed height of column (m), Q the volumetric flow rate ($\text{m}^3 \text{min}^{-1}$), and t the time pass after starting the operation of biosorption fixed bed column (min).

t_b , t_e can be determined by rearranging Eq. 4.33 to:

$$t_b = \frac{q_{mc}\rho_p AL}{QC_o} - \frac{\ln(19)}{k_{TH}} \quad (4.34a)$$

$$t_e = \frac{q_{mc}\rho_p AL}{QC_o} + \frac{\ln(19)}{k_{TH}} \quad (4.34b)$$

One of the advantages of Thomas model is the determination of the minimum bed depth of column (L_{min}) which is the depth the column required to reach the breakthrough immediately after operated. From the definition, substitution $t = 0$ and $C_{eff}/C_o = 0.05$ into Eq. 4.33 leads to:

$$L_{min} = \frac{Q\ln(19)}{Aq_{mc}\rho_p k_{TH}} = \frac{u\ln(19)}{q_{mc}\rho_p k_{TH}} \quad (4.35)$$

where u is superficial velocity (equal to Q/A).

To evaluate the efficiency of sorption column, the retardation factor (r_f) is often employed to determine the rate at which the contaminants move within the column, i.e. the contaminant will move faster in the system with lower r_f than that in the system with higher r_f . In fact, r_f is determined from the treated volume per void volume that gives $C_{eff}/C_o = 0.5$. Replacing $C_{eff}/C_o = 0.5$ to Eq. 4.33 gives $t_{50\%}$:

$$t_{50\%} = \frac{q_{mc}\rho_p AL}{QC_o} = \frac{q_{mc}\rho_p L}{uC_o} = \frac{q_{mc}m}{QC_o} \quad (4.36)$$

Therefore

$$\begin{aligned} V_{50\%} &= Q \times t_{50\%} = \frac{q_{mc}m}{C_o} \\ r_f &= \frac{V_{50\%}}{V_v} = \frac{V_{50\%}}{(AL)\varepsilon} = \frac{q_{mc}m}{(AL)C_o\varepsilon} = \frac{q_{mc}\rho_p}{C_o\varepsilon} \\ r_f &= \frac{q_{mc}\rho_p}{C_o\varepsilon} \end{aligned} \quad (4.37)$$

The results of bed depth and flow rate on breakthrough curve of each heavy metal in the biosorption column are shown in Figs. 4.11 and 4.12, respectively. This revealed that Pb^{2+} required the longest time period to reach the breakthrough concentration than the other metals in all cases at the same condition. This emphasized again that this alga had the greatest sorption capacity for Pb^{2+} . In addition, the figures show that the column service time decreased when the bed depth was decreased and the flow rate was increased. The parameters for the column study such as breakthrough time, retardation factor, and parameters obtained from Thomas model are summarized in Table 4.9.

In this study, the lowest algal dose was obtained from operating the column with the flow rate of 6 mL min^{-1} with the bed volume of about 7.07 mL (bed height 4 cm) for all metal ions. The average sorption capacity in the unit of mol kg^{-1} calculated from the breakthrough curve could be prioritized from high to low as: Pb^{2+} (0.136) > Cu^{2+} (0.085) > Cd^{2+} (0.083). From Thomas model, the sorption capacities for the various metals could also be prioritized with the same order: Pb^{2+} (0.129) > Cu^{2+} (0.087) > Cd^{2+} (0.084). This agreed with the order of maximum sorption capacities obtained from Langmuir equation in batch experiments. In addition, the average retardation factors for the different metals also followed this order where: Pb^{2+} (410) > Cu^{2+} (276) > Cd^{2+} (229) from actual breakthrough curve and Pb^{2+} (429) > Cu^{2+} (283) > Cd^{2+} (241) from Thomas model parameters. This could be interpreted that algal biomass retained Pb^{2+} better than Cu^{2+} and Cd^{2+} , respectively.

MTZ in this study was found to increase with an increase in flow rate for all metals. MTZ was also found to expand over the length of the column and therefore the system with a greater length would see a longer MTZ at the very end of the column.

Table 4.9 Fixed bed biosorption parameters

Column operation	Pb ²⁺			Cu ²⁺			Cd ²⁺		
<i>L</i> (cm)	2	4	4	2	4	4	2	4	4
<i>Q</i> (mL min ⁻¹)	6.02	6.02	10.48	6.00	6.00	10.55	5.89	5.89	10.48
<i>u</i> (cm min ⁻¹)	3.41	3.41	5.93	3.39	3.40	5.97	3.33	3.33	5.93
ε (-)	0.57	0.42	0.35	0.57	0.42	0.42	0.57	0.42	0.42
<i>u_{pw}</i> (cm min ⁻¹)	6.02	8.03	16.77	6.00	8.00	14.07	5.89	7.86	13.98
Breakthrough analysis	Pb ²⁺			Cu ²⁺			Cd ²⁺		
<i>q</i> (mol kg ⁻¹)	0.158	0.149	0.101	0.076	0.103	0.077	0.085	0.091	0.072
<i>t_b</i> (min)	46	150	55	6	105	25	10	58	15
<i>t_{50%}</i> (min)	110	230	104	60	180	82	65	154	55
<i>t_e</i> (min)	240	360	172.5	226.5	260	190	175	312	150
<i>V_b</i> (mL)	277	903	576	36	630	264	59	342	157
Sorbent usage (g L ⁻¹)	1.81	1.11	1.74	13.90	1.59	3.79	8.49	2.93	6.38
<i>r_f</i> (-)	331	462	436	180	360	288	192	302	192
MTZ (cm)	1.62	2.33	2.72	1.95	2.38	3.47	1.89	3.26	3.60
Thomas model analysis	Pb ²⁺			Cu ²⁺			Cd ²⁺		
<i>q_{mc}</i> (mol kg ⁻¹)	0.159	0.121	0.107	0.072	0.109	0.081	0.086	0.093	0.075
<i>K_{TH}</i> (m ³ mol ⁻¹ min ⁻¹)	0.251	0.303	0.538	0.345	0.354	0.426	0.380	0.237	0.446
<i>R</i> ²	0.978	0.998	0.998	0.980	0.999	0.985	0.992	0.995	0.989
<i>t_b</i> (min)	13.5	121.8	49.6	0.0	98.4	8.5	0.0	34.0	4.6
<i>t_{50%}</i> (min)	122	235	107	62	182	85	69	158	60
<i>t_e</i> (min)	230	349	164	151	265	161	142	282	115
<i>V_b</i> (mL)	81	733	520	0	591	90	0	201	48
Sorbent usage (g L ⁻¹)	6.14	1.36	1.92	-	1.69	11.14	-	5.00	20.86
<i>r_f</i> (-)	367	472	448	187	364	298	203	310	209
MTZ (cm)	1.88	2.60	2.79	2.00	2.51	3.79	2.00	3.52	3.84
<i>L_{min}</i> (cm)	1.78	1.93	2.14	2.83	1.83	3.60	2.14	3.14	3.69

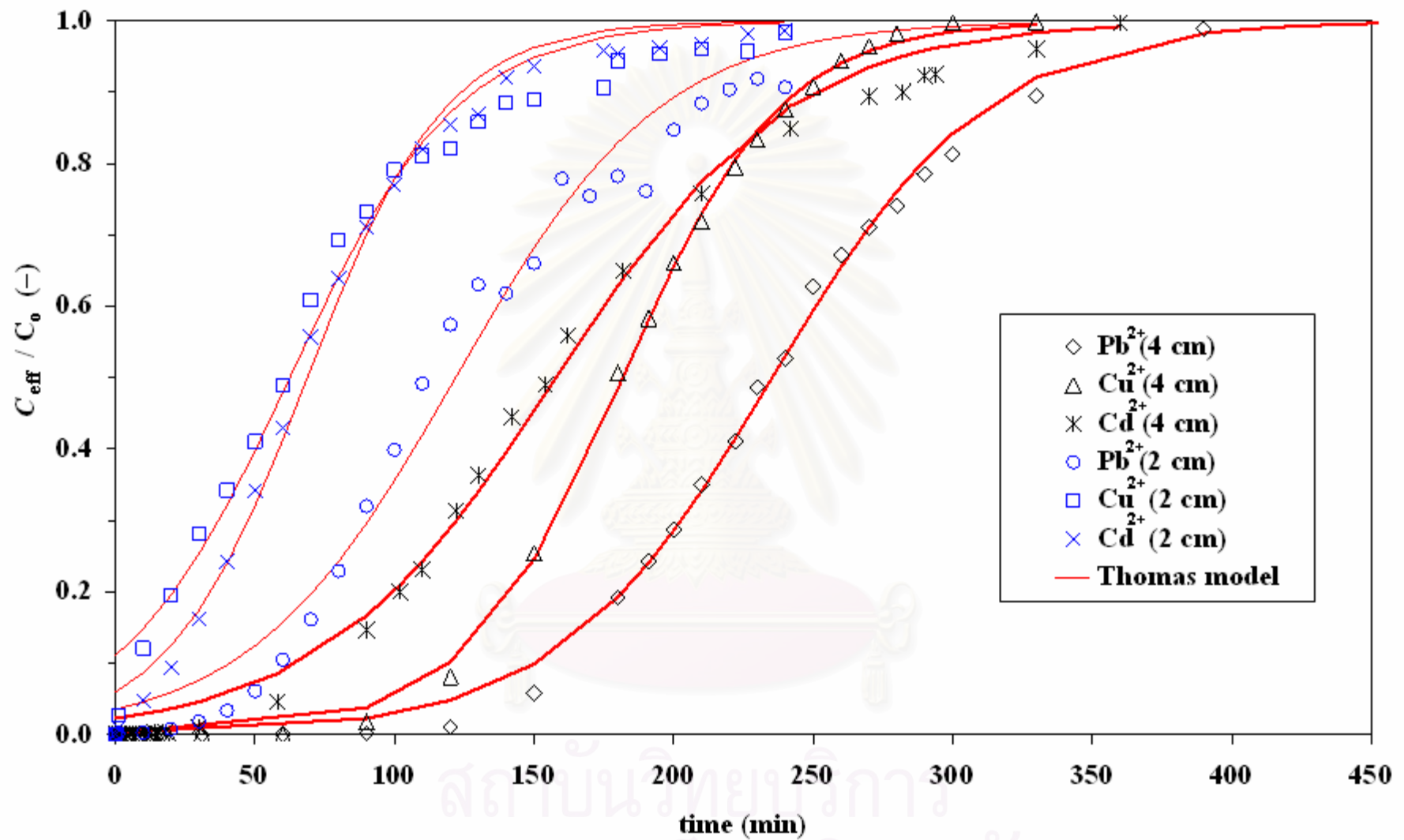


Figure 4.11 Effect of bed depth on breakthrough curve
 ($Q = 6 \text{ mL min}^{-1}$, $C_0 = 0.1 \text{ mol m}^{-3}$, $\text{pH} = 5$, $T = 294 \text{ K}$, $\rho_p = 140 \text{ kg m}^{-3}$)

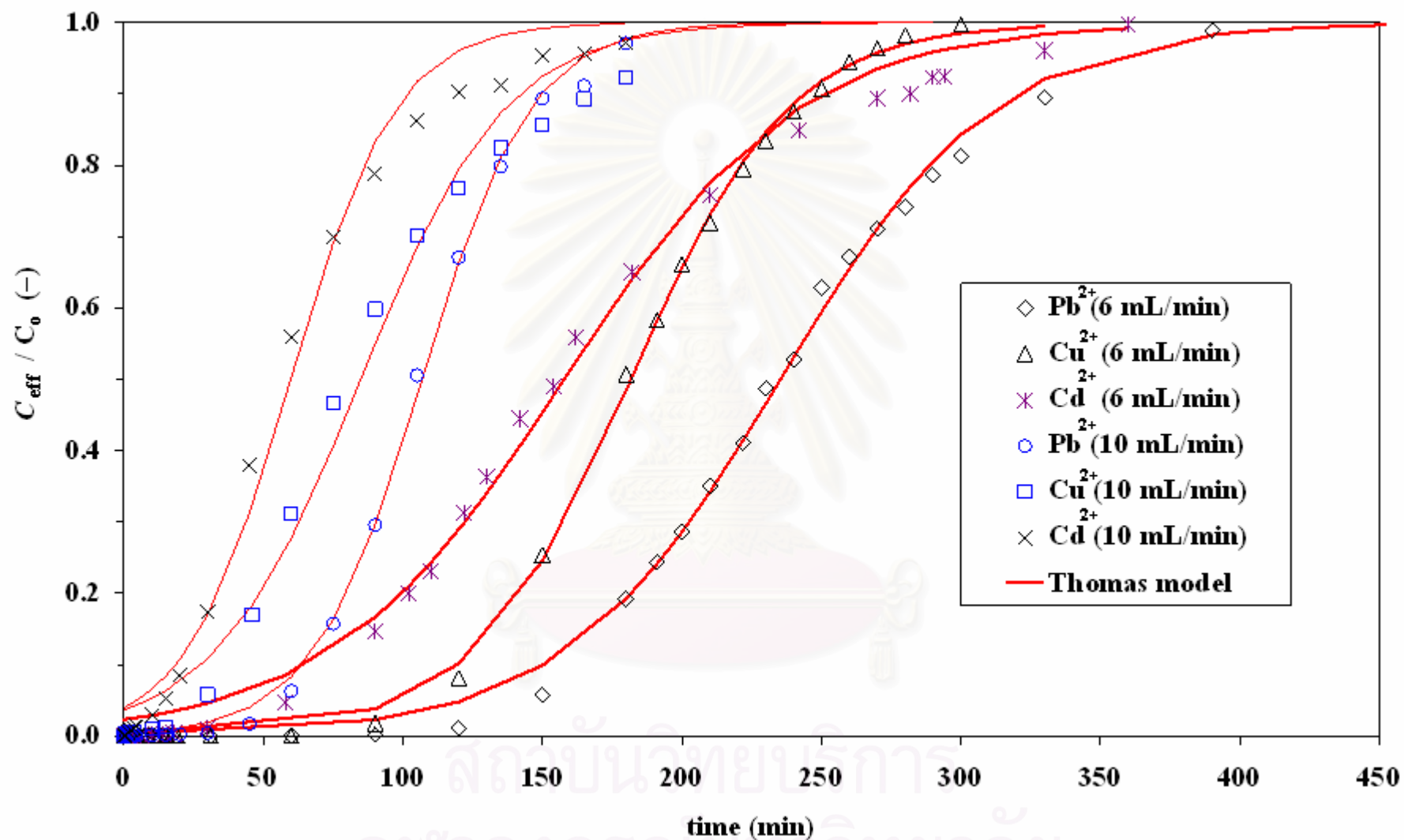


Figure 4.12 Effect of flow rate on breakthrough curve

($L = 4 \text{ cm}$, $C_0 = 0.1 \text{ mol m}^{-3}$, $\text{pH} = 5$, $T = 294 \text{ K}$, $\rho_p = 140 \text{ kg m}^{-3}$, Bed volume = 7.07 mL)

4.10 Metal release VS Biosorption mechanism

During the sorption in the fixed bed column, metals ions deposited in the algal biomass such as Ca^{2+} , Mg^{2+} etc. were observed to be released significantly. The releases of such metal elements suggested that ion exchange could play a significant role as a biosorption mechanism as the heavy metals could replace Ca^{2+} and Mg^{2+} in the algal structure. The amount of the metals released from the alga was calculated by integrating Ca^{2+} and Mg^{2+} concentration-volume profiles in Fig. 4.13 using Eq. 4.38 and the results are summarized in Table 4.10.

$$\text{Accumulated metal ion released (meq kg}^{-1}\text{)} = \frac{1000 \int_0^V C_{\text{released}}(V) dV}{m_{\text{biomass}}} \quad (4.38)$$

where $C_{\text{released}}(V)$ is the released metal concentration as a function of volume fed to the column (eq m^{-3}), V and m_{biomass} have the same meanings as those in Eq. 3.4.

Table 4.10 demonstrates that major ions involved in biosorption mechanism ordered from the most to the lesser significant were Ca^{2+} followed by Mg^{2+} and Mn^{2+} . It is interesting to note that, although the alga originally contained high amounts of Al^{3+} and some of K^{+} and Li^{+} (Apiratikul, 2003), these were only slightly released during the biosorption. It could be that Al^{3+} , K^{+} , and Li^{+} had different charges than Pb^{2+} , Cu^{2+} , and Cd^{2+} , and this could not be exchanged favorably with the heavy metal ions, or they might constitute the component in the solid state under the binding sites resulting in difficulties in the exchange with the metal ions. However, this conclusion could not be drawn from the findings in this work. The total metal released from the algal biomass was quite close to the amount of heavy metal uptake, especially for Cu^{2+} and Cd^{2+} which suggested that ion exchange was one of the main sorption mechanisms for the biosorption of heavy metals by this alga. However, the amount of Pb^{2+} uptaken by the algal biomass was found to be higher than that of total metal released (release = 83% of Pb^{2+} uptaken) indicating that Pb^{2+} could be adsorbed on some free binding sites in the biomass. In other words, the biosorption mechanism of Pb^{2+} involved both ion exchange and adsorption at the proportion of about 83% and 17%, respectively.

Table 4.10 Relationship between heavy metal uptake and metal release during biosorption

Heavy metal ion (M ²⁺)	Ca ²⁺ release (meq kg ⁻¹)	Mg ²⁺ release (meq kg ⁻¹)	Mn ²⁺ release (meq kg ⁻¹)	Al ³⁺ release (meq kg ⁻¹)	K ⁺ release (meq kg ⁻¹)	Li ⁺ release (meq kg ⁻¹)	Total release (meq kg ⁻¹)	M ²⁺ uptake (meq kg ⁻¹)	Release:uptake
Pb ²⁺	171	48	40	1	3	0	263	316	0.83
Cu ²⁺	92	22	30	0	5	1	150	151	0.99
Cd ²⁺	106	38	32	0	0	1	177	171	1.04

สถาบันวิทยบริการ
จุฬาลงกรณ์มหาวิทยาลัย

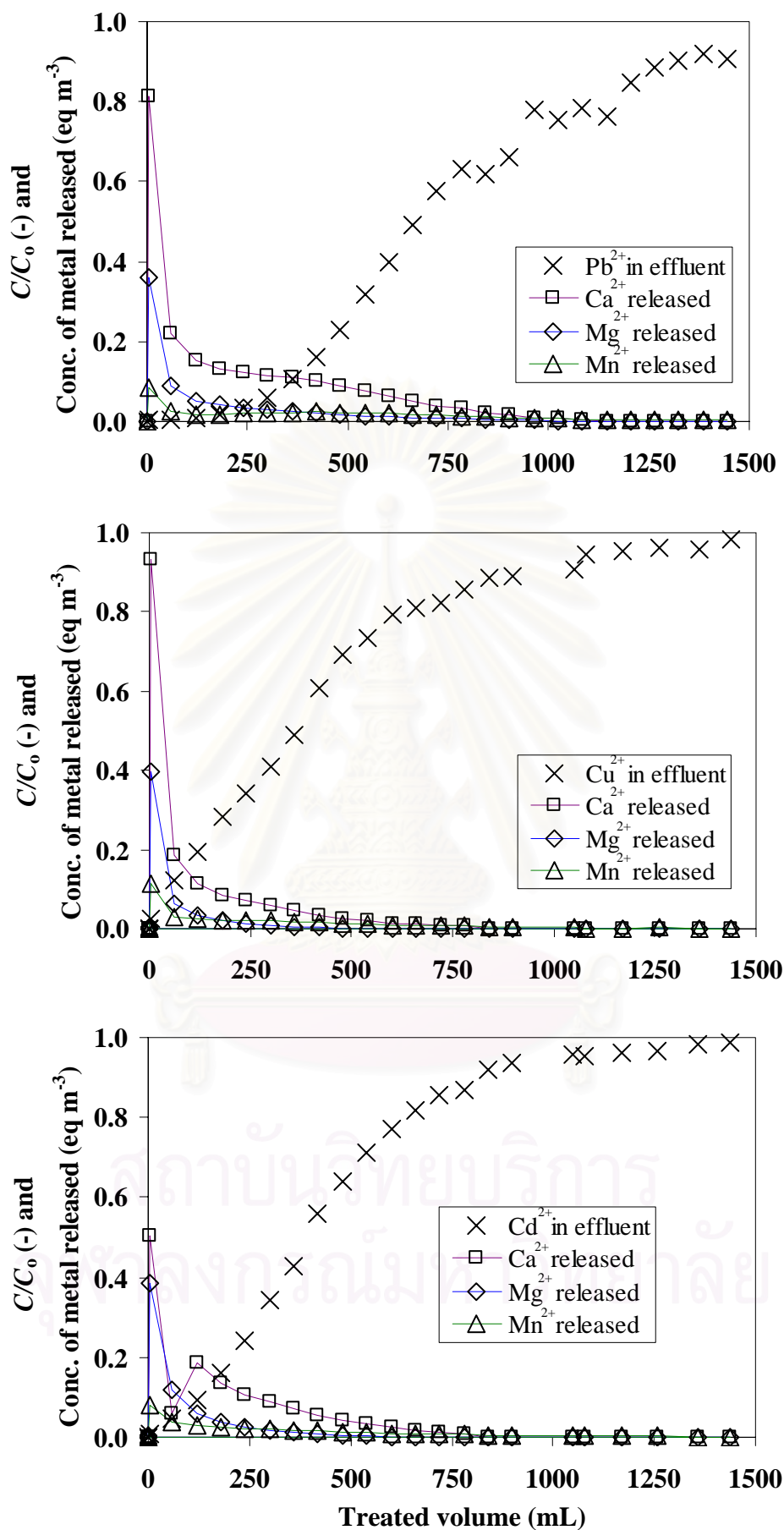


Figure 4.13 Amounts of metal ions released during the column sorption experiment ($C_0 = 0.1 \text{ mol m}^{-3}$, $\text{pH} = 5$, Flow rate = 6 mL min^{-1} , Bed depth = 2 cm, algal mass = 0.5 g , packing density = 141 g L^{-1})

4.11 Concluding remarks

This chapter demonstrated the biosorption of the three heavy metals ions (Cu^{2+} , Cd^{2+} , and Pb^{2+}) with dried biomass of the unwanted agricultural by-product, *Caulerpa lentillifera*. The sorption of these metal ions rapidly reached the equilibrium within 10-20 minutes. The smaller particle size of algal biomass provided the quicker time to reach equilibrium. However, there was no effect of particle size on equilibrium sorption capacity. The External mass transfer and intraparticle diffusion seemed to be the rate limiting step. The order of the maximum sorption capacity of this biomass was $\text{Pb}^{2+} > \text{Cu}^{2+} > \text{Cd}^{2+}$. The sorption occurred due potentially to the physical force between metal ions and the binding sites of the algal biomass as monolayer sorption character. The maximum sorption capacity and sorption affinity was found to be a function of pH.

The studying of binary component biosorption model using three concepts consist of competitive, uncompetitive, and partial competitive sorption isotherm models suggested that the partial competitive isotherm model could accurately predict the sorption performance. Antagonistic competitive effect was found to occur for the sorption in binary component systems where the sorption capacity of primary metal ion decreased with the presence of the secondary metal ions. The maximum sorption capacity of the pooled binding site of the two metal ions was about 0.1 mol kg^{-1} for the binary component system. It was also illustrated that the effect of pH on metal sorption on this biomass could well be explained using a similar type of isotherm model as that for the sorption of binary metal component systems. The experimental results matched with the HSAB theory of Pearson where the maximum sorption capacity of Cd^{2+} was always found to be lower than those of Cu^{2+} and Pb^{2+} .

The sorption capacities obtained from the column experiment was in the same range with those from the batch scale. The ion exchange was believed to be a principle mechanism of the sorption where metals originally attached onto the biomass structure were replaced by the heavy metal ions.

CHAPTER V

ZEOLITE FORMATION AND UTILIZATION FOR METAL SORPTION

5.1 Effect of NaOH:CFA

The effect of NaOH:CFA ratio on the CEC value of the product is displayed in Fig. 5.1. The increasing of the NaOH:CFA ratio resulted in an increase in CEC value for the range of the ratio between 0:1 to 2.5:1. However, CEC decreased when the ratio increased from 2.5:1 to 3:1. This may be due to the change of zeolite structure. Although the ratio of 2.5:1 seemed to give the highest sorption characteristics, the fusion product was very difficult to handle. Therefore the optimal weight ratio for the conversion of CFA to zeolite was suggested at 1.75:1. The CEC of the obtained zeolite (1.75:1) was about 140 meq / 100 g, a significantly higher figure than 6 – 7 meq / 100 g obtained from the original CFA. This implied the possibility in turning the modified CFA which was originally a waste from industrial activity, into high CEC value zeolite which could be applied in various environmental applications such as removing of heavy metal ions from wastewater. The obtained zeolite characterization was studied using several techniques described in Section 3.3.3 and the results are described in Section 5.2.

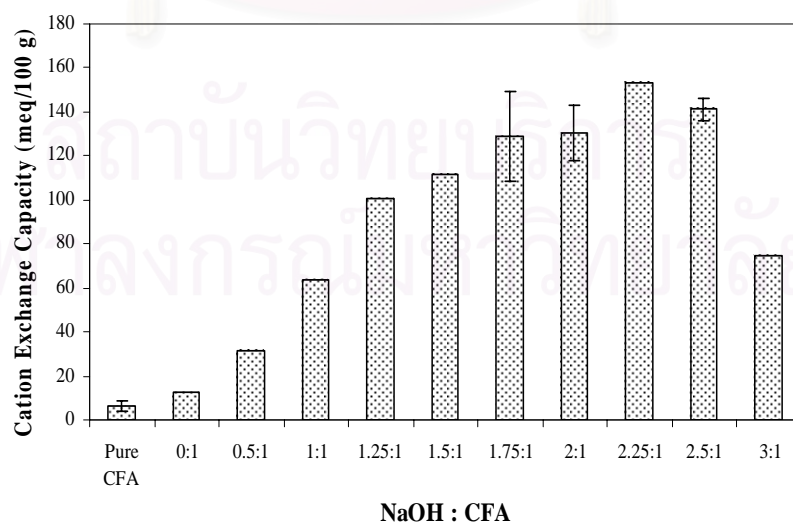


Figure 5.1 Effect of NaOH:CFA ratio on CEC

5.2 Sorbent characterization

The elemental composition analysis by XRF in Table 5.1 indicated that CFA contained large quantities of silica and alumina which are the two main components in zeolite. The XRD pattern in Fig. 5.2 suggests that the zeolite product was of X-type. The micrographs of CFA and zeolite were taken by Scanning Electron Microscope (SEM) and shown in Figs. 5.3(a) and 5.3(b), respectively. The figure shows that the zeolite obtained from modified CFA had rougher surface than original CFA. This was due to the the structure of CFA changed into crystal of zeolite X. The specific surface area (SAA) and specific pore volume (SPV) obtained from N₂-BET technique were 344 m² g⁻¹ and 0.4921 cm³ g⁻¹, respectively, while the values of CFA were about 47.71 m² g⁻¹ and 0.0649 cm³ g⁻¹, respectively. This meant modifying CFA to zeolite provided higher SAA and SPV than unmodified CFA. The density of the obtained zeolite determined by the gas pycnometer technique was 2.10 g cm⁻³ while that of CFA was 2.24 g cm⁻³ whereas the density of the zeolite and CFA determined by the water pycnometer technique were about 2.245 and 2.42 g cm⁻³, respectively. The particle size distribution in Fig. 5.4 shows that the size of zeolite fell in a range of 0.5 – 300 micron with an average of about 38.5 micron. Fig. 5.5 illustrates the relation between zeta potential and the pH of the solution and the results indicated that zeolite's surface had negative charge at pH higher than 3. In other words the Point of Zero Charge or PZC was less than 3. Hence, the zeolite could be used as sorbent for positively charged contaminants such as heavy metal ions above this pH range.

Table 5.1 Elemental composition of zeolite (amount in % by weight)

Parameter Amount (%)	Na	Mg	Al	Si	K	Ca	Ti	Mn	Fe	Rb	Sr	P	S	Zn
CFA	0.99	0.56	5.75	24.33	2.78	4.12	0.27	0.14	6.86	0.03	0.20	0.25	0.42	-
Obtained Zeolite	7.15	0.70	6.38	13.27	0.74	4.61	0.72	0.29	10.67	-	0.26	-	-	0.06

nd = not detected with the accuracy of the selected analytical method

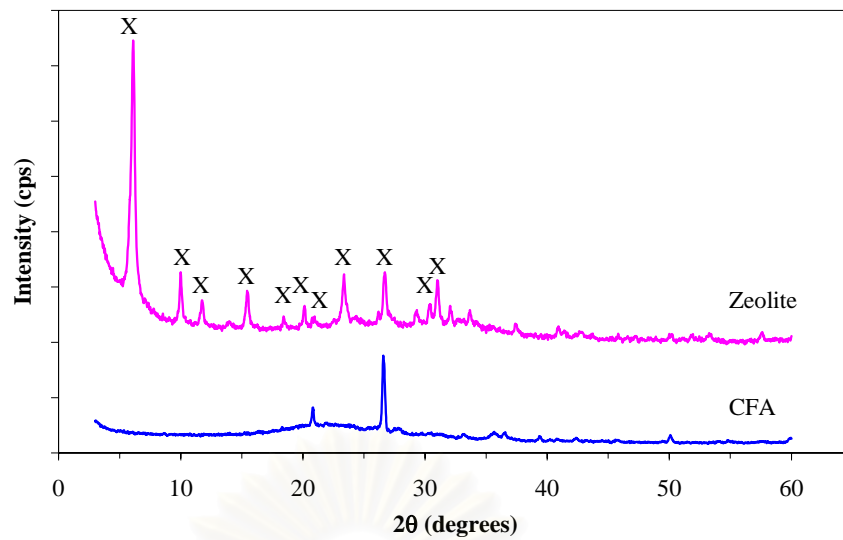


Figure 5.2 XRD characteristic peak of original CFA and obtained zeolite

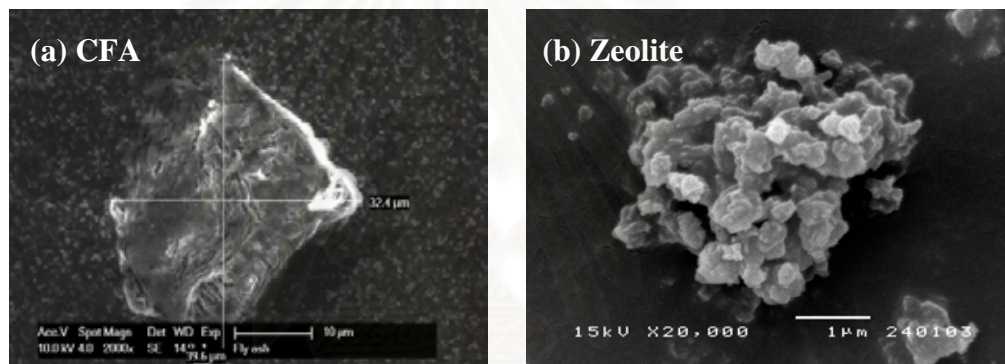


Figure 5.3 SEM micrograph of original CFA and obtained zeolite

สถาบันวิทยบริการ
จุฬาลงกรณ์มหาวิทยาลัย

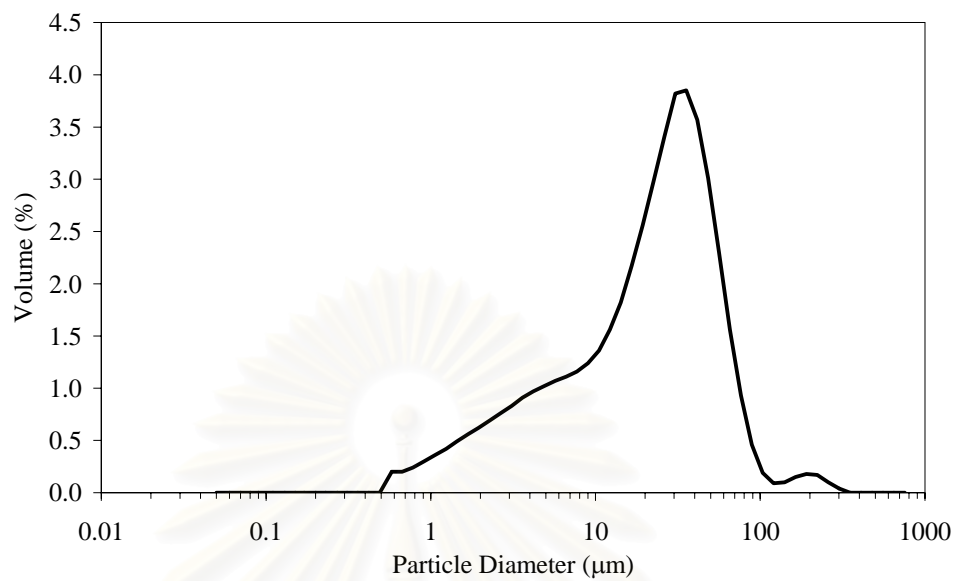


Figure 5.4 Particle size distribution of zeolite

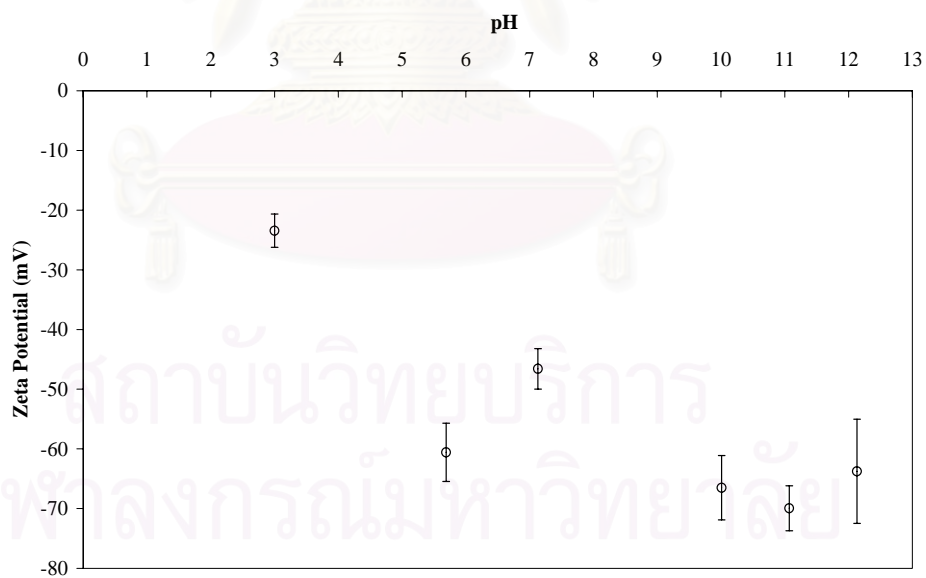


Figure 5.5 Relationship between surface charge of zeolite and pH

5.3 Effect of initial concentration on sorption kinetics

The time-profiles of the sorption capacities of Pb^{2+} , Cu^{2+} , and Cd^{2+} by zeolite for a range of initial concentration from 0 – 5 mol m^{-3} and a sorbent dose of 1 g L^{-1} are given in Fig. 5.6. Although it took slightly longer for the systems at high initial metal concentrations to reach equilibrium than those with low initial concentration, generally the sorption reached equilibrium within 120 min. Experimental data were analyzed with the sorption kinetic models (Eqs. 2.7 and 2.9) and the resulting parameters of each kinetic model which were determined by nonlinear fitting using STATISTICA version 6.0 are summarized in Table 5.2. This table also demonstrates that the order of equilibrium sorption capacity from both models ($q_{e,1}$ and $q_{e,2}$) increased with initial concentration. This was due to the existence of equilibrium between the liquid phase concentration and the sorption capacity of the zeolite such that an increase in the initial concentration shifted the equilibrium towards a higher sorption capacity region. On the other hand, the kinetic rate constants (k_1 and k_2) were adversely affected by the initial concentration. This indicated that the systems with lower initial metal concentration reached equilibrium more slowly than the systems with higher initial concentration.

The pseudo second order kinetic model was shown to be a better model for this set of experimental data than the pseudo first order kinetic model for all cases (considered from a higher determination coefficient, R^2). Azizian and Yahyaei (2006) stated that an additional criterion in the discrimination between the pseudo first and pseudo second order kinetic models was that the first order rate constant decreased with an increase in initial concentration if the reaction obeyed the second order model. The experimental data from this work agreed well with their criterion, and this strongly confirmed the applicability of the second order model. Hence, the pseudo second order kinetic model was thereafter used as a representative model in this study, and the model prediction of experimental data was plotted as solid lines in Fig. 5.6.

Table 5.2 Sorption kinetic parameters (initial concentration range of 0 – 5 mol m⁻³)(a) Pb²⁺

C_o (mM)	Pseudo first order model			Pseudo second order model		
	$q_{e,1}$ (mol kg ⁻¹)	k_1 (min ⁻¹)	R^2	$q_{e,2}$ (mol kg ⁻¹)	k_2 (kg mol ⁻¹ min ⁻¹)	R^2
0.1	0.101	13.4	1.00	0.102	237	1.00
0.5	0.337	2.35	0.995	0.343	39.4	1.00
1	0.584	2.11	0.935	0.649	2.56	1.00
3	1.07	0.615	0.778	1.36	0.205	0.994
5	1.28	0.705	0.726	1.68	0.173	0.997

(b) Cu²⁺

C_o (mM)	Pseudo first order model			Pseudo second order model		
	$q_{e,1}$ (mol kg ⁻¹)	k_1 (min ⁻¹)	R^2	$q_{e,2}$ (mol kg ⁻¹)	k_2 (kg mol ⁻¹ min ⁻¹)	R^2
0.1	0.0502	1.53	0.962	0.0531	30.0	1.00
0.5	0.154	0.514	0.990	0.162	5.13	1.00
1	0.309	0.579	0.983	0.328	3.03	1.00
3	0.698	0.371	0.989	0.738	0.833	1.00
5	0.913	0.246	0.966	0.991	0.287	0.999

(c) Cd²⁺

C_o (mM)	Pseudo first order model			Pseudo second order model		
	$q_{e,1}$ (mol kg ⁻¹)	k_1 (min ⁻¹)	R^2	$q_{e,2}$ (mol kg ⁻¹)	k_2 (kg mol ⁻¹ min ⁻¹)	R^2
0.1	0.0508	2.71	0.936	0.0591	23.6	0.998
0.5	0.171	0.943	0.938	0.193	4.85	1.00
1	0.266	1.80	0.977	0.294	5.56	1.00
3	0.456	2.08	0.941	0.522	2.20	0.999
5	0.651	1.05	0.979	0.694	2.05	1.00

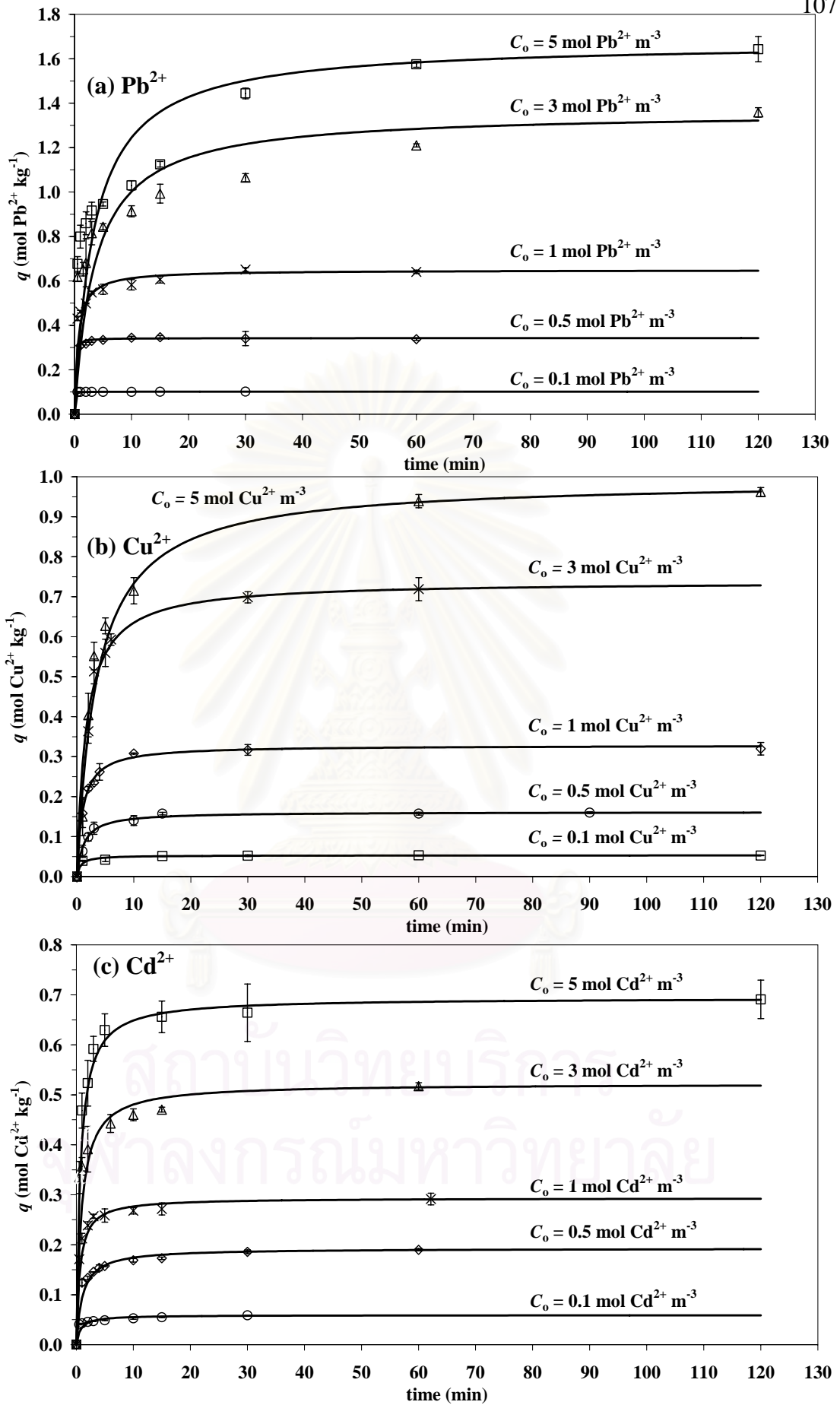


Figure 5.6 Relationship between contact time and sorption capacity (q) at various concentration using sorbent dose of 1 g L^{-1}

5.4 Effect of sorbent dose on sorption kinetics

The time-profiles of the sorption capacity of Pb^{2+} , Cu^{2+} , and Cd^{2+} by zeolite for a range of sorbent dose from $0.5 - 3 \text{ g L}^{-1}$ at an initial heavy metal concentration of 5 mol m^{-3} are provided in Fig. 5.7 and the parameters of each kinetic model are summarized in Table 5.3. Again, equilibrium was reached within 120 minutes and the pseudo second order kinetic model was better than pseudo first order kinetic model for the prediction of experimental data in all cases. The equilibrium sorption capacity decreased with an increase in the sorbent dose. This was not uncommon as an increase in the sorbent dose provided more space for the sorbate and the population of sorbate in the sorbent therefore decreased. This could also be explained using Eq. 2.1 as an increase in the sorbent dose increased the denominator in this equation, reducing the sorption capacity at equilibrium. In terms of kinetic rate constants, no general trend could be observed from this experiment. The values of k_2 for Pb^{2+} seemed to increase with zeolite dose whereas k_2 for the other two metals did not show clear trends with zeolite dose. As a general observation, the rate constant (k_2) seemed to vary directly with the sorbent dose.

Table 5.3 Sorption kinetic parameters (sorbent dose range of 0.5 – 3 g L⁻¹)(a) Pb²⁺

X_0 (g L ⁻¹)	Pseudo first order model			Pseudo second order model		
	$q_{e,1}$ (mol kg ⁻¹)	k_1 (min ⁻¹)	R^2	$q_{e,2}$ (mol kg ⁻¹)	k_2 (kg mol ⁻¹ min ⁻¹)	R^2
0.5	1.97	0.705	0.818	2.31	0.0898	0.976
1	1.28	0.705	0.726	1.68	0.173	0.997
2	1.11	1.45	0.825	1.37	0.348	0.999
3	1.04	1.76	0.852	1.26	0.425	0.999

(b) Cu²⁺

X_0 (g L ⁻¹)	Pseudo first order model			Pseudo second order model		
	$q_{e,1}$ (mol kg ⁻¹)	k_1 (min ⁻¹)	R^2	$q_{e,2}$ (mol kg ⁻¹)	k_2 (kg mol ⁻¹ min ⁻¹)	R^2
0.5	0.950	0.362	0.938	1.06	0.320	0.993
1	0.913	0.246	0.966	0.991	0.287	0.999
3	0.550	1.38	0.807	0.706	0.538	0.996

(c) Cd²⁺

X_0 (g L ⁻¹)	Pseudo first order model			Pseudo second order model		
	$q_{e,1}$ (mol kg ⁻¹)	k_1 (min ⁻¹)	R^2	$q_{e,2}$ (mol kg ⁻¹)	k_2 (kg mol ⁻¹ min ⁻¹)	R^2
0.5	0.619	0.857	0.804	0.753	0.540	0.999
1	0.651	1.05	0.979	0.694	2.05	1.00
2	0.512	2.26	0.879	0.625	1.03	0.996
3	0.530	1.13	0.974	0.576	2.12	1.00

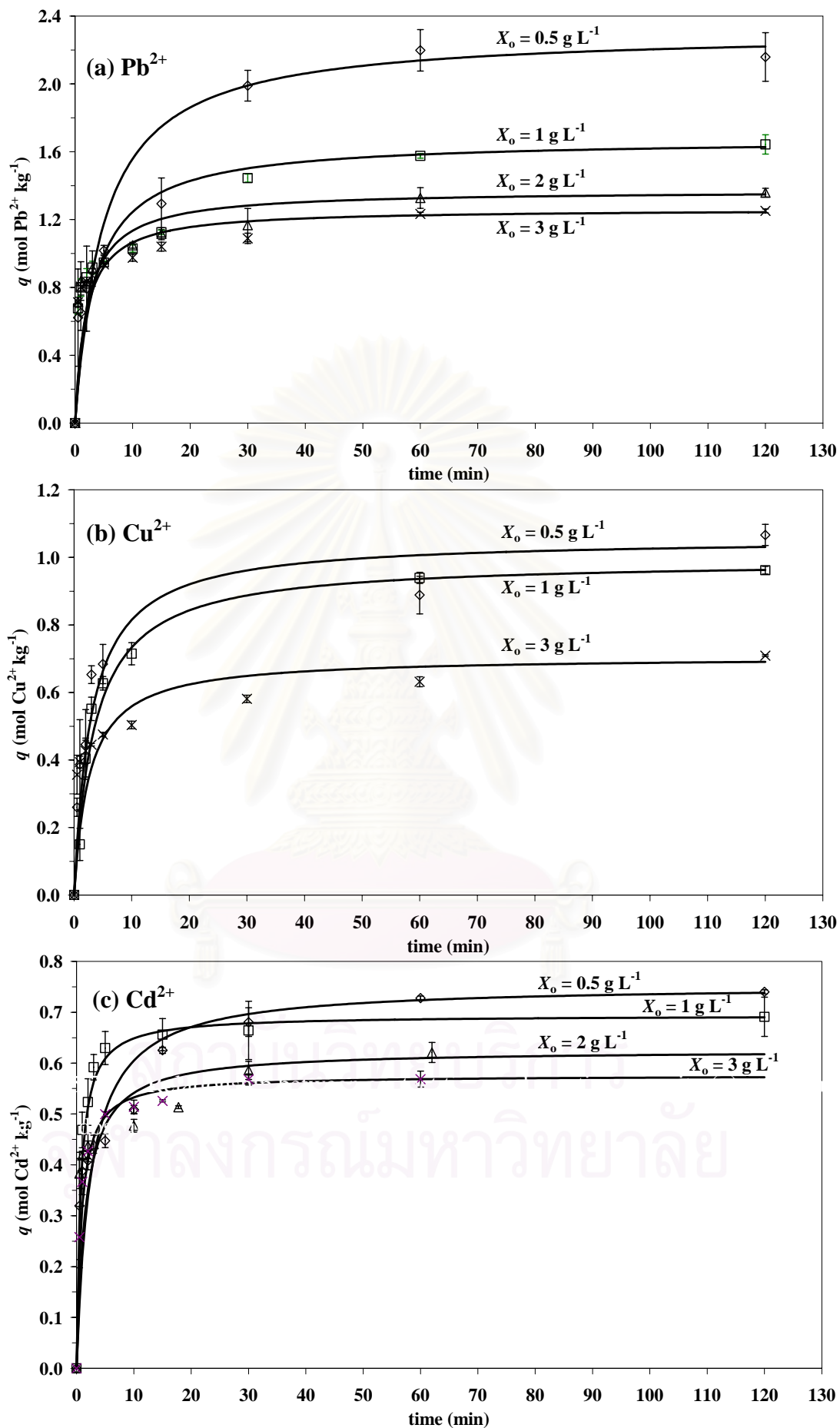


Figure 5.7 Relationship between contact time and sorption capacity (q) at various sorbent dose using initial concentration of 5 mol m^{-3}

5.5 Mechanism in sorption kinetics

Sorption kinetic models based on reaction mechanisms (Eqs. 2.12, 2.15, 2.17, 2.21, and 2.22) were tested for the compatibility with experimental data. Model parameters were obtained from the characterization of the zeolite product as stated in Section 5.1 and briefly summarized as follows: mean particle diameter (d_p) at approx. 3.85×10^{-5} m and bulk density (ρ_b) of 2100 kg m^{-3} . This makes a specific surface area (A) of $74.22 \text{ m}^2 \text{ kg}^{-1}$. The other models parameters and variables were summarized in Table 5.4.

The results from the model as summarized in Table 5.4 illustrates that, the external mass transfer coefficient (K_L) from the external mass transfer model, which was determined from parameter h (initial sorption rate) from the pseudo second order kinetic model, inversely varied with the initial concentration for all metal ions. K_L of Pb^{2+} was considerably higher than those of Cu^{2+} and Cd^{2+} for the range of initial concentration between $0.1 - 1 \text{ mol m}^{-3}$, particularly at low initial concentration range (e.g. at 0.1 and 0.5 mol m^{-3}) where the difference was as high as two order of magnitude (about 100 times larger). However, the effect of sorbent dose on the mass transfer coefficient differed for each metal ion. For Pb^{2+} , K_L increased gradually with the sorbent dose reaching the maximum value at approx. $3 \times 10^{-5} \text{ m s}^{-1}$. On the other hand, K_L of Cu^{2+} convergently decreased to about $1.24 \times 10^{-5} \text{ m s}^{-1}$. However, no general trend for the effect of sorbent dose on the mass transfer coefficient of Cd^{2+} could be observed from this set of experimental data.

The results from Vermeulen model on the equilibrium sorption capacity ($q_{e,v}$) provided a similar trend with that calculated from the pseudo second order kinetic model, and the accuracy of the prediction from Vermeulen model was reasonably high with the determination coefficient (R^2) of more than 0.836. The calculation revealed that the effective diffusion coefficient ($D_{e,v}$) for Pb^{2+} and Cu^{2+} decreased with an increase in the initial concentration whilst the trend for Cd^{2+} could not be defined. On the other hand, an increase in the sorbent dose from $0.5 - 3 \text{ g L}^{-1}$ resulted in an enhancing Vermeulen effective diffusion coefficient of Pb^{2+} . No general trend for the effect of sorbent dose on the effective diffusion coefficient of Cu^{2+} was observed, whereas a parabolic trend for Cd^{2+} with the maximum obtained at the sorbent dose of 2 g L^{-1} was obtained.

Table 5.4 Sorption kinetic parameters based on reaction mechanism

Metal ion	C_o (mol m ⁻³)	X_o (g L ⁻¹)	External mass transfer model		Vermeulen model			Weber-Morris model			
			$h = q_e^2 k_2$ (mol kg ⁻¹ min ⁻¹)	K_L (m s ⁻¹)	$q_{e,v}$ (mol kg ⁻¹)	$D_{e,v}$ (m ² s ⁻¹)	R^2	K_{WM} (mol kg ⁻¹ min ^{-0.5})	$D_{e,WM}$ (m ² s ⁻¹)	I (mol kg ⁻¹)	RC (%)
Pb ²⁺	0.105	1	2.45	5.25×10 ⁻³	0.101	7.51×10 ⁻¹²	1.000	2.32×10 ⁻⁴	2.82×10 ⁻¹⁸	0.100	98.5
	0.485	1	4.63	2.14×10 ⁻³	0.338	1.01×10 ⁻¹²	0.996	1.64×10 ⁻²	1.23×10 ⁻¹⁵	0.296	86.3
	1.02	1	1.08	2.38×10 ⁻⁴	0.598	6.13×10 ⁻¹³	0.957	2.76×10 ⁻²	9.74×10 ⁻¹⁶	0.499	76.9
	3.05	1	0.380	2.80×10 ⁻⁵	1.13	1.48×10 ⁻¹³	0.868	5.96×10 ⁻²	1.03×10 ⁻¹⁵	0.739	54.3
	5.08	1	0.485	2.14×10 ⁻⁵	1.44	1.02×10 ⁻¹³	0.836	1.06×10 ⁻¹	2.17×10 ⁻¹⁵	0.708	42.3
	5.23	0.5	0.479	2.06×10 ⁻⁵	2.32	2.23×10 ⁻¹³	0.938	2.74×10 ⁻¹	7.61×10 ⁻¹⁵	0.388	16.8
	5.22	2	0.655	2.82×10 ⁻⁵	1.17	2.98×10 ⁻¹³	0.939	9.15×10 ⁻²	2.40×10 ⁻¹⁵	0.725	52.8
	5.18	3	0.679	2.94×10 ⁻⁵	1.08	4.12×10 ⁻¹³	0.888	7.44×10 ⁻²	1.87×10 ⁻¹⁵	0.726	57.4
Cu ²⁺	0.101	1	0.0845	1.88×10 ⁻⁴	0.0504	5.47×10 ⁻¹³	0.964	4.12×10 ⁻³	3.25×10 ⁻¹⁵	0.0345	64.9
	0.500	1	0.134	6.02×10 ⁻⁵	0.157	1.48×10 ⁻¹³	0.988	7.86×10 ⁻²	1.27×10 ⁻¹³	0.00*	-8.80
	0.970	1	0.326	7.56×10 ⁻⁵	0.317	1.82×10 ⁻¹³	0.998	9.97×10 ⁻²	4.97×10 ⁻¹⁴	0.0655	20.0
	3.04	1	0.454	3.35×10 ⁻⁵	0.711	1.22×10 ⁻¹³	0.991	2.00×10 ⁻¹	3.97×10 ⁻¹⁴	0.0753	10.2
	5.10	1	0.282	1.24×10 ⁻⁵	0.951	6.00×10 ⁻¹⁴	0.967	1.61×10 ⁻¹	1.42×10 ⁻¹⁴	0.0603	6.09
	4.96	0.5	0.357	1.62×10 ⁻⁵	0.977	9.45×10 ⁻¹⁴	0.972	2.88×10 ⁻¹	4.01×10 ⁻¹⁴	0.0776	7.34
	4.85	3	0.268	1.24×10 ⁻⁵	0.590	2.67×10 ⁻¹³	0.868	7.55×10 ⁻²	6.17×10 ⁻¹⁵	0.312	44.3
Cd ²⁺	0.083	1	0.0825	2.24×10 ⁻⁴	0.0518	8.66×10 ⁻¹³	0.948	6.45×10 ⁻³	6.41×10 ⁻¹⁵	0.0362	61.2
	0.479	1	0.180	8.44×10 ⁻⁵	0.177	2.77×10 ⁻¹³	0.969	2.86×10 ⁻²	1.19×10 ⁻¹⁴	0.0949	49.3
	0.953	1	0.479	1.13×10 ⁻⁴	0.271	5.74×10 ⁻¹³	0.989	8.04×10 ⁻²	4.04×10 ⁻¹⁴	0.122	41.6
	2.82	1	0.599	4.77×10 ⁻⁵	0.466	6.35×10 ⁻¹³	0.962	6.12×10 ⁻²	7.39×10 ⁻¹⁵	0.296	56.7
	4.80	1	0.989	4.63×10 ⁻⁵	0.664	3.54×10 ⁻¹³	0.993	1.35×10 ⁻¹	2.03×10 ⁻¹⁴	0.338	48.7
	4.89	0.5	0.306	1.4×10 ⁻⁵	0.675	1.25×10 ⁻¹³	0.884	8.24×10 ⁻²	6.45×10 ⁻¹⁵	0.279	37.0
	4.91	2	0.402	1.84×10 ⁻⁵	0.528	6.08×10 ⁻¹³	0.900	3.67×10 ⁻²	1.86×10 ⁻¹⁵	0.372	59.5
	4.95	3	0.704	3.20×10 ⁻⁵	0.540	3.29×10 ⁻¹³	0.988	2.33×10 ⁻¹	8.78×10 ⁻¹⁴	0.108	18.8

* The calculated value was negative value which close to zero (-0.0142) but in the reality this value must not be negative value

Weber-Morris model often predicted higher effective diffusion coefficient ($D_{e,WM}$) than those from Vermeulen model, and in particular, the trend of $D_{e,WM}$ did not follow the same trend as that of $D_{e,v}$. This could be because $D_{e,WM}$ was determined using only the linear region which, on the one hand, depended on the judgement of the “linear region”, and this might induce statistical bias. Hence, for this work, Vermeulen model was recommended for the determination of effective diffusion coefficient. However, Weber-Morris model still was useful in the examination of the dominant transport mechanism between external mass transfer and intraparticle diffusion. As described in Section 2.6, the intercept (I) of the plot between q and \sqrt{t} provided an insight evaluation of the relative significance of the external mass transfer step. However, only an intercept value might not be enough as a criterion in the investigation of rate limiting step as it only gives the information on the magnitude of external mass transfer without taking into account the intraparticle diffusion. The equilibrium sorption capacity should then be incorporated with the intercept to allow a better examination, and this, in this work, was proposed as a parameter, “Relative Coefficient (RC)”, which is expressed as the ratio between the intercept (I) and the equilibrium sorption capacity as follows:

$$RC(\%) = 100 \times \frac{I}{q_e} \quad (5.1)$$

where I takes the same meaning as that in Eq. 2.15 and q_e the equilibrium sorption capacity obtained from the best fitted kinetic model. Higher RC would indicate the external mass transfer step as a stronger rate limiting step, whereas the lower RC indicated that the intraparticle diffusion step was the rate limiting step. In this work, q_e from the pseudo second order kinetic model was applied in Eq. 5.1 and RCs from the various experiments were reported in Table 5.4. It can be seen from the table that an increase in the initial concentration generally resulted in a decrease in RC for Pb^{2+} . This indicated that the external mass transfer was more significant as a rate limiting step particularly at low than high initial concentrations. RC for Cu^{2+} also decreased with an increase initial concentration, but the value of RC was mostly lower than 50%. This suggested that the sorption of Cu^{2+} was controlled primarily by intraparticle diffusion. For Cd^{2+} , no general trend could be concluded on the determination of rate limiting step and RC took the values between about 40 – 60%. An increase in the sorbent dose from 0.5 – 3 g L⁻¹ increased RC of Pb^{2+} indicating that the external mass transfer became

more significant at higher sorbent dose. The effect of sorbent dose on the rate controlling mechanism could not be clearly observed for Cu^{2+} , but the external mass transfer seemed to be more important at higher initial concentration. The relationship between RC and sorbent dose for the sorption Cd^{2+} was found to be parabolic with the maximum taken place at the sorbent dose of 2 g L^{-1} . It should be noted that the negative value of I and RC for Cu^{2+} at $C_0 = 0.5 \text{ mol m}^{-3}$ occurred as the linear regression in calculation of K_{WM} resulted in the y-intercept below horizontal axis. The reason could be that the process was highly limited by intraparticle diffusion step.

In conclusion, the sorption of Pb^{2+} was often controlled by the external mass transfer process (RC always higher than 50%). On the other hand, the sorption of Cu^{2+} was generally found to involve with the intraparticle diffusion process (RC always lower than 50%). The sorption on Cd^{2+} seemed to involve equally the external mass transfer and the intraparticle diffusion as RC generally varied in a range of 40 – 60%. This suggested that the rate of sorption could be enhanced by

- increasing shaking rate for Pb^{2+} sorption
- increasing temperature for Cu^{2+} sorption
- increasing shaking rate and temperature for Cd^{2+} sorption.

5.6 Sorption isotherm

The sorption equilibrium curve was constructed from the kinetic data with sufficient contact time as shown in Fig 5.8. As the contact time increased, the bulk liquid phase concentration (C_t) decreasingly converged to equilibrium bulk liquid phase concentration (C_e), and solid phase concentration or the sorption capacity (q_t) increasingly converged to equilibrium sorption capacity (q_e). The liquid phase concentration at time ' t ' (C_t) and equilibrium concentration (C_e) can be calculated by rearranging Eq. 2.1 as follows:

$$C_t = C_o - \frac{mq_t}{V} \quad (5.2a)$$

$$C_e = C_o - \frac{mq_e}{V} \quad (5.2b)$$

Each experiment provided a dot line with the final point lied on the equilibrium line as illustrated in Fig. 5.8. Each equilibrium data were fitted with the isotherm models (Eqs 2.28, 2.31, and 2.32) and the isotherm parameters are summarized in Table 5.5.

Table 5.5 Sorption isotherm

Metal ion	Langmuir isotherm			Dubinin-Radushkevich isotherm			
	q_{\max} (mol kg ⁻¹)	b (m ³ mol ⁻¹)	R^2	q_{\max} (mol kg ⁻¹)	β (mol ² kJ ⁻²)	E (kJ mol ⁻¹)	R^2
Pb ²⁺	2.03	1.29	0.994	1.61	-0.0770	2.55	0.970
Cu ²⁺	1.43	0.468	0.993	0.989	-0.203	1.57	0.974
Cd ²⁺	0.870	0.797	0.980	0.640	-0.119	2.05	0.923

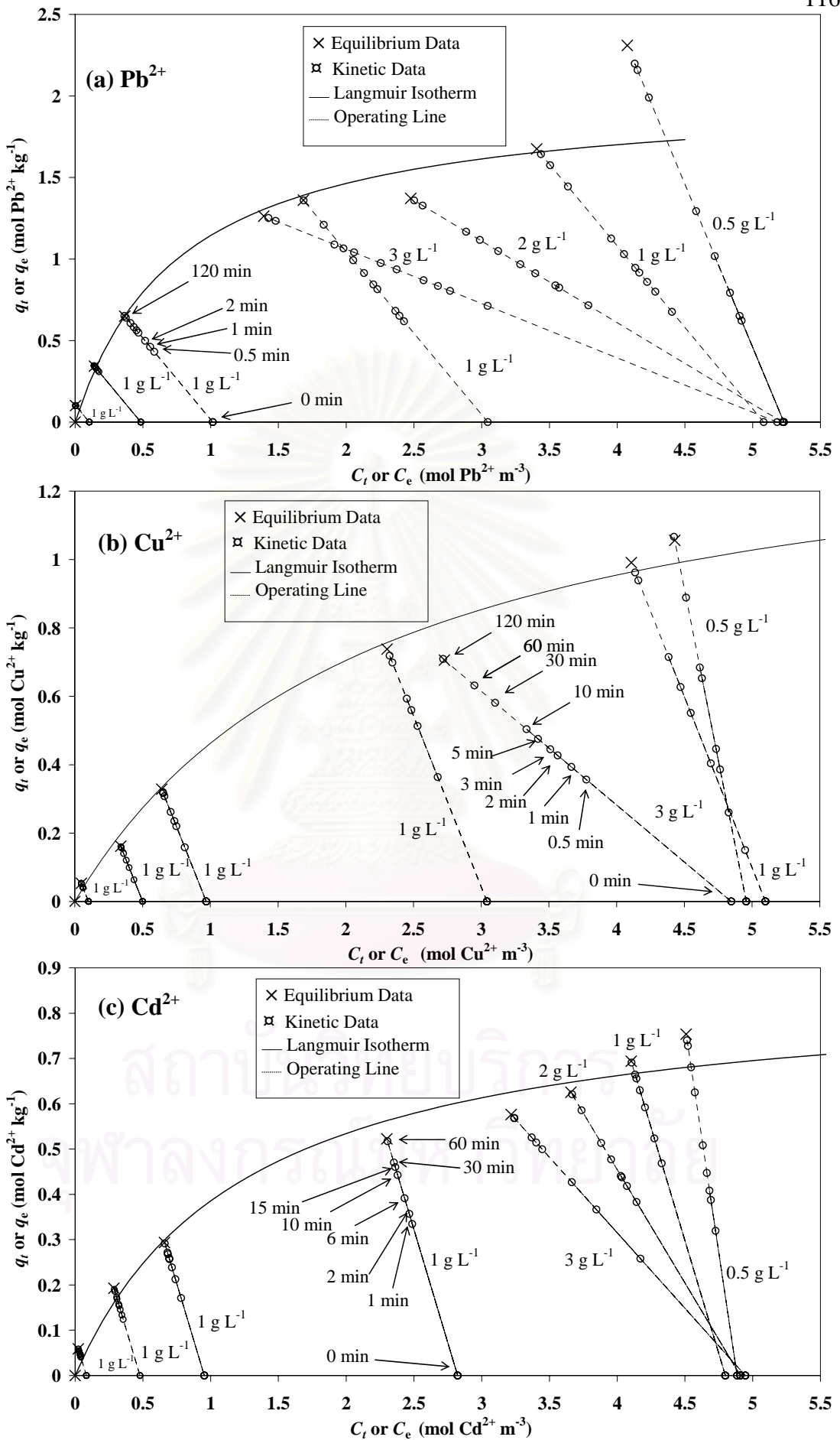


Figure 5.8 Sorption isotherm with kinetic tracking plots

Langmuir isotherm suggested that the order of maximum sorption capacity (q_{max}) could be prioritized from high to low as: $Pb^{2+} > Cu^{2+} > Cd^{2+}$, indicating that the zeolite product from this work had more binding sites for Pb^{2+} than Cu^{2+} and Cd^{2+} , respectively. On the other hand, the Langmuir affinity constant (b) could be prioritized from high to low as: $Pb^{2+} > Cd^{2+} > Cu^{2+}$ which suggested that Pb^{2+} was the most easily bonded component to the binding sites of the zeolite, followed by Cd^{2+} and Cu^{2+} , respectively.

Dubin-Radushkevich isotherm model was employed to evaluate the energy of sorption. The analysis from Dubin-Radushkevich isotherm showed that the mean sorption energies were 2.55, 1.57, and 2.05 kJ mol⁻¹ for Pb^{2+} , Cu^{2+} , and Cd^{2+} , respectively. Smith (1981) illustrated that the range of energy of sorption at 2–20 kJ mol⁻¹ could be considered physi-sorption in nature. Therefore it was possible that physical means such as electrostatic force played a significant role as a sorption mechanism for the sorption of heavy metal ions in this work.

5.7 Effect of sorbent dose and initial concentration on sorption equilibrium

The effect of sorbent dose and initial concentration on equilibrium study is important in designing the treatment unit, and the relationships between these parameters were often constructed. For example, on the investigation of the sorption of nickel ions on baker yeast, Padmavathy et al. (2003) proposed the relationship between equilibrium sorption capacity and initial metal concentration as:

$$q_e \text{ (in mg g}^{-1}\text{)} = \frac{C_o \text{ (in mg L}^{-1}\text{)}}{8.95 \times 10^{-2} C_o + 3.57} \text{ for the sorbent dose of } 1 \text{ g L}^{-1} \text{ and the relationship}$$

between sorption capacity and sorbent dose as: $q_e \text{ (in mg g}^{-1}\text{)} = 7.15m_s^{-0.686} \text{ (in g L}^{-1}\text{)}$ for an initial concentration of about 100 mg L⁻¹. Suthiparinyanont (2003) observed that the sorption capacity for Cu^{2+} , Cd^{2+} , and Pb^{2+} increased with an increase in initial metal concentration, except for Zn^{2+} where an increase in initial concentration from 1-1.5 mol m⁻³ led to a slower rate of change in the sorption capacity. However, the exact reason for the finding could not be drawn from that work. Kumar and Kumaran (2005), who studied the removal of methylene blue by mango seed kernel powder, suggested the relationship between equilibrium sorption capacity and initial dye concentration as:

$$q_e = \frac{0.4167C_o^2 + 4.0086C_o}{0.5833C_o - 4.0086} \text{ for sorbent dose } 0.6 \text{ g L}^{-1}, \text{ while the relationship between}$$

the q_e and adsorbent mass fitted with: m (in g) = $\frac{0.0003q_e(\text{in mg g}^{-1})}{0.0242q_e - 1}$ for an initial dye concentration of 100 mg L⁻¹. Ho and Ofomaja (2006) reported that the relationship between coconut copra meal dose and %Removal at an initial concentration of about 128 mg-Cd²⁺ L⁻¹ (1.14 mol Cd²⁺ m⁻³) could be fitted by;

$$\% \text{Removal} = \frac{m_s(\text{in g L}^{-1})}{7.97 \times 10^{-2} + 1.60 \times 10^{-2} m_s}, \text{ while the relationship between the sorbent}$$

$$\text{dose and sorption capacity was: } q_e(\text{in mg g}^{-1}) = \frac{1}{6.20 \times 10^{-2} + 1.25 \times 10^{-2} m_s(\text{in g L}^{-1})}.$$

In this work, the effect of sorbent dose (X_o) and initial concentration (C_o) was found to simultaneously control the equilibrium parameters such as equilibrium sorption capacity (q_e) and removal percentage (%Removal). The relationship between these parameters could be achieved by combining Eqs. 2.28 and 5.2b where $\frac{m}{V}$ is defined as X_o , and this leads to:

$$q_e = \frac{q_{\max} b(C_o - X_o q_e)}{1 + b(C_o - X_o q_e)} \quad (5.3)$$

In this equation, X_o represents sorbent dose (g L⁻¹ or kg m⁻³) and the other parameters take the same meanings as those in Eqs. 2.1 and 2.28. Rearranging Eq. 5.3 gives:

$$(bX_o)q_e^2 - (1 + bC_o + q_{\max} bX_o)q_e + (q_{\max} bC_o) = 0 \quad (5.4)$$

The above relationship is quadratic equation and therefore the solutions can be obtained from:

$$q_e = \frac{(q_{\max} bX_o + bC_o + 1) \pm \sqrt{b^2 C_o^2 + 2b(1 - q_{\max} bX_o)C_o + (1 + q_{\max} bX_o)^2}}{2bX_o} \quad (5.5)$$

As $q_e = 0$ when $C_o = 0$, if the operation between the two terms was “plus”, the substitution of C_o with zero gives: $q_e = \frac{(q_{\max} bX_o + 1)}{bX_o}$ which was not equal to zero.

Hence, the operation must be negative and the actual exact solution of Eq. 5.4 can be expressed as:

$$q_e = \frac{(q_{\max} bX_o + bC_o + 1) - \sqrt{b^2 C_o^2 + 2b(1 - q_{\max} bX_o)C_o + (1 + q_{\max} bX_o)^2}}{2bX_o} \quad (5.5)$$

With this information, the determination the effect of initial concentration and sorbent dose on removal percentage can also be achieved by combining Eqs 2.1 and 3.3 where q , C_f , and $\frac{m}{V}$ were substituted by q_e , C_e , and X_o , respectively. This leads to:

$$\% \text{Removal} = 100 \frac{q_e X_o}{C_o} \quad (5.6)$$

In this equation, %Removal represents the removal percentage at equilibrium. The other parameters take the same meanings as those in Eqs. 2.1 and 2.28. Substitution of q_e from Eq. 5.5 into Eq. 5.6 gives:

$$\% \text{Removal} = 50 \frac{(q_{\max} b X_o + b C_o + 1) - \sqrt{b^2 C_o^2 + 2b(1 - q_{\max} b X_o) C_o + (1 + q_{\max} b X_o)^2}}{b C_o} \quad (5.7)$$

5.8 Model verification

New sets of sorption experiments were carried out to verify the models in Eqs 5.5 and 5.7. It should be noted that the contact time of about 2 hours were assumed, from experience in Sections 5.3 and 5.4, to be adequate for the system to reach equilibrium. The results from the experiments along with the model predictions were compared as illustrated in Figs. 5.9 – 5.11 for Pb^{2+} , Cu^{2+} , and Cd^{2+} , respectively.

Parameters employed to verify the model prediction were: (i) the coefficient of determination (R^2), (ii) average of %Error, and (iii) relative standard distribution (RSD) of %Error. These are calculated from:

$$R^2 = 1 - \frac{\sum_{i=1}^N (y_i - y_{c,i})^2}{\sum_{i=1}^N (y_i - \bar{y})^2} \quad (5.8a)$$

$$E_i = \left| \frac{y_i - y_{c,i}}{y_i} \right| \quad (5.8b)$$

$$\text{Average of Error (\%)} = \frac{100 \times \sum_{i=1}^N E_i}{N} \quad (5.8c)$$

$$\text{RSD of Error (\%)} = 100 \times \sqrt{\frac{\sum_{i=1}^N (E_i - \bar{E})^2}{N \bar{E}^2}} \quad (5.8d)$$

where y_i is the actual model variables (can be either q_e or %Removal) at point i obtained from experimental data, $y_{c,i}$ the predicted actual model variables from the model at the same point as y_i , \bar{y} the average of actual model variables from all interested experimental data, E_i the error at point i , \bar{E} the average of error from all experimental data, and N the number of experimental data.

The parameters for model verification were shown in Table 5.6 whereas the accuracy of the models was plotted in the Fig. 5.12. A high R^2 , low average of percentage error (Average of %Error), and low relative standard deviation of percentage error (RSD of %Error) indicated high accuracy of the model in the prediction of sorption characteristics. Note that the model could predict the sorption performance for Pb^{2+} and Cd^{2+} better than that of Cu^{2+} .

5.9 Concluding remarks

The sorption of three heavy metal ions, *i.e.* Pb^{2+} , Cu^{2+} , and Cd^{2+} using zeolite X modified from coal fly ash was evaluated here. Sorption kinetic mechanism was analyzed which revealed that generally both external mass transfer and intraparticle diffusion were the rate limiting step for Pb^{2+} and Cd^{2+} while Cu^{2+} seemed to generally be governed by intraparticle diffusion. The maximum sorption capacity (q_{max}) of the metal ions calculated from Langmuir isotherms was always higher than that reported in literature (Table 5.7) indicating that zeolite from this work could well be used as a high performance sorbent in sequestering of contaminated metals in wastewater. A general mathematical model for predicting the sorption parameters (q_e and %Removal) was proposed. The model could simultaneously integrate the effects of initial concentration and sorbent dose, and provide a relatively accurate prediction of sorption and this is applicable for further reference. Overall, this work illustrates the possibility in the conversion of the unwanted industrial materials such as coal fly ash from power plants to a high performance zeolite sorbent which could be useful for the removal of heavy metal ions from the wastewater.

Table 5.6 Parameters for model verification

Variables	Metal	R^2	Average Error (%)	RSD* of Error (%)	Max Error (%)	Min Error (%)	%Data with error less than 10%	No. of Data
q_e	Pb ²⁺	0.928	14.7	64.0	31.0	0.303	37.5	24
	Cu ²⁺	0.872	22.9	95.6	79.8	0.893	37.5	24
	Cd ²⁺	0.922	19.0	77.2	52.7	0.632	33.3	24
	All Data	0.929	18.9	86.3	79.8	0.303	36.1	72
%Removal	Pb ²⁺	0.821	14.7	64.0	31.0	0.303	37.5	24
	Cu ²⁺	0.672	22.9	95.6	79.8	0.893	37.5	24
	Cd ²⁺	0.704	19.0	77.2	52.7	0.632	33.3	24
	All Data	0.783	18.9	86.3	79.8	0.303	36.1	72

*RSD = Relative Standard Deviation = 100*Standard Deviation/Aver

Table 5.7 Maximum sorption capacities for heavy metals of various sorbents

Sorbent	q_{max} (mol kg ⁻¹)	pH	Reference
<i>S. cinnamomeum</i>	Pb(0.36) > Cd(0.19) > Cu(0.14)	4.0	Puranik and Paknikar, 1999
<i>P. chrysogenum</i>	Pb(0.34) > Cu(0.20) > Cd(0.11)	4.0	Puranik and Paknikar, 1999
<i>Durvillaea potatorum</i>	Pb(1.55) > Cu(1.30)	5.0	Matheickal and Yu, 1999
<i>Ecklonia radiata</i>	Pb(1.26) > Cu(1.11)	5.0	Matheickal and Yu, 1999
<i>Aspergillus niger</i>	Cu(0.073) > Pb(0.049) > Cd(0.035)	5.0	Kapoor and Viraragharan, 1999
<i>Sphaerotilus natans</i>	Pb(0.65) = Cu(0.65) > Cd(0.23)	5.0	Pagnanelli et al., 2001
Bone char	Cu(0.709) > Cd(0.477)	5.0	Ko et al., 2001
Pine bark	Cu(0.149) > Cd(0.126)	*	Al-Asheh et al., 2000
<i>Chlorella vulgaris</i> ,	Pb(0.816)	5.0	El-Naas et al., in press
Rice husk ash	Pb(0.061)	5.6–5.8	Feng et al., 2004
<i>Cymodocea nodosa</i>	Cu(0.83)	4.5	Sanchez et al, 1999
<i>Padina</i> sp	Cu(0.80)	5.0	Kaewsarn, 2002
GAC**	Cu(0.043) > Cd(0.0219)	5.4-5.7	Üçer et al., 2006
Modified GAC by Citric â	Cu(0.235)	4.9	Chen et al., 2003
<i>Caulerpa lentillifera</i>	Pb(0.14) > Cu(0.13) > Cd(0.042)	5.0	This work
Sepiolite	Cd(0.152)	6.0	Álvarez-Ayuso and García-Sánchez, 2003
Zeolite Na-P1	Pb(1.29) > Cu(1.05) > Cd(1.16)	*	Lee et al., 2006
Zeolite Faujasite	Pb(1.23)	*	Lee et al., 2006
Zeolite Sodalite	Pb(0.798)	*	Lee et al., 2006
Zeolite Analcime	Pb(0.745)	*	Lee et al., 2006
Zeolite Cancrinite	Pb(0.537)	*	Lee et al., 2006
Zeolite Clinoptilolite	Cu(1.41)	6-7	Erdem et al., 2004
Zeolite Clinoptilolite	Cu(0.405) > Pb(0.130) > Cd(0.043)	6.2	Sprynskyy et al., 2006
Zeolite X	Pb (2.03) > Cu (1.43) > Cd (0.870)	5.0	This work

*Not defined

**Granular Activated Carbon

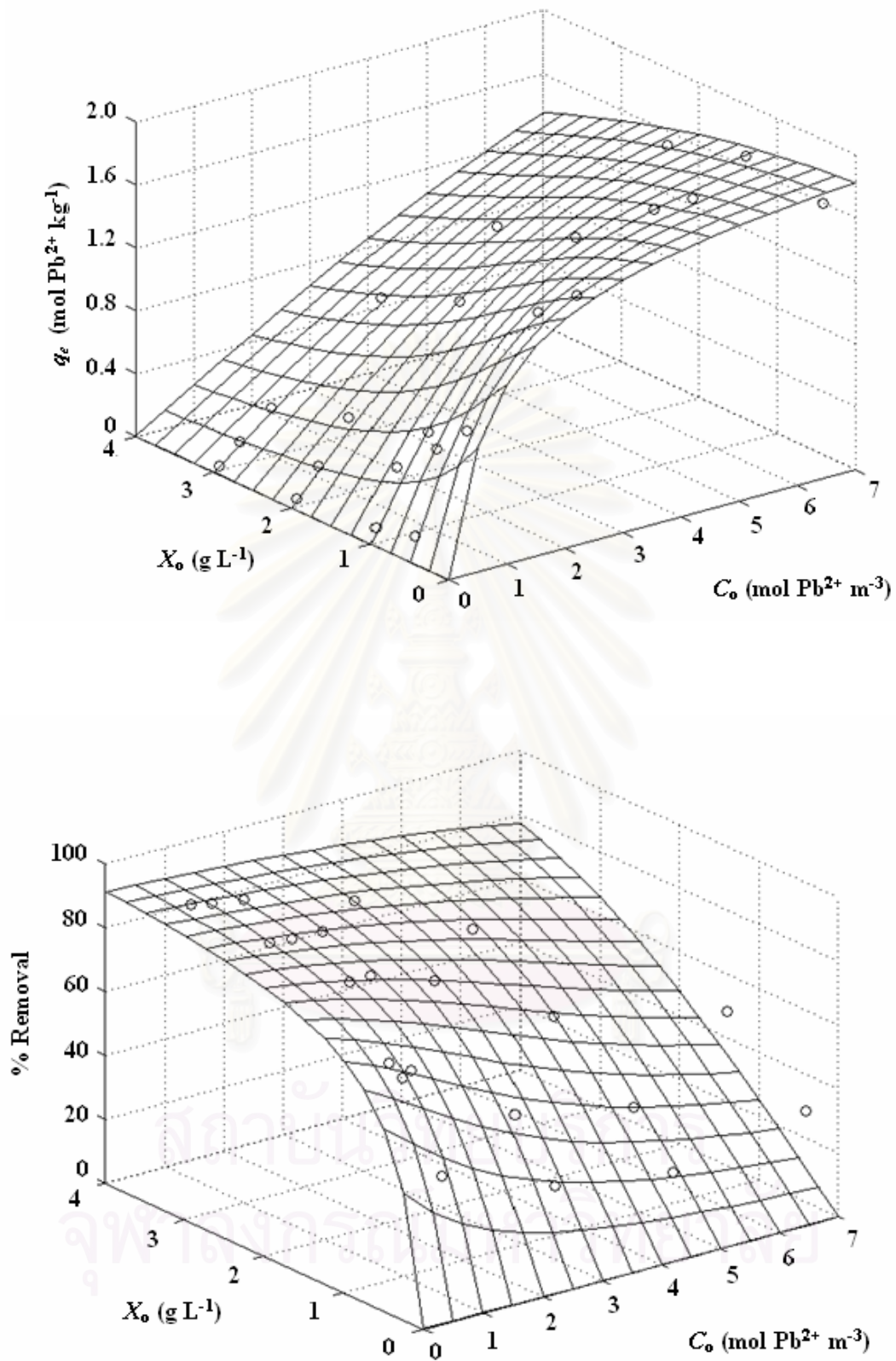


Figure 5.9 Relationship between sorption parameters (q_e and %Removal) of Pb^{2+} and operating parameters (C_o and X_o)

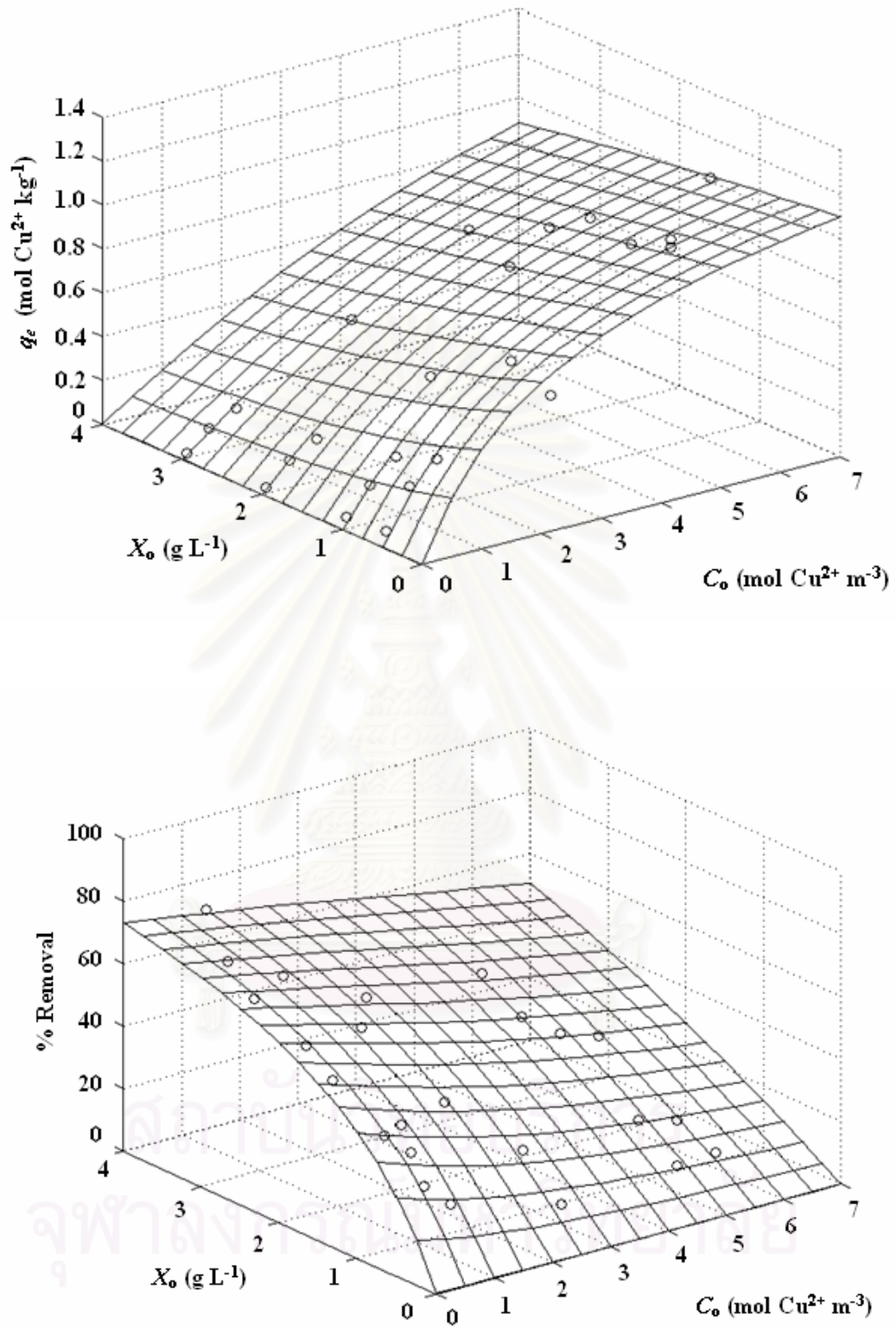


Figure 5.10 Relationship between sorption parameters (q_e and %Removal) of Cu²⁺ and operating parameters (C_o and X_o)

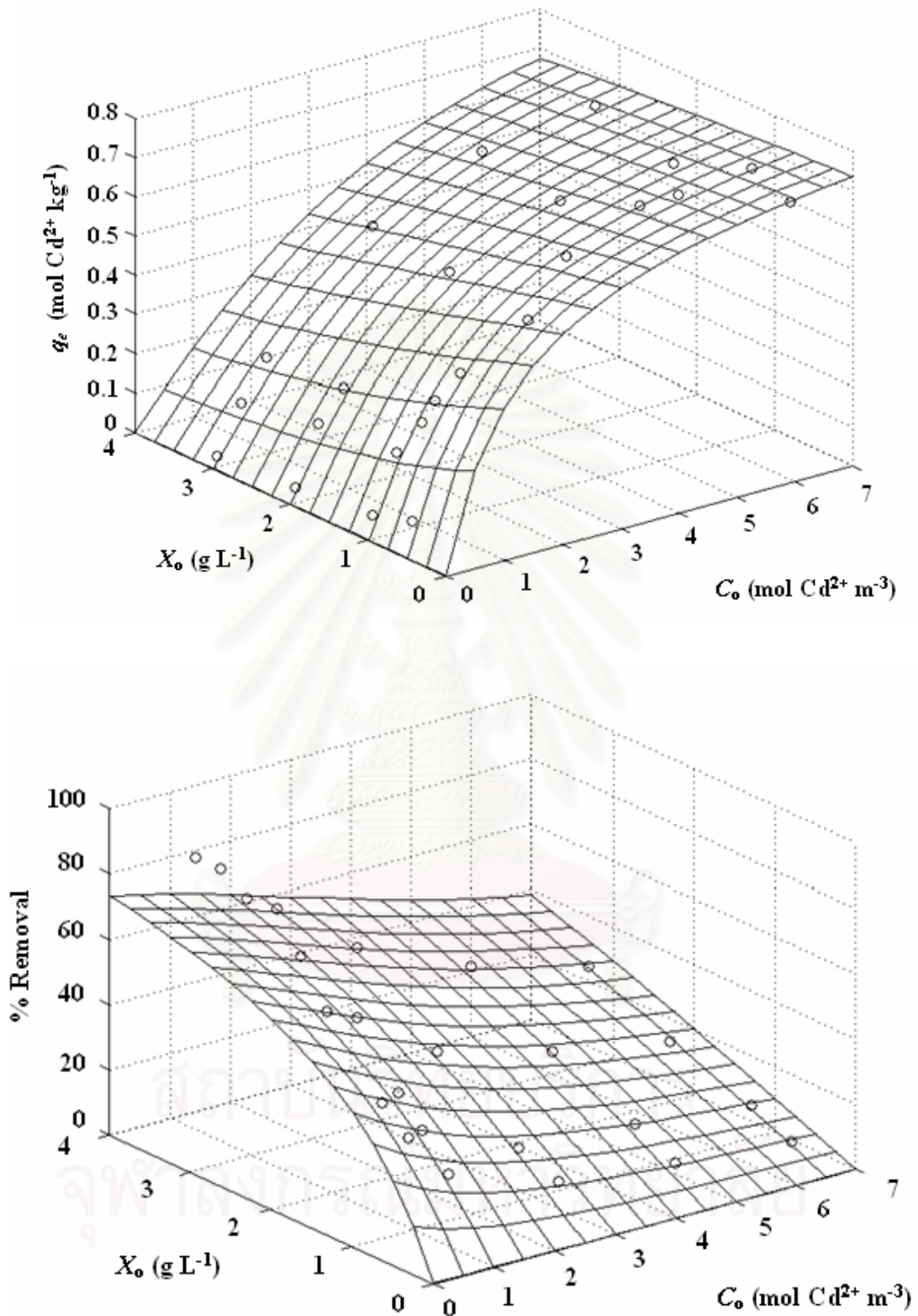


Figure 5.11 Relationship between sorption parameters (q_e and %Removal) of Cd²⁺ and operating parameters (C_o and X_o)

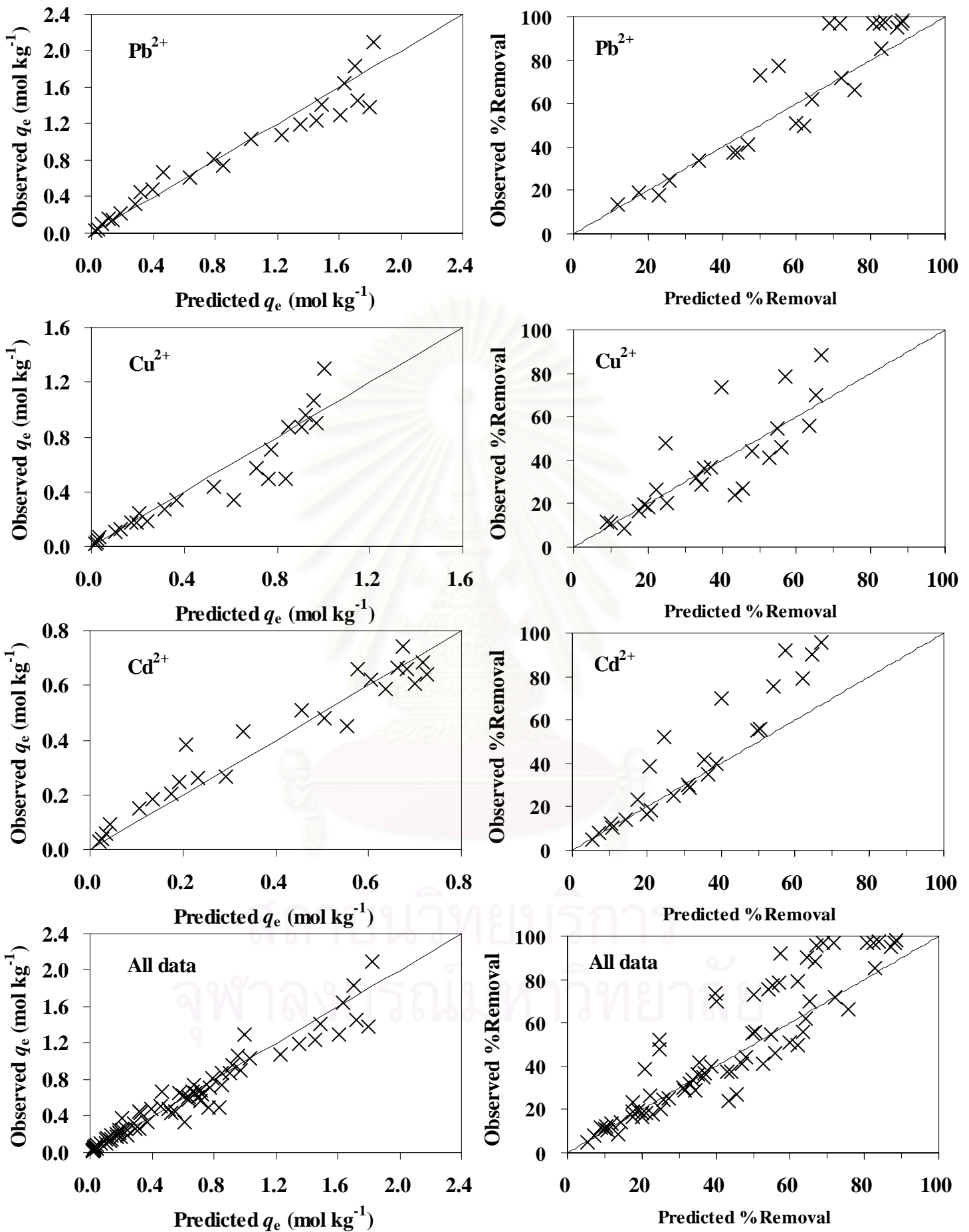


Figure 5.12 Accuracy of the models prediction

CHAPTER VI

COMPARISON BETWEEN CAULERPA LENTILLIFERA AND ZEOLITE X MODIFIED FROM COAL FLY ASH

6.1 Sorption point of view

The unwanted materials examined here were from two completely different sources: (i) agricultural and (ii) industrial activities. For agricultural work, the excess biomass of *Caulerpa lentillifera* was used directly as biosorbent which was found to have some capacities for the sorption of heavy metals. On the other hand, coal fly ash was converted to zeolite X and was proven to have even greater capacities for the sorption of heavy metals. Both sorbents exhibited similar sorption characteristics:

- (i) Physical force i.e. electrostatic force was involved with metal sorption.
- (ii) The order of maximum metal sorption capacity could be prioritized from high to low as $Pb^{2+} > Cu^{2+} > Cd^{2+}$.

The differences in sorption characteristics of the two sorbents were as follows:

- (i) The negative charges of algal biomass was caused by functional groups while that of zeolite was by Al atom in a three dimensional framework of Si and Al tetrahedral unit of zeolite structures
- (ii) Zeolite X provided a higher maximum sorption capacity for all metals than *Caulerpa lentillifera*.

The reason that the maximum sorption capacity of zeolite X was higher than that of *Caulerpa lentillifera* was that the zeolite contained higher specific surface area than the algal biomass as summarized in Table 6.1. It could be seen from the table that surface area based maximum sorption capacity of the zeolite was lower than that of the algal biomass. This was due to the greater denominator (specific surface area) in calculation of maximum sorption capacity based on surface area. However, mass based maximum sorption capacity was often used in comparison of efficiency between various sorbents in literatures since it was generally used in the design of actual wastewater treatment systems rather than surface area based maximum sorption capacity.

Table 6.1 Summary of maximum sorption capacity of the two sorbents

Sorbent	Maximum Sorption capacity based on mass (mol kg ⁻¹)	Specific surface area (m ² g ⁻¹)	Maximum Sorption capacity based on surface area (μmol m ⁻²)
<i>Caulerpa lentillifera</i>	Pb ²⁺ : 0.14 Cu ²⁺ : 0.13 Cd ²⁺ : 0.042	4.94	Pb ²⁺ : 28.3 Cu ²⁺ : 26.3 Cd ²⁺ : 8.50
Zeolite X	Pb ²⁺ : 2.03 Cu ²⁺ : 1.43 Cd ²⁺ : 0.870	344	Pb ²⁺ : 5.90 Cu ²⁺ : 4.16 Cd ²⁺ : 2.53

6.2 Economic point of view

Production costs of *Caulerpa lentillifera* and zeolite X modified from coal fly ash are summarized in Tables 6.2 and 6.3.

Table 6.2 Estimated cost of 1 kg *Caulerpa lentillifera*

a) Electrical cost	Electrical power (kW)	Time used (h)	Electricity consumed (unit)	Electricity charge* (฿)
- Oven for drying	1.6	48	76.8	127.49
			Total =	<u>127.49</u>
b) Material cost	Amount used	Cost per unit	Value (฿)	
- Tap water**	1000 L	0.01581 ฿ L ⁻¹	15.81	
- DI water	100 L	0.42 ฿ L ⁻¹	42	
(For washing process)			Total =	<u>57.81</u>

Productivity of the algal biomass = 2000 g

Total cost = 185.3

Specific cost = 92.6 ฿ kg⁻¹

* 1.66 ฿ unit⁻¹ (According to the electricity tariff applicable to any government institution and agency (69 kV and over), 2000)

**According to the Water Tariffs for government agency and industry, 1999.

Table 6.3 Estimated cost of 1 kg Zeolite X modified from CFA

a) Electrical cost	Electrical power (kW)	Time used (h)	Electricity consumed (unit)	Electricity charge* (฿)
- Furnace	6.99	2	13.98	23.21
- Shaker water bath	1.5	24	36	59.76
- Oven for crystallization	1.6	2	3.2	5.31
- Centrifuge	1.4	2	2.8	4.65
- Oven for drying	1.6	12	19.2	31.87
			Total =	<u>124.80</u>
b) Material cost	Amount used	Cost per unit	Value (฿)	
- NaOH anhydrous	140 g	350 ฿ per 500 g	98	
- Tap water** for zeolization process	0.68 L	0.01581 ฿ L ⁻¹	0.01075	
- DI water for zeolization process	0.68 L	0.42 ฿ L ⁻¹	0.2856	
- Tap water** for washing process	0.68 L	0.01581 ฿ L ⁻¹	0.379	
- DI water for washing process	0.68 L	0.42 ฿ L ⁻¹	10.08	
			Total =	<u>108.76</u>

Productivity of the Zeolite = 68 g

Total cost = 233.55

Specific cost = 3434.6 ฿ kg⁻¹

* 1.66 ฿ unit⁻¹ (According to the electricity tariff applicable to any government institution and agency (69 kV and over), 2000)

**According to the Water Tariffs for government agency and industry, 1999.

The two tables show that the expense of *Caulerpa lentillifera* is lower than that of the Zeolite X of the same amount. It can be suggested from the data of sorption and cost analysis that *Caulerpa lentillifera* biomass should be used for wastewater with low strength of heavy metal concentration (but the effluent might not meet the standard of discharging wastewater) while zeolite was more applicable with high strength wastewater. However, the estimated cost of zeolite in this work was lower than the cost of commercial zeolite which was about 20,000 ฿ kg⁻¹.

CHAPTER VII

CONCLUSIONS AND RECOMMENDATIONS

7.1 Summaries, achievements and contributions

This work proposed some simple methods for the conversion of unwanted materials to some useful products and also suggested the potential in using *Caulerpa lentillifera* as a low cost biosorbent in the wastewater containing low concentration of heavy metal while the higher concentration case suited better with the zeolite X modified form CFA. The major achievements and original contributions of this research are:

- 1) Agricultural and industrial wastes were converted to sorbent which helped reduce the quantities of solid waste.
- 2) Optimal NaOH:CFA ratio was suggested for the conversion of CFA to zeolite for the Nation Power Supply Co.Ltd. (Thailand) and this might be rightly applied in other power plants with similar CFA composition.
- 3) The metal sorption mechanisms were thoroughly investigated.
- 4) Mathematical modelings were developed to explain the sorption behavior such as effect of secondary metal ion on the sorption, effect of pH on the sorption, and effect of sorbent dose and initial concentration.

The findings from this dissertation contributed greatly to the current state of the art which facilitates further design the zeolite modifying process, and the development of sorption process to apply with the treatment of actual wastewater.

สถาบันวิทยบริการ
จุฬาลงกรณ์มหาวิทยาลัย

7.2 Suggestions and recommendations

The information on the biosorption using *Caulerpa lentillifera* provided in this work should be adequate for the actual application. This was based on the fact that the alga after employed as biosorbent for heavy metals should only go to secure landfill as the regeneration of such biosorbent should not be economical feasible. The work on the modified CFA, on the other hand, could still find much wider research applications. Further studies should be conducted in the following areas:

- 1) Effect of parameters of several units in fusion process such as settling time, shaking rate, time, and temperature etc. This aims at the production of zeolite with better sorption behavior such as higher CEC.
- 2) Effect of pH and counter ions on sorption characteristic by the zeolite.
- 3) Effect of temperature on the sorption process by the zeolite.
- 4) Testing for the continuous system such as column operation.
- 5) Sorption mechanism involved in the metal removal, e.g. ion exchange process of the metal with other light metals in the zeolite (potentially Na^+).
- 6) More complex mathematical modeling for metal sorption combining the two mass transfer steps, external mass transfer and intraparticle diffusion.
- 7) Electrostatic modeling of metal sorption on zeolite surface by the model such as surface complexation model.
- 8) Metal recovery and regeneration of spent zeolite.
- 9) Durability and stability of the zeolite sorbent in metal removal.

REFERENCES

- Abollino, O., Aceto, M., Malandrino, M., Sarzanini, C., and Mentasti, E. 2003. sorption of heavy metals on Na-montmorillonite. Effect of pH and organic substances. Water Research. 37: 1619-1627.
- Acemioglu, B. 2004. Batch kinetic study of sorption of methylene blue by perlite. Chemical Engineering Journal. 106: 73–81.
- Agrawal, A., and Sahu, K.K. 2006. Kinetic and isotherm studies of cadmium adsorption on manganese nodule residue. Journal of Hazardous Materials. in press.
- Aksu, Z., and Acikel, U. 1999. A Single-staged Biosorption Process for Simultaneous Removal of Copper(II) and Chromium(VI) by using *C. vulgaris*. Process Biochemistry. 34: 589-599.
- Aksu, Z., and İšoğlu, İ.A. 2005. Removal of copper(II) ions from aqueous solution by biosorption onto agricultural waste sugar beet pulp. Process Biochemistry. 40(9): 3031-3044.
- Al-Asheh, S., Banat, F., Al-Omari, R., and Duvnjak, Z. 2000. Predictions of binary sorption isotherms for the sorption of heavy metals by pine bark using single isotherm data. Chemosphere. 41: 659 – 665.
- Alimohamadi, M., Abolhamd, G., and Keshtkar, A. 2005. Pb(II) and Cu(II) biosorption on *Rhizopus arrhizus* modeling mono- and multi component systems modeling mono- and multi component systems. Minerals Engineering. 18: 1325–1330.
- Allen, S.J., McKay, G., and Khader, K.Y.H. 1989. Intraparticle Diffusion of a Basic Dye During Adsorption onto sphagnum Peat. Environmental Pollution. 56: 39-50.
- Álvarez-Ayuso, E., and Nugteren, H.W. 2005. Purification of chromium(VI) finishing wastewaters using calcined and uncalcined Mg-Al-CO₃-hydrotalcite. Water Research. 39(12): 2535-2542.
- Alvarez-Ayuso, E., Garcia-Sanchez, A., and Querol, X. 2003. Purification of metal electroplating waste waters using zeolites. Water Research. 37: 4855–4862.

- Apiratikul, R. 2003. Biosorption of Heavy Metals Mixture Solution by Green Macroalga, *Caulerpa lentillifera*. M.Sc. Thesis, Environmental Management (Inter-Department), Graduate School, Chulalongkorn University.
- Arpa, C., Basyilmaz, E., Bektas, S., Genc, O., and Yurum, Y. 2000. Cation exchange properties of low rank Turkish coals: removal of Hg, Cd and Pb from waste water. Fuel processing Technology. 68: 111-120.
- Azizian, S. 2004. Kinetic models of sorption: a theoretical analysis. Journal of Colloid and Interface Science. 276: 47-52.
- Banerjee, K. 2000. Economic evaluation of biosorption in compareision with other technologies for heavy metal removal. M.Sc. Thesis, Environmental Engineering, Griffith University, Queensland.
- Barrer, R.M., 1982. Hydrothermal chemistry of zeolites. London: Academic Press.
- Bektas, N., Agim, B.A., and Kara, S. 2004. Kinetic and equilibrium studies in removing lead ions from aqueous solutions by natural sepiolite. Journal of Hazardous Materials. 112: 115-122.
- Benguella, B., and Benaissa, H. 2002. Cadmium removal from aqueous solutions by chitin: kinetic and equilibrium studies. Water Research. 36(10): 2463-2474.
- Bergaut, V., and Singer, A. 1996. High capacity cation exchanger by hydrothermal zeolitization of coal fly ash. Applied Clay Science. 10(5): 369-378.
- Boyd, G.E., Adamson, A.W., and Meyers, L.S. 1947. The exchange adsorption of ions from aqueous solution by organic zeolites. II Kinetics. J. Am. Chem. Soc. 69: 2836-2848.
- Breck, D.W. 1974. Zeolite molecular sieves: structure, chemistry, and use. New York: Wiley.
- Brierley, J.A., and Vance, D.B. 1988. Recovery of precious metals by microbial biomass. In P.R. Norris and D.P. Kelly (eds.), BioHydroMetallurgy: Proceedings of the International Symposium on Science Technology Letters. pp. 477-486. Kew, Surrey, U.K.
- Chang, C.F., Chang, C.Y., Chen, K.H., Tsai, W.T., Shie, J.L., and Chen, Y.H. 2004. Adsorption of naphthalene on zeolite from aqueous solution. Journal of Colloid and Interface Science. 277: 29-34.

- Chen, J. P., Wu, S., Chong, K.H. 2003. Surface modification of a granular activated carbon by citric acid for enhancement of copper adsorption, Carbon 41(10): 1979-1986.
- Chojnacka, K. 2005. Biosorption of Cr(III) ions by eggshells. Journal of Hazardous Materials. 121(1-3): 167-173.
- Chokwiwattanawanit, A. 2000. Efficiency of the macroalgae *Caulerpa lentillifera* and *Acanthophora spicifera* for the treatment of nitrogen compound from shrimp pond effluent. M.Sc. Thesis, Environmental Science, Inter-department of Environmental Science, Graduate School, Chulalongkorn University.
- Chu, H.K., Hashim, A.M., Phang, M.S., and Samuel B.V. 1997. Biosorption of Cadmium by Algal Biomass: Sorption and Desorption Characteristics. Water Science and Technology. 35(7): 115-122.
- Conrad, K., and Hansen, H.C.B. 2007. Sorption of zinc and lead on coir. Bioresource Technology. 98 (1): 89-97.
- Crank, J. 1975. The Mathematics of Diffusion (second ed.), Clarendon, Oxford 91 pp.
- Davidson, J.M. and McDouga, J.R. 1973. Experimental and Predicted Movement of Three Herbicides in a Water-Saturated Soil. Journal of Environmental Quality. 2(4): 428-433.
- Davis, T.A., Llanes, F., Volesky, B., and Mucci, A. 2003a. Metal selectivity of *Sargassum* sp. and their alginates in relation to their α -L-guluronic acid content and conformation. Environmental Science and Technology. 37(2): 261-267.
- Davis, T.A., Llanes, F., Volesky, B., Diaz-Pulido, G., McCook, L., and Mucci, A. 2003b. A $^1\text{H-NMR}$ study of Na-alginates extracted from *Sargassum* sp. in relation to metal biosorption. Applied Biochemistry and Biotechnology. 110(2): 75-90.
- Dortch, M., Zakikhani, M., Furey, J., Meyer, R., Fant, S., Gerald, J., Qasim, M., Fredrickson, H., and Honea, P. 2005. Data Gap Analysis and Database Expansion of Parameters for Munitions Constituents. Engineer Research and Development Center, US Army Corps of Engineers.
- Dubin, M.M., and Radushkevich, L.V. 1947. Equation of the characteristic curve of activated charcoal. Chemisches Zentralblatt. 1: 875-889.

- El-Kamash, A., Zaki, A.M., El, A.A., and Geleel, M.A. 2005. Modeling batch kinetics and thermodynamics of zinc and cadmium ions removal from waste solutions using synthetic zeolite. Journal of Hazardous Materials. 127(1-3): 211-220.
- Elliott, H.A., and Huang, C.P. 1981. Adsorption characteristics of some Cu(II) complexes on alumino silicates. Water Research. 15: 849–854.
- El-Naas, M.H., Al-Rub, F.A., Ashour, I., Marzouqi, M.A. Effect of Competitive Interference on the Bio-sorption of Lead (II) by *Chlorella vulgaris*. Chemical Engineering and Processing (in press).
- Erdem, E., Karapinar, N., and Donat R. 2004. The removal of heavy metal cations by natural zeolites. Journal of Colloid and Interface Science. 280: 309–314.
- Feng, Q., Lin, Q., Gong, F., Sugita, S., and Shoya, M. 2004. Adsorption of lead and mercury by rice husk ash. Journal of Colloid and Interface Science. 278(1): 1-8.
- Figueira, M.M., Volesky, B., Ciminelli, S.T.V., and Roddick, A.F. 2000. Biosorption of Metals in Brown Seaweed Biomass. Water Research. 34(1): 196-204.
- Freundlich, H., 1907. Über die Adsorption in Lösungen, Zeitschrift für Physikalische Chemie (Leipzig). 57A: 385 – 470.
- Gupta, A., Gaur, V., and Verma, N. 2004. Breakthrough analysis for adsorption of sulfur-dioxide over zeolites. Chemical Engineering and Processing. 43: 9 - 22.
- Hammami, A., Ballester, A., Blázquez, M.L., González, F., and Muñoz, J. 2002. Effect of the presence of lead on the biosorption of copper, cadmium and zinc by activated sludge. Hydrometallurgy. 67: 109–116.
- Hidenobu, W., Tachibana, Y., and Hosaka, M. 2001. Removal of dimethyl sulfide and *t*-butylmercaptan from city gas by adsorption on zeolites. Microporous and Mesoporous Material. 46: 237-247.
- Ho, Y.S. 1995. Adsorption of heavy metals from waste streams by peat. Ph.D. Dissertation, University of Birmingham, Birmingham, U.K.
- Ho, Y.S., and Ofomaja, A.E. 2006. Pseudo-second-order model for lead ion sorption from aqueous solutions onto palm kernel fiber. Journal of Hazardous Materials. 129(1-3): 137-142.
- Ho, Y.S., Wase, D.A.J., and Forster, C.F. 1996. Kinetic studies of competitive heavy metal sorption by *Sphagnum moss* peat. Environmental Technology. 17: 71-77.

- Hobson, J.P. 1969. Physical sorption isotherms extending from ultrahigh vacuum to vapor pressure. Journal of Physical Chemistry. 73: 2720–2727.
- Inthorn, D., Nagase, H., Isaji, Y., Hirata, K., and Miyamoto, K. 1996. Removal of Cadmium from aqueous solution by the Filamentous Cyanobacterium *Tolypothrix tenuis*. Journal of Fermentation and Bioengineering. 82: 580-584.
- Jalali, R., Ghafourian, H., Asef, Y., Davarpanah, J.S., and Sepehr, S. 2002. Removal and Recovery of Lead using Nonliving Biomass of Marine Algae. Journal of Hazardous Materials. B92: 253-262.
- Janoš, P., Michálek, P., and Turek, L. Sorption of ionic dyes onto untreated low-rank coal – oxihumolite: A kinetic study. Dyes and Pigments, in press.
- Jansson-Charrier, M., Guibal, E., Roussy, J., Delanghe, B., and Le Cloirec, P. 1996. Vanadium (IV) sorption by chitosan: Kinetics and equilibrium. Water Research. 30(2): 465-475.
- Kaewsarn, P., 2000. Single and Multi-Component Biosorption of Heavy Metal Ions by Biosorbents from Marine Alga *Durvillaea Potatorum*. Ph.D. Dissertation, Environmental Engineering, Griffith University, Queensland.
- Kaewsarn, P. 2002. Biosorption of copper(II) from aqueous solution by pre-treated biomass of marine algae *Padina* sp.. Chemosphere. 47: 1081-1085.
- Kalavathy, M. H., Karthikeyan, T., Rajgopal, S., and Miranda, L.R. 2005. Kinetic and isotherm studies of Cu(II) adsorption onto H₃PO₄ – activated rubber wood sawdust. Journal of Colloid and Interface Science. 292(2): 354-362.
- Kapoor, A., and Viraraghavan, T. 1998. Biosorption of heavy metals on *Aspergillus niger*: Effect of pre-treatment. Bioresource Technology. 630: 109-113.
- Kapoor, A., Viraragharan, T., and Cullimore, R.D. 1999. Removal of heavy metals using the fungus *Aspergillus niger*. Bioresource Technology. 70: 95-104.
- Ko, D.C.K., Cheung, C.W., Choy, K.K.H., Porter, J.F., and McKay, G. 2004. Sorption equilibria of metal ions on bone char. Chemosphere. 54: 273–281.
- Kojima, H., and Lee, K.Y. 2001. Photosynthetic Microorganisms in Environmental Biotechnology. Hong Kong: Springer Verlag Hong Kong Ltd.
- Kolay, P. K., Singh, D. N., and Murti, M. V. R. 2001. Synthesis of zeolites from a lagoon ash. Fuel. 80(5): 739-745.
- Kratochvil, D., Fourest, E., and Volesky, B. 1995. Biosorption of copper by *Sargassum fluitans* biomass in fixed-bed column. Biotechnol. Lett. 17(7): 777-782.

- Kumar, K.V., and Kumaran, A. 2005. Removal of methylene blue by mango seed kernel powder. Biochemical Engineering Journal. 27(1): 83-93.
- Kumar, Y. P., King, P., and Prasad, V.S.R.K. 2006. Equilibrium and kinetic studies for the biosorption system of copper(II) ion from aqueous solution using *Tectona grandis* L.f. leaves powder. Journal of Hazardous Materials. in press.
- Kwon, J.S., Yun, S.T., Kim, S.O., Mayer, B., and Hutcheon, I. 2005. Sorption of Zn(II) in aqueous solutions by scoria. Chemosphere. 60(10): 1416-1426.
- Lagergren, S. 1898. Zur Theorie der sogenannten adsorption gelöster stoffe. Kungliga Svenska Vetenskapsakademiens. Handlingar. 24(4): 1–39.
- Langmuir, I. 1918. The sorption of gases on plane surfaces of glass, mica and platinum. Journal of the American Chemical Society. 40: 1361-1403.
- Lee, H.S., and Suh, J.H. 2001. Interference of Aluminum in Heavy Metal Biosorption by a Seaweed Biosorbent. Korean Journal of Chemical Engineering. 18(5): 692-697.
- Lee, M.G., Yi, G., Ahn, B.J., and Roddick, F. 2000 (Check). Conversion of Coal Fly Ash into Zeolite and Heavy Metal Removal Characteristics of the Products. Korean Journal of Chemical Engineering. 17(3): 325-331.
- Lee, R.E. 1989. Phycology. Cambridge, UK: Cambridge University Press.
- Ma, W., and Tobin, J.M. 2003. Development of multimetal binding model and application to binary metal biosorption onto peat biomass. Water Research. 37: 3967–3977.
- Malkoc, E. Ni(II) removal from aqueous solutions using cone biomass of *Thuja orientalis*. Journal of Hazardous Materials., in press.
- Matheickal, T.J. 1998. Biosorption of Heavy Metals from Waste Water using Macro-Algae *Durvillaea Potatorum* and *Ecklonia Radiata*. Ph.D. diss., Environmental Engineering, Griffith University, Queensland.
- Matheickal, T.J., and Yu, Q. 1999. Biosorption of Lead(II) and Copper(II) from Aqueous Solution by Pre-Treated Biomass of Australian Marine Algae. Bioresource Technology. 69: 223-229.
- McBain, J.W. 1932. The Sorption of Gases and Vapors by Solids. London: Routledge.

- McLean, R.J.C., and Beveridge, T.J. 1990. Metal-binding capacity of bacterial surfaces and their ability to form mineralized aggregates. In H.L. Ehrlich and C.L Brierley (eds.), Microbial Mineral Recovery, pp. 185-222. New York: McGraw-Hill Publishing.
- Molina, A., and Poole, C. 2004. A comparative study using two methods to produce zeolites from fly ash. Minerals Engineering. 17(2): 167-173.
- Montes-Hernandez, G., and Rihs, S. simplified method to estimate kinetic and thermodynamic parameters on the solid–liquid separation of pollutants. Journal of Colloid and Interface Science. in press.
- Noeline, B.F., Manohar, D.M., and Anirudhan, T.S. 2005. Kinetic and equilibrium modelling of lead(II) sorption from water and wastewater by polymerized banana stem in a batch reactor. Separation and Purification Technology. 45(2): 131-140.
- Oliveira, E.A., Montanher, S.F., Andrade, A.D., Nóbrega, J.A., and Rollemberg, M.C. 2005. Equilibrium studies for the sorption of chromium and nickel from aqueous solutions using raw rice bran. Process Biochemistry. 40(11): 3485-3490.
- Önala, Y., Akmil-Başara, C., Erenb, D., Sarıcı-Özdemira, Ç., and Depcib, T. 2006. Adsorption kinetics of malachite green onto activated carbon prepared from Tunçbilek lignite. Journal of Hazardous Materials. 128(2-3): 150-157.
- Padmavathy, V., Vasudevan, P., and Dhingra, S.C. 2003. Biosorption of nickel(II) ions on Baker's yeast. Process Biochemistry. 38(10): 1389-1395.
- Pagnanelli, F., Trifonia, M., Beolchini, F., Esposito, A., Toroa, L., and Vegliò, F. 2001. Equilibrium biosorption studies in single and multi-metal systems. Process Biochemistry. 37: 115-124.
- Pagnanelli, F., Esposito, A., Toro, L., and Veglio, F. 2003. Metal speciation and pH effect on Pb^{2+} , Cu^{2+} , Zn^{2+} and Cd^{2+} biosorption onto *Sphaerotilus natans*: Langmuir-type empirical model. Water Research. 37: 627–633.
- Pearson, R.G. 1963. Hard and Soft Acids and Bases. Journal of the American Chemical Society. 85: 3533–3539.
- Pigaga, A., Ju kenas, R., Virbalyt , D., Klimantavi i t , M.G., and Pak tas, V. 2005. The use of cement kiln dust for the removal of heavy metal ions from aqueous solutions. Transactions of the Institute of Metal Finishing. 83(4): 210-214(5).

- Pitcher, S.K., Sladea, R.C.T., and Ward, N.I. 2004. Heavy metal removal from motorway stormwater using zeolites. Science of the Total Environment. 334–335: 161–166.
- Puranik, P.R., Paknikar, K.M. 1999. Influence of co-cations on biosorption of lead and zinc – a comparative evaluation in binary and multimetal systems. Bioresource Technology. 70: 269 – 276.
- Qodah, A. 2000. Adsorption of dyes using shale oil ash. Water Research. 34(17): 4295–4303.
- Querol, X., Moreno, N., and Umana, J.C., Alastuey, A., Hernandez, E., Lopez-Soler, A. and Plana, F. 2002. Synthesis of zeolites from coal fly ash: an overview. International Journal of Coal Geology. 50: 413– 423.
- Rabo, J.A., and Schoonover, M.W. 2001. Early discoveries in zeolite chemistry and catalysis at Union Carbide, and follow-up in industrial catalysis. Applied Catalysis A. General 222: 261–275.
- Remacle, J. 1990. The cell wall and metal binding.. In B. Volesky (ed.), Biosorption of Heavy Metals, pp. 83-92. Boca Raton: CRC Press..
- Ricordel, S., Taha, S., Cisse, I., and Dorange, G. 2001. Heavy metal removal by sorption onto peanut husks carbon: characterization, kinetic study and modeling. Separation and purification technology. 24(3): 389-401.
- Sag, Y., Aksu, Z., Acikel, U., and Kutsal, T. 1998. A comparative study for the simultaneous biosorption of Cr(VI) and Fe(III) on *C. vulgaris* and *R. arrhizus*: Application of the competition sorption models. Process Biochemistry. 33(3): 273-281.
- Sag, Y., and Aktay, Y. 2000. Mass transfer and equilibrium studies for the sorption of chromium ions onto chitin. Process Biochemistry. 36(1-2): 157-173.
- Sag, Y., and Kutsal T. 1996. Fully Competitive Biosorption of Chromium(VI) and Iron(III) Ions from Binary Metal Mixtures by *R. arrhizus*: Use of the Competitive Langmuir Model. Process Biochemistry. 31(6): 573-585.
- Sanchez, A., Ballester, A., Blazques, L.M., Gonzalez, F., Munoz, J., and Hammami, A. 1999. Biosorption of Copper and Zinc by *Cymodocea nodosa*. FEMS Microbiology Reviews. 23: 527-536.

- Sanguanduan, N. 2002. Heavy metal removal by ion exchange resin made from corn cob, soybean hull and sunflower stalks. M.Eng. Thesis, Environmental Engineering, Faculty of Engineering, Chulalongkorn University.
- Sawyer, C.N., McCarty, P.L., and Parkin, G.F. 1990. Chemistry for environmental engineering. fourth ed. McGrawHill. Singapore.
- Selatnia, A., Boukazoula, A., Kechid, N., Bakhti, M. Z., Chergui, A., and Kerchich, Y. 2004. Biosorption of lead (II) from aqueous solution by a bacterial dead *Streptomyces rimosus* biomass. Biochemical Engineering Journal. 19(2): 127-135.
- Selim, H.M., and Iskandar, I.S. 1999. Fate and transport of heavy metals in the vadose zone. USA: CRC press.
- Sengupta, A.K. 2002. Environmental Separation of Heavy Metals. (n.p.): CRC Press.
- Shawabkeh, R., Al-Harashsheh, A., Ham, M., and Khlaifat, A. 2004. Conversion of oil shale ash into zeolite for cadmium and lead removal from wastewater. Fuel. 83(7-8): 981-985.
- Shen, J., and Duvnjak, Z. 2005. Adsorption kinetics of cupric and cadmium ions on corncob particles. Process Biochemistry. 40(11): 3446-3454.
- Shih, W.H. and Chang, H.L. 1996. Conversion of fly ash into zeolites for ion-exchange applications. Materials Letters. 28(4-6): 263-268.
- Shin, E.W., Karthikeyan, K.G., and Tshabalala, M.A. 2007. Adsorption mechanism of cadmium on juniper bark and wood. Bioresource Technology. 98(3): 588-594.
- Shukla, S.S., Yu, L.J., Dorris, K.L., and Shukla, A. 2005. Removal of nickel from aqueous solutions by sawdust. Journal of Hazardous Materials. 121(1-3): 243-246.
- Singh, K.K., Singh, A.K., and Hasan, S.H. 2006. Low cost bio-sorbent 'wheat bran' for the removal of cadmium from wastewater: Kinetic and equilibrium studies Bioresource Technology. 97(8): 994-1001.
- Singh, S., Rai, B.N., and Rai, L.C. 2001. Ni (II) and Cr (VI) sorption kinetics by microcystis in single and multimetallic system. Process Biochemistry. 36: 1205-1213.
- Sips, R. 1948. On the structure of a catalyst surface. Journal of Chemical Physics. 16: 490-495.

- Smith, J.M. 1981. Chemical Engineering Kinetics. McGraw-Hill. New York.
- Somerset, V. S., Petrik, L. F., White, R. A., Klink, M.J., Key, D., and Iwuoha, E.I. 2005. Alkaline hydrothermal zeolites synthesized from high SiO₂ and Al₂O₃ co-disposal fly ash filtrates. Fuel. 84(18): 2324-2329.
- Sprynskyy, M., Artur, B.B., Terzyk, P., and Namieśnik, J. 2006. Study of the selection mechanism of heavy metal (Pb²⁺, Cu²⁺, Ni²⁺, and Cd²⁺) adsorption on clinoptilolite. Journal of Colloid and Interface Science. 304(1): 21-28.
- Srivastava, V. C., Mall, I. D., and Mishra, I. M. 2006. Characterization of mesoporous rice husk ash (RHA) and adsorption kinetics of metal ions from aqueous solution onto RHA. Journal of Hazardous Materials. 134(1-3): 257-267.
- Steenbruggen, G., and Hollman, G.G. 1998. The synthesis of zeolites from fly ash and the properties of the zeolite products. Journal of Geochemical Exploration. 62: 305–309.
- Subbiah, A., Cho, B.K., Blint, R.J., Gujar, A., Price, G.L., and Yie, J.E. 2003. NO_x reduction over metal-ion exchanged novel zeolite under lean conditions: activity and hydrothermal stability. Applied Catalysis B. Environmental 42: 155–178.
- Sungkhum, V. 2002. Sorption of Heavy Metals by Green Macroalga, *Caulerpa lentillifera*. M.Sc. Thesis, Environmental Management (Inter-Department), Graduate School, Chulalongkorn University.
- Suthiparinyanont, P. 2003. Pretreatment of Green Macroalga, *Caulerpa lentillifera* for Heavy Metal Removal. M.Sc. Thesis, Environmental Management (Inter-Department), Graduate School, Chulalongkorn University.
- Szoztak, R. 1989. Molecular Sieve Principles of Synthesis and Identification. New York: Van Nostrand Reinhold.
- Tan, K.H., 2000. Environmental Soil Science. (n.p.):Marcel Dekker.
- Thomas, H.G., 1948. Chromatography: a problem in kinetic. Annals of the New York Academy of Sciences. 49, 161-182.
- Tongkam, M. 1999. Synthesis of zeolites from coal fly ash. M.Sc. Thesis, Chemical Technology, Faculty of Science, Chulalongkorn University.
- Turatum, P. 2001. Synthesis of zeolite beta from lignite fly ash. M.Eng. Thesis, Chemical Engineering, Faculty of Engineering, Chulalongkorn University.

- Üçer, A., Uyanik, A., and Aygün, Ş.F. 2006. Adsorption of Cu(II), Cd(II), Zn(II), Mn(II) and Fe(III) ions by tannic acid immobilized activated carbon. Separation and Purification Technology. 47(3): 113-118.
- Vasudevan, P., Padmavathy, V., and Dhingra, S.C. 2003. Kinetics of biosorption of cadmium on Baker's yeast. Bioresource Technology. 89(3): 281-287.
- Veglio, F., and Beolchini, F. 1997. Removal of Metals by Biosorption: A Review. Hydrometallurgy. 44: 301-316.
- Vermeulen, T. 1953. Theory for irreversible and constant pattern solid diffusion. Industrial and Engineering Chemistry. 45(8): 1664-1670.
- Vijayaraghavan, K., Palanivelu, K., and Velan, M. 2006. Biosorption of copper(II) and cobalt(II) from aqueous solutions by crab shell particles. Bioresource Technology. 97(12): 1411-1419.
- Volesky, B. 1990. Biosorption of Heavy Metals. Boca Raton: CRC Press.
- Volesky, B. 2004. Sorption and Biosorption. St.Lambert, Quebec: BV-Sorbex Inc.
- Vymazal, J. 1995. Algae and element cycling in wetlands. Boca Raton. Lewis Press.
- Wase, J., and Foster, C. 1996. Biosorbents for Metal Ions. Taylor & Francis. UK.
- Weber, W.J., and Morris, J.C. 1962. Advance in water pollution research : removal of biological resistant pollutions from wastewater by adsorption. In Proceedings of the International Conference on Water Pollution Symposium.Vol. 2, Pergamon Press, Oxford, 231 – 266.
- Wild, A. 1993. Soils and the Environment. U.K.: Cambridge University Press.
- Wong, J.P.K., Wong, S.Y., and Tam, N.F.Y. 2000. Nickel Biosorption by Two Chlorella Species, *C. Vulgaris* (a commercial species) and *C. Miniata* (a local isolate). Bioresource Technology. 73: 133-137.
- Xu, H., Liu, Y., and Tay, J.H. 2006. Effect of pH on nickel biosorption by aerobic granular sludge. Bioresource Technology. 97(3): 359-363.
- Yin, P., Yu, Q., Jin, B., and Ling, Z. 1999. Biosorption Removal of Cadmium from Aqueous Solution by Using Pretreated Fungal biomass Cultured from Starch Wastewater. Water Research. 33(8): 1960-1963.
- Yu, Q., and Kaewsarn, P. 1999. Binary Sorption of Copper(II) and Cadmium(II) from Aqueous Solutions by Biomass of Marine Alga *Durvillaea potatorum*. Separation Science and Technology. 34(8): 1595-1605.

- Yu, Q., and Kaewsarn, P. 2000. Sorption of Ni²⁺ from Aqueous Solutions by Pretreated Biomass of Marine Macroalga *Durvillaea potatorum*. Separation Science and Technology. 35(5): 689-701.
- Yun, Z.Y., Xu, Y., Xu, J.H., Wu, Z.Y., Wei, Y.L., Zhou, Z.P., and Zhu, J.H. 2004. In situ FTIR investigation on the adsorption of nitrosamines in zeolites. Microporous and Mesoporous Materials. 72: 127–135.
- Zhou, L.J., Huang, L.P., and Lin, G.R. 1998. Sorption and Desorption of Cu and Cd²⁺ by Macroalgae and Microalgae. Environmental Pollution. 101: 67-75.
- Zulkali, M.M.D., Ahmad, A.L., and Norulakmal, N.H. 2006. Oryza sativa L. husk as heavy metal adsorbent: Optimization with lead as model solution. Bioresource Technology. 97(1): 21-25.



สถาบันวิทยบริการ
จุฬาลงกรณ์มหาวิทยาลัย

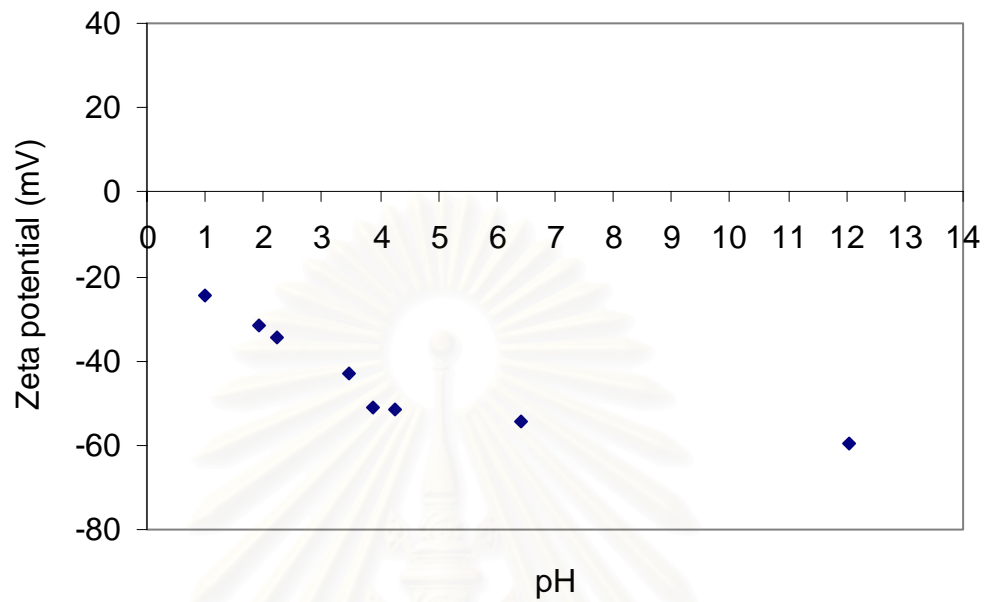


APPENDICES

สถาบันวิทยบริการ
จุฬาลงกรณ์มหาวิทยาลัย

APPENDIX A

Surface charge of *Caulerpa lentillifera*



Source : unpublished result from Meevasana (Ph.D. candidate at National Research Center for Environmental and Hazardous Waste Management)

สถาบันวิทยบริการ
จุฬาลงกรณ์มหาวิทยาลัย

APPENDIX B

Raw data of heavy metal biosorption by *Caulerpa lentillifera*

B.1 Single component data

Co, Pb (mg/l)	Co, Pb (mg/l)	M (g)	Co, Cu (mg/l)	Ce, Cu (mg/l)	M (g)	Co, Cd (mg/l)	Ce, Cd (mg/l)	M (g)
57.46	2.00	0.5007	6.11	1.00	0.5004	15.20	2.52	0.5005
57.46	1.87	0.5004	6.11	0.88	0.5001	15.20	2.97	0.5008
57.46	1.98	0.5006	6.11	1.10	0.5004	15.20	3.47	0.5012
79.28	3.47	0.5008	12.61	1.54	0.5002	32.94	6.25	0.5016
79.28	2.49	0.5004	12.61	1.71	0.5001	32.94	6.84	0.5016
79.28	2.74	0.5002	12.61	1.61	0.5005	32.94	6.93	0.5001
122.77	5.76	0.5001	17.94	3.26	0.5006	41.43	11.24	0.5004
122.77	5.23	0.5001	17.94	3.22	0.5003	41.43	9.58	0.5004
122.77	4.20	0.5003	17.94	3.08	0.5002	41.43	10.65	0.5012
181.21	8.86	0.5008	25.22	4.62	0.5006	53.16	14.66	0.5005
181.21	8.48	0.5001	25.22	4.43	0.5003	53.16	14.43	0.5003
181.21	10.92	0.5002	25.22	3.50	0.5002	53.16	16.09	0.5005
248.16	15.04	0.5009	36.23	7.45	0.5004	73.55	28.35	0.5016
248.16	19.10	0.5004	36.23	5.80	0.5002	73.55	26.37	0.501
248.16	18.64	0.5001	36.23	5.97	0.5	73.55	28.79	0.5015
498.6	289.15	0.5007	54.88	11.9	0.5002	96.97	39.99	0.5017
498.6	272.95	0.5004	54.88	12.39	0.5007	96.97	41.23	0.501
498.6	280.25	0.5006	54.88	12.86	0.5007	96.97	45.65	0.5008
			77.97	19.09	0.5001	114.99	56.82	0.5004
			77.97	18.08	0.5003	114.99	53.55	0.5015
			77.97	20.09	0.5009	114.99	58.11	0.5015

สถาบันวิทยบริการ
จุฬาลงกรณ์มหาวิทยาลัย

B.2 Binary components data

	Co, Pb	Ce, Pb	Co, Cu	Ce, Cu	M		Co, Pb	Ce, Pb	Co, Cd	Ce, Cd	M
	(mg/l)	(mg/l)	(mg/l)	(mg/l)	(g)		(mg/l)	(mg/l)	(mg/l)	(mg/l)	(g)
Vary Pb Fix Cu 0.1 mM (~ 6 ppm) 30 mL	14.12	0	4.82	0	0.5006	Vary Pb Fix Cd 0.1 mM (~ 10 ppm) 30 mL	13.27	0	9.69	1.91	0.5005
	14.12	0	4.82	0.16738	0.5008		13.27	0	9.69	1.80	0.5007
	14.12	0	4.82	0	0.5		13.27	0	9.69	1.86	0.5001
	36.63	0.1233	5.52	0.00537	0.5003		29.10	0	9.59	2.12	0.5001
	36.63	0.2123	5.52	0.00505	0.5002		29.10	0	9.59	2.09	0.5007
	36.63	0.2123	5.52	0.00503	0.5003		29.10	0	9.59	2.11	0.5008
	46.86	0.2249	4.54	0.00779	0.5		46.71	0.20	9.84	2.27	0.5005
	46.86	0.2017	4.54	0.00466	0.5005		46.71	0.16	9.84	2.36	0.5005
	46.86	0.5776	4.54	0.00403	0.5004		46.71	0.30	9.84	2.80	0.5005
	97.78	4.2628	5.42	0.01483	0.5008		105.26	4.24	9.78	2.81	0.5003
	97.78	3.2474	5.42	0.01353	0.5002		105.26	3.38	9.78	2.55	0.5006
	97.78	4.253	5.42	0.018	0.5002		105.26	4.44	9.78	2.87	0.5009
	158.69	8.8709	5.83	0.01458	0.5		173.83	9.30	9.90	3.77	0.5009
	158.69	8.2559	5.83	0.0134	0.5008		173.83	8.73	9.90	3.45	0.5011
	158.69	11.28	5.83	0.01632	0.50098		173.83	11.32	9.90	4.29	0.5022
	213.98	17.788	5.61	0.0123	0.5005		230.02	18.37	9.48	4.07	0.5017
	213.98	17.196	5.61	0.02584	0.5002		230.02	18.48	9.48	3.74	0.5005
213.98	18.632	5.61	0.01593	0.5009	230.02	20.19	9.48	4.31	0.5018		
Vary Pb Fix Cu 0.78 mM (50 ppm) 60 mL	7.62	1E-05	48.95	5.19	1.0026	Vary Pb Fix Cd 0.44 mM (50 ppm) 60 mL	10.14	0	41.65	23.76	1.0005
	7.62	1E-05	48.95	8.05	1		10.14	0	41.65	25.30	1.0000
	7.62	1E-05	48.95	8.51	1.0037		10.14	0	41.65	24.14	1.0005
	20.74	0.39	46.26	16.37	1.0034		16.02	2.14	43.28	28.73	1.0003
	20.74	1.64	46.26	11.98	1.0039		16.02	1.14	43.28	24.81	1.0010
	20.74	0.0019	46.26	8.19	1		16.02	1.27	43.28	26.73	1.0007
	45.97	5.50	48.17	19.55	1.0001		45.82	5.48	43.19	29.52	1.0010
	45.97	5.00	48.17	13.34	1.0012		45.82	4.97	43.19	30.42	1.0000
	45.97	6.92	48.17	15.23	1.0012		45.82	6.96	43.19	29.12	1.0009
	62.02	20.46	49.15	19.86	1.0001		98.89	9.89	47.94	33.65	1.0004
	62.02	19.14	49.15	18.068	1.0012		98.89	10.80	47.94	35.74	1.0009
	62.02	17.37	49.15	17.32	1.0012		98.89	11.32	47.94	34.32	1.0002
					125.34	19.98	45.83	33.24	1.0004		
					125.34	21.53	45.83	34.52	1.0009		
					125.34	20.42	45.83	35.17	1.0002		

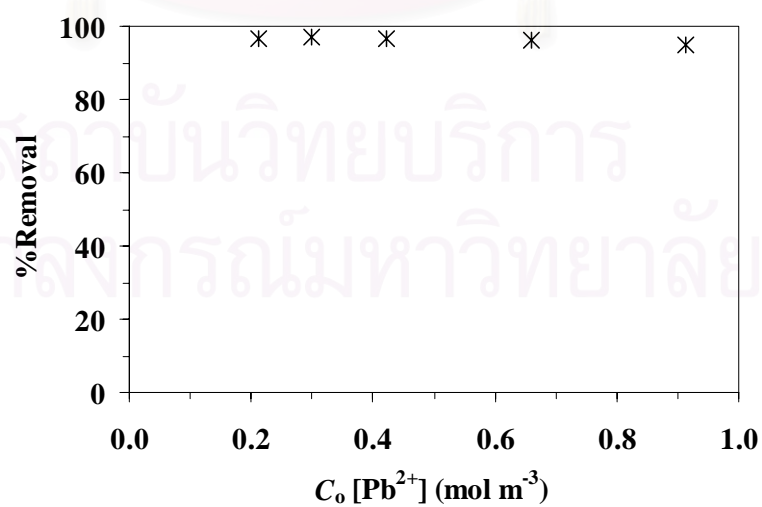
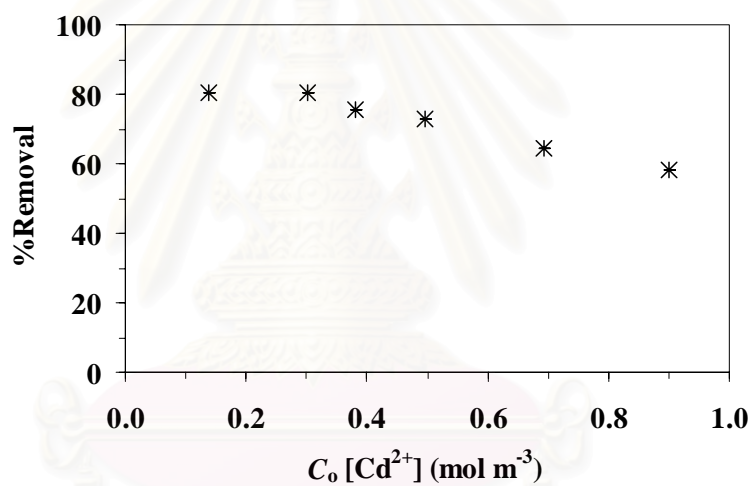
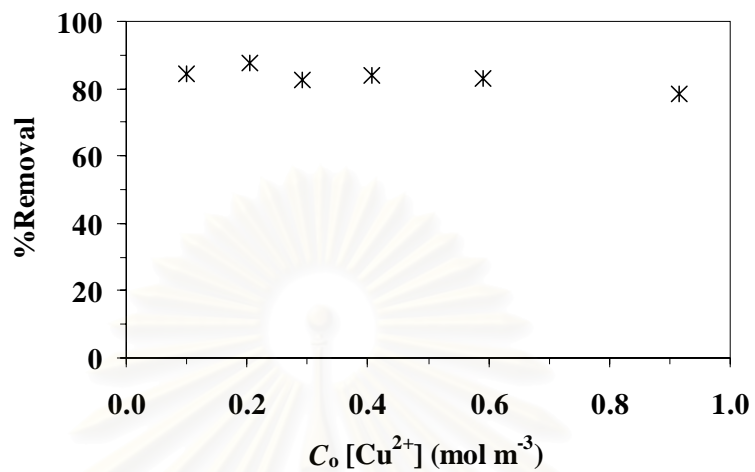
	Co, Cu	Ce, Cu	Co, Pb	Ce, Pb	M		Co, Cu	Ce, Cu	Co, Cd	Ce, Cd	M
	(mg/l)	(mg/l)	(mg/l)	(mg/l)	(g)		(mg/l)	(mg/l)	(mg/l)	(mg/l)	(g)
Vary Cu Fix Pb 0.1 mM (~ 20 ppm) 30 mL	4.82	0.891	14.123	0	0.5006	Vary Cu Fix Cd 0.1 mM (~ 10 ppm) 30 mL	4.09	0.99	8.65	5.93	0.5009
	4.82	0.943	14.123	0	0.5008		4.09	0.58	8.65	5.01	0.5002
	4.82	0.971	14.123	0	0.5000		4.09	1.58	8.65	6.46	0.5007
	9.78	1.891	14.114	0	0.5005		9.39	0.75	9.52	2.02	0.5006
	9.78	1.943	14.114	0	0.5003		9.39	0.69	9.52	2.11	0.5009
	9.78	1.971	14.114	0	0.5003		9.39	0.76	9.52	2.33	0.5006
	16.03	3.641	16.396	0	0.5008		17.28	1.09	10.14	2.25	0.5005
	16.03	3.980	16.396	0	0.5010		17.28	1.06	10.14	2.29	0.5001
	16.03	3.641	16.396	0	0.5015		17.28	1.31	10.14	2.54	0.5003
	32.76	8.628	20.630	0.913	0.5004		32.46	5.21	9.79	2.72	0.5001
	32.76	8.398	20.630	0.543	0.5012		32.46	4.59	9.79	2.32	0.5005
	32.76	8.896	20.630	0.590	0.5012		32.46	5.48	9.79	2.58	0.5003
	50.35	13.660	19.922	0.733	0.5002		51.09	9.45	9.53	3.28	0.5004
	50.35	12.705	19.922	0.547	0.5003		51.09	10.14	9.53	3.45	0.5007
	50.35	13.812	19.922	0.400	0.5004		51.09	10.78	9.53	3.58	0.5009
	69.24	23.660	21.193	0.736	0.5002		69.44	15.50	9.59	4.02	0.5005
	69.24	22.705	21.193	0.665	0.5013		69.44	13.75	9.59	3.69	0.5007
69.24	23.812	21.193	0.388	0.5009	69.44	16.41	9.59	4.19	0.5004		
Vary Cu Fix Pb 0.24 mM (50 ppm) 60 mL	7.71	1.56	38.73	6.03	1.0020	Vary Cu Fix Cd 0.44 mM (50 ppm) 60 mL	6.64	0.10	42.19	22.53	1.0006
	7.71	1.50	38.73	6.24	1.0005		6.64	0.83	42.19	24.86	1.0002
	7.71	1.46	38.73	9.91	1.0005		6.64	0.37	42.19	20.29	1
	20.89	9.29	39.07	9.78	1.0008		19.86	4.23	43.06	24.78	1
	20.89	6.53	39.07	6.37	1.0003		19.86	2.83	43.06	25.36	1.0002
	20.89	8.37	39.07	10.27	1.0002		19.86	4.36	43.06	24.54	1.0003
	48.17	19.55	45.97	5.50	1.0001		41.10	24.00	42.28	31.68	1.0001
	48.17	17.34	45.97	5.00	1.0012		41.10	17.70	42.28	25.58	1.0003
48.17	15.23	45.97	6.92	1.0012	41.10	18.67	42.28	30.91	1.0005		

2. Binary components data (Continue)

	Co, Cd	Ce, Cd	Co, Pb	Ce, Pb	M		Co, Cd	Ce, Cd	Co, Cu	Ce, Cu	M
	(mg/l)	(mg/l)	(mg/l)	(mg/l)	(g)		(mg/l)	(mg/l)	(mg/l)	(mg/l)	(g)
Vary Cd Fix Pb 0.1 mM (~ 20 ppm) 30 mL	9.69	1.91	13.27	0	0.5005	Vary Cd Fix Cd 0.1 mM (~ 10 ppm) 30 mL	23.09	18.26	4.26	1.17	0.5006
	9.69	1.80	13.27	0	0.5007		23.09	16.54	4.26	0.81	0.5
	9.69	1.86	13.27	0	0.5001		23.09	16.37	4.26	0.75	0.5007
	18.70	3.83	12.26	0	0.501		56.56	17.55	5.13	0.97	0.5001
	18.70	3.51	12.26	0	0.5003		56.56	18.20	5.13	0.93	0.5003
	18.70	5.34	12.26	0	0.5019		56.56	20.82	5.13	0.83	0.5006
	23.10	8.13	12.09	0	0.5001		90.70	43.84	4.96	0.85	0.5007
	23.10	6.04	12.09	0	0.5007		90.70	59.95	4.96	0.77	0.5005
	23.10	7.32	12.09	0	0.5000		90.70	50.46	4.96	0.70	0.5002
	55.33	21.96	21.77	0.63	0.5003		121.43	66.44	5.01	0.96	0.5003
	55.33	21.73	21.77	0.72	0.5012		121.43	64.48	5.01	0.66	0.5002
	55.33	24.38	21.77	0.61	0.5007		121.43	68.25	5.01	0.87	0.5004
	87.38	35.42	20.35	0.72	0.5011						
	87.38	34.85	20.35	0.65	0.5006						
	87.38	37.43	20.35	0.58	0.5012						
Vary Cd Fix Pb 0.24 mM (50 ppm) 60 mL	9.31	4.99	39.49	6.08	1.0025	Vary Cd Fix Cd 0.44 mM (50 ppm) 60 mL	11.43	4.21	46.87	9.56	1.0009
	9.31	4.55	39.49	6.38	1.0035		11.43	6.18	46.87	16.02	1.0033
	9.31	4.34	39.49	9.76	1.0016		11.43	4.89	46.87	8.77	1.0055
	21.61	15.82	39.11	9.91	1.0000		27.51	20.79	50.18	16.91	1.0009
	21.61	17.59	39.11	6.32	1.0000		27.51	20.03	50.18	14.24	1.0000
	21.61	17.68	39.11	10.46	1.0025		27.51	21.72	50.18	15.43	1.0006
	43.19	29.52	45.82	5.48	1.0010		50.79	35.64	48.39	19.53	1.0001
	43.19	30.42	45.82	4.97	1.0000		50.79	33.10	48.39	12.99	1.0003
	43.19	29.12	45.82	6.96	1.0009		50.79	27.93	48.39	14.23	1.0005

สถาบันวิทยบริการ
จุฬาลงกรณ์มหาวิทยาลัย

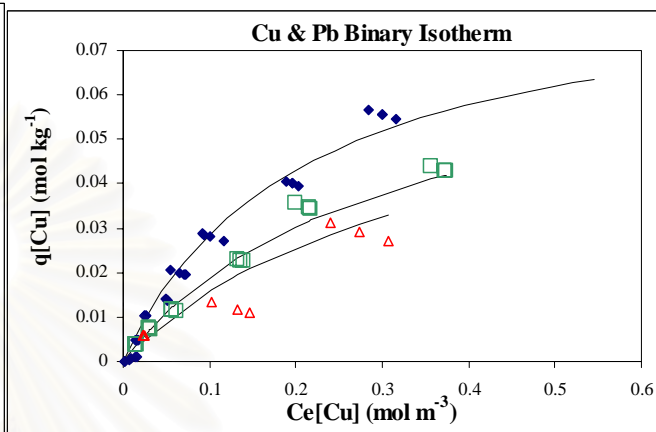
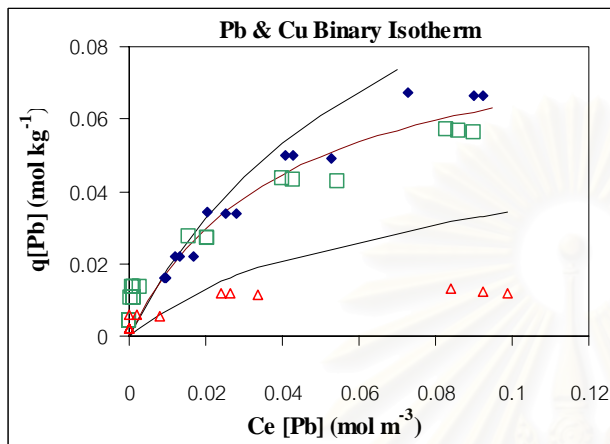
APPENDIX C

Removal percentage of metal sorption by *Caulerpa lentillifera*

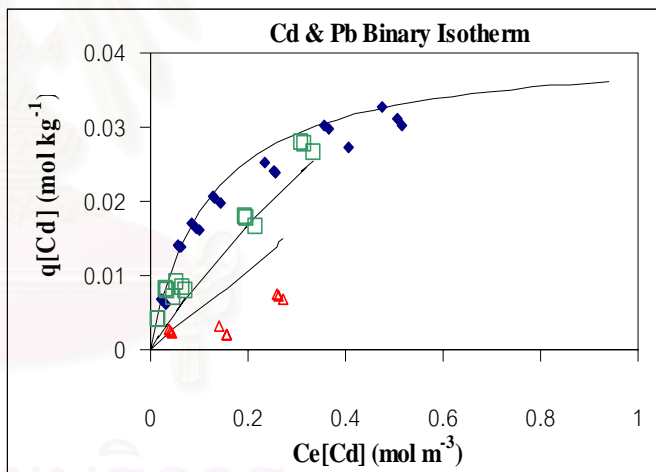
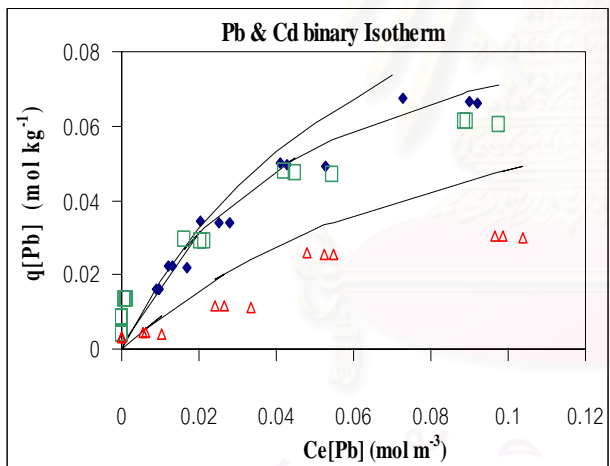
APPENDIX D

Two dimensional curves of binary sorption isotherm

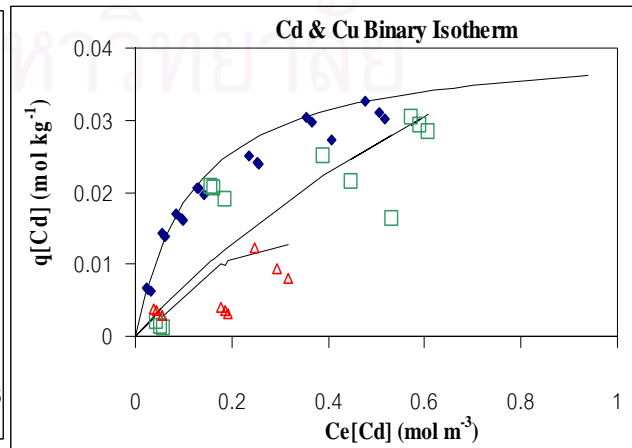
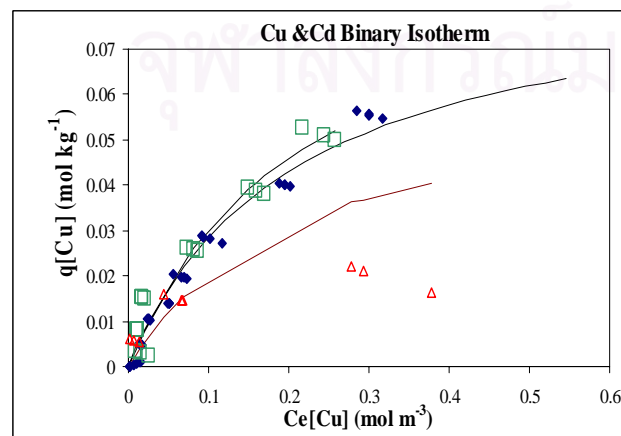
C.1 Pb^{2+} - Cu^{2+} system



C.2 Pb^{2+} - Cd^{2+} system



C.3 Cu^{2+} - Cd^{2+} system



APPENDIX E

Paper Publications (Research Articles)

1. **Apiratikul, R.**, and Pavasant, P. 2006. Sorption isotherm model for binary component sorption of copper, cadmium, and lead ions using dried green macroalga, *Caulerpa lentillifera*. Chemical Engineering Journal. 119: 135–145.
2. Pavasant, P., **Apiratikul, R.**, Sungkhum, V., Suthiparinyanont, P., Wattanachira, S., Marhaba, T.F. 2006. Biosorption of Cu^{2+} , Cd^{2+} , Pb^{2+} , and Zn^{2+} using dried marine green macroalga *Caulerpa lentillifera*. Bioresource Technology. 97: 2321–2329.
3. **Apiratikul, R.**, and Pavasant, P. Biosorption mechanism of heavy metals by dried green macro alga, *Caulerpa lentillifera*. Submitted to Bioresource Technology.
4. **Apiratikul, R.**, and Pavasant, P. Sorption of Cu^{2+} , Cd^{2+} , and Pb^{2+} using modified zeolite from coal fly ash. Submitted to Chemical Engineering Journal.

APPENDIX F

Paper Publications (Conference Articles)

1. **Ronbanchob Apiratikul**, Prasert Pavasant. Treatment of heavy metals using fixed-bed biosorption column by green macroalga, *Caulerpa lentillifera*. 2004. The Regional symposium on Chemical Engineering (RSCE 2004), 1-3 December 2004, The Grand Hotel, Bangkok.
2. **Ronbanchob Apiratikul**, DOUNGMANEE Rungsuk, Varong Pavarajarn, Prasert Pavasant. Conversion of coal fly ash to zeolite. 2006. RGJ Ph.D. Congress VII, 20 – 22 April 2006, Jomtien Palm Beach Resort, Choburi.
3. Viriya Madacha, **Ronbanchob Apiratikul**, Prasert Pavasant. Heavy metals uptake by dried *Caulerpa lentillifera* 2006. JGSEE and Kyoto University 2nd Joint International Conference on: Sustainable Energy and Environment "Technology and Policy Innovations", 21 - 23 Nov. 2006, Nai Lert Park Hotel, Bangkok.
4. DOUNGMANEE Rungsuk, **Ronbanchob Apiratikul**, Prasert Pavasant. Zeolite synthesis from fly ash from coal-fired power plant by fusion method 2006. JGSEE and Kyoto University 2nd Joint International Conference on: 21 - 23 Nov. 2006, Nai Lert Park Hotel, Bangkok.
5. **Ronbanchob Apiratikul**, Parichat Norranattrakul, Prasert Pavasant. Sorption of heavy metal ions using zeolite modified from coal fly ash. 2006. The Regional symposium on Chemical Engineering (RSCE 2006), 3-5 December 2006, Nanyang Executive Center, Singapore.

สถาบันวิทยบริการ
จุฬาลงกรณ์มหาวิทยาลัย

BIOGRAPHY

Mr. Ronbanchob Apiratikul was born on 27th October 1980 in Bangkok, Thailand. He finished his higher secondary courses from Triam udom suksa high school (Bangkok) in March 1998. After that he studied in the major of Environmental Engineering, Faculty of Engineering at Chulalongkorn University and graduated his bachelor's degree in 2002. He began his further study for Master's degree in International Environmental Management at Chulalongkorn University and received his Master's degree in April 2004. In the same year, he continued his Ph.D. study in the same field and university as Master's degree. During his doctoral learning, he was granted a Royal Golden Jubilee Ph.D. scholarship (grant number PHD/0248/2546) by Thailand Research Fund and joined the Regional Symposium on Chemical Engineering at Singapore with a Conference Grant for Ph.D. student supported by Graduate School of Chulalongkorn University. He achieved his Ph.D. degree in April 2007.



สถาบันวิทยบริการ
จุฬาลงกรณ์มหาวิทยาลัย